อนุภาคนาโนไคโตซานกับอะลูมิเนียมไฮดรอกไซด์เจล
ในการเป็นระบบนำส่งวัคซีนไข้หวัดใหญ่ทางจมูก

นายอนุวัช มิตรประทาน

วิทยานิพนธ์นี้เป็นส่วนหนึ่งของการศึกษาตามหลักสูตรปริญญาเภสัชศาสตรมหาบัณฑิต
สาขาวิชาเภสัชอุตสาหกรรม ภาควิชาวิทยาการเภสัชกรรมและเภสัชอุตสาหกรรม
คณะเภสัชศาสตร์ จุฬาลงกรณ์มหาวิทยาลัย
ปีการศึกษา 2555

CHITOSAN NANOPARTICLES WITH ALUMINIUM HYDROXIDE GEL AS NASAL

DELIVERY SYSTEM FOR INFLUENZA VACCINE

Mr. Anawatch Mitpratan

A Thesis Submitted in Partial Fulfillment of the Requirements

for the Degree of Master of Science in Pharmacy Program in Industrial Pharmacy

Department of Pharmaceutics and Industrial Pharmacy

Faculty of Pharmaceutical Sciences

Chulalongkorn University

Academic Year 2012

Thesis Title   CHITOSAN NANOPARTICLES WITH ALUMINIUM HYDROXIDE GEL AS NASAL DELIVERY SYSTEM FOR INFLUENZA VACCINE.

By   Mr. Anawatch Mitpratan

Field of Study   Industrial Pharmacy

Thesis Advisor   Professor Garnpimol C. Ritthidej, Ph.D.

Thesis Co-advisor Associate Professor Vimolmas Lipipun, Ph.D.

Accepted by the Faculty of Pharmaceutical Sciences, Chulalongkorn University in Partial Fulfillment of the Requirements for the Master's Degree

…………………………………………..…Dean of the Faculty of
Pharmaceutical Sciences

(Associate Professor Pintip Pongpech, Ph.D.)

THESIS COMMITTEE

…………………………………………..Chairman

(Associate Professor Poj Kulvanich, Ph.D.)

…………………………………….…….Thesis Advisor

(Professor Garnpimol C. Ritthidej, Ph.D.)

…………………………………………..Thesis Co-advisor

(Associate Professor Vimolmas Lipipun, Ph.D.)

…………………………………………..Examiner

(Phanphen Wattanaarsakit, Ph.D.)

…………………………………………..External Examiner

(Assistant Professor Wiwat Pichayakorn, Ph.D.)

อนุวัช มิตรประทาน : อนุภาคนาโนไคโตซานกับอะลูมิเนียมไฮดรอกไซด์เจลในการ
เป็นระบบนำส่งวัคซีนไข้หวัดใหญ่ทางจมู ก.   (CHITOSAN NANOPARTICLES
WITH ALUMINIUM HYDROXIDE GEL AS NASAL DELIVERY SYSTEM FOR
INFLUENZA VACCINE) อ.ที่ปรึกษาวิทยานิพนธ์หลัก : ศ.ดร.กาญจน์พิมล ฤทธิเดช ,
อ.ที่ปรึกษาวิทยานิพนธ์ร่วม : รศ.ดร.วิมลมาศ ลิปิพันธ์, 113 หน้า.

การศึกษานี้เป็นการเตรียม ระบบนำส่งที่มีศักยภาพสำหรับการให้วัคซีนไข้หวัดใหญ่
ทางจมูกโดยใช้หลักการเกิดเจลระหว่างประจุของไคโตซานกับโซเดียม ไตรโพลีฟอสเฟต เพน
ตาเบสิก (ทีพีพี) และร่วมกับ การเกิดคอนจูเกตกับ อะลูมิเนียมไฮดรอกไซด์เจล โดยศึกษาสภาวะ
การเตรียมที่มีผลต่อคุณสมบัติเชิงเคมีและฟิสิกส์ของอนุภาคที่เตรียมได้   โปรตีนซีรั่มจากวัว
(bovine serum albumin) ใช้เป็นแอนติเจนต้นแบบสำหรับการประเมินผลก่อนการศึกษาการ
กระตุ้นภูมิคุ้มกัน จากผลการทดลองแสดงให้เห็นว่าขนาดของอนุภาคลดลงโดยการลดความ
เข้มข้นของสารละลายไคโตซานและมีอัตราส่วนน้ำหนักของไคโตซาน :ทีพีพี ที่เหมาะสม (3:1)
ค่าความเป็นกรด -ด่างของสารลายไคโตซานที่เหมาะสมอยู่ที่ 4.5 ซึ่งจะทำให้ได้ขนาดอนุภาคที่
เล็กลงในขณะที่การเพิ่มความเป็นกรด -ด่างจะทำให้ได้ขนาดอนุภาคที่ใหญ่ขึ้นและค่าศักย์ซีตา
ลดลง นอกจากนี้ปริมาณของทวีน 80 และอะลูมิเนียมไฮดรอกไซด์เจลรวมทั้งลำดับการผสมยังมี
ผลต่อขนาดอนุภาคด้วย อนุภาคนาโน ที่ได้มีลักษณะเป็นทรงกลมเคลือบด้วยชั้นที่มีลักษณะฟู
ของอะลูมิเนียมไฮดรอกไซด์เจล มีประสิทธิภาพการกักเก็บยาประมาณ 52 - 57% โปรตีนที่ถูก
เก็บกักไว้ในอนุภาคยังคงสภาพ ซึ่งแสดงโดยผลของโซเดียมโดเดซิลซัลเฟตโพลีอะคริลาไมด์
เจลอิเล็กโตรโฟรีซิสและเซอร์คูลาร์ไดโครอิซึม การทดสอบในเซลล์อาร์เอ็มพีไอ 2650 แสดงให้
เห็นว่าสูตรตำรับที่เป็นอนุภาคไม่สามารถเปิดช่องว่างระหว่างเซลล์ (ไทท์ จังชัน) ได้ แต่จะทำให้
เกิดการนำเข้าสู่เซลล์อย่างมาก สูตรตำรับที่คัดเลือกมาเพื่อศึกษาต่อในสัตว์ไม่มีความเป็นพิษต่อ
เซลล์เพาะเลี้ยง การให้อนุภาคนาโนไคโตซานกับอะลูมิเนียมไฮดรอกไซด์เจล ที่นำส่งแอนติเจน
ไข้หวัดใหญ่จะเหนี่ยวนำให้เกิดการตอบสนองทางภูมิคุ้มกันได้สูงกว่าสูตรตำรับอื่น ๆ ที่ให้ทาง
จมูก การตอบสนองจะไม่แตกต่างจากการให้วัคซีนโดยการฉีดเข้ากล้ามเนื้อ นอกจากนี้ มีเพียง
สูตรตำรับที่คอนจูเกตร่วมกับอะลูมิเนียมไฮดรอกไซด์เจลที่เหนี่ยวนำให้เกิด S-IgA ในหนูทุกตัว
จากสูตรที่ทดสอบทั้งหมด

ภาควิชา วิทยาการเภสัชกรรมและเภสัชอุตสาหกรรม ลายมือชื่อนิสิต..
สาขาวิชา   เภสัชอุตสาหกรรม   ลายมือชื่อ อ.ที่ปรึกษาวิทยานิพนธ์หลัก...................
ปีการศึกษา   2555   ลายมือชื่อ อ.ที่ปรึกษาวิทยานิพนธ์ร่วม ....

5376567833 : MAJOR INDUSTRIAL PHARMACY

KEYWORDS : CHITOSAN / ALUMINIUM HYDROXIDE GEL / NANOPARTICLES / INFLUENZA / VACCINE

ANAWATCH MITPRATAN : CHITOSAN NANOPARTICLES WITH ALUMINIUM HYDROXIDE GEL AS NASAL DELIVERY SYSTEM FOR INFLUENZA VACCINE. ADVISOR : PROF. GARNPIMOL C. RITTHIDEJ, Ph.D., CO-ADVISOR : ASSOC. PROF. VIMOLMAS LIPIPUN, Ph.D., 113 pp.

In this study, the potential delivery system for nasal administration of Influenza vaccine was prepared by ionotropic gelation of chitosan (CS) with sodium tripolyphosphate pentabasic (TPP) and consequent conjugation with aluminium hydroxide gel. The preparation conditions influencing on physicochemical characteristics were evaluated. Bovine serum albumin (BSA) was used as model antigen for the evaluation prior to immunization study. The results demonstrated that the particle size decreased by decreasing of chitosan solution concentration with the optimum weight ratio of chitosan : TPP (3:1). The appropriate pH of chitosan solution at 4.5 resulted in slight decreasing of particle size while increasing the pH caused increasing the particle size and decreasing zeta potential. Moreover, the amount of tween 80 and aluminium hydroxide gel and order of mixing also affected the size. The obtained nanoparticles had spherical structure surrounded by fluffy coating of aluminium hydroxide gel and showed loading efficiency about 52 - 57%. The integrity of entrapped protein was maintained as shown by sodium dodecyl sulphate-polyacrylamide gel electrophoresis and circular dichroism. The testing in RMPI 2650 cells showed that the particulate formulations could not open the tight junctions but dramatically induced cellular uptake. The formulations selected for further studies in animals were relatively non-toxic to the cell culture. Upon i.n. administration, influenza antigen loaded chitosan nanoparticles conjugated with aluminium hydroxide gel induced higher immune response than other i.n. formulations. The i.n. vaccination response was not different from those induced by i.m. vaccination ($p > 0.05$). Moreover, only conjugated formulation could induce S-IgA in all mice among the tested formulations.

Department : __Pharmaceutics and Industrial Pharmacy__ Student's Signature _____

Field of Study : ____Industrial Pharmacy____ Advisor's Signature _____

Academic Year : ____2012____ Co-advisor's Signature _____

ACKNOWLEDGEMENTS

CONTENTS

LIST OF TABLES

LIST OF FIGURES

Figure   **Page**

LIST OF ABBREVIATIONS

%	percentage
A$^{\circ}$	angstrom
ºC	degree Celsius (centigrade)
μg	microgram (s)
μm	micrometer (s)
ACUC	animal care and use committee
APCs	antigen presenting cells
ATCC	american type culture collection
BSA	bovine serum albumin
BBB	blood brain barrier
CD	circular dichroism
cm	centimeter (s)
cm^2	square centimeter (s)
CS	chitosan
CSNP(s)	chitosan nanoparticle (s)
CTL	cytotoxic T lymphocytes
Da	dalton (s)
DC(s)	dendritic cell (s)
DLS	dynamic light scattering
DMSO	dimethyl sulfoxide

ELISA	enzyme-linked immunosorbent assay
EDTA	ethylenediaminetetraacetic acid
et al.	et alli, and other
etc.	et cetera
FACS	fluorescence-assisted cell sorter
FAE	follicle associated epithelium
FD-4	fluorescein isothiocyanate conjugated dextran, molecular weight 4000
FITC-BSA	bovine serum albumin-fluorescein isothiocyanate
FTIR	fourier-transform infrared
GISN	Global Influenza Surveillance Network
HA	hemagglutinin
HBSS	hank's balance salt solution
HIV	human immunodeficiency virus
HRP	horseradish peroxidase
ICR	imprinting control region
i.n.	intranasal
i.m.	intramuscular
IgA	immunoglobulin A
IgG	immunoglobulin G
IgG1	immunoglobulin G1
IgG2a	immunoglobulin G2a

IR	infrared
ISCOM	immune stimulating complex
KBr	potassium bromide
kDa	kilodalton (s)
kg	kilogram (s)
LAIV	live attenuated influenza vaccine
LDV	laser doppler velocimetry
LE	loading efficiency
M-cells	microfold cells
mA	milliampere (s)
MALT	mucosa-associated lymphoid tissue
MCC	mucociliary clearance
MEM	minimum essential medium
mg	milligram (s)
MHC	major histocompatibility complex
min	minute (s)
ml	milliliter (s)
mm	millimeter (s)
mM	millimolar (s)
MPL	monophosphoryl lipid A
MTT	3-(4,5-dimethylthiazol-2-yl)-2,5-diphenyl tetrazolium bromide
MW	molecular weight

N	normal
NA	neuraminidase
NaCl	sodium chloride
NALP3	Nod-like receptor protein 3
NALT	nasal-associated lymphoid tissue
NEP	nuclear export protein
nm	nanometer (s)
No.	number
o/w	oil in water
OD	optical density
PBS	phosphate buffered saline
pDNA	plasmid deoxyribonucleic acid
PMSF	phenylmethylsulfonyl fluoride
rpm	round per minute
S-IgA	secretory immunoglobulin A
SD	standard deviation
SDS-PAGE	sodium dodecyl sulphate-polyacrylamide gel electrophoresis
SEM	scanning electron microscope
TEM	transmission electron microscopy
TEER	trans-epithelial electrical resistance
TEMED	N,N,N',N'-tetramethylethylenediamine

Th cells	T helper cells
TIV	trivalent inactivated influenza vaccine
TMB	3, 3′,5 ,5′-tetramethylbenzidine
TMC	N-trimethyl chitosan
TPP	sodium tripolyphosphate pentabasic
UV	ultraviolet
v/v	volume by volume
w/v	weight by volume

CHAPTER I

INTRODUCTION

Influenza is an infectious disease of many animal species, which birds are thought to be the main animal reservoirs of influenza virus. Influenza virus infections cause considerable morbidity and mortality worldwide each year, particularly in children and elderly people. The WHO publication, 2005, stated that there were about 3 to 5 million yearly cases of severe illness and about 300,000 to 500,000 yearly deaths worldwide (WHO, 2005:online). It imposes a considerable economic burden in the form of hospital and other health care costs and lost productivity. In the United States of America estimated put the cost of influenza epidemics to the economy at US$ 71-167 billion per year (WHO, 2003: online). The antiviral drugs for influenza can effectively prevent and treat the illness for the infection. However, there were some reports about the viral resistance to these medicines (Hsu et al., 2012; Barr et al., 2010; WHO, 2009: online). Therefore, vaccination is an effective method to prevent the influenza infection.

Influenza vaccine was derived from virus-loaded fluid from the influenza virus infected embryonic egg, in egg-based manufacturing. Recently, the cell-based influenza vaccine was approved by US FDA. However, most of influenza vaccines are used as parenteral administration in the inactivated form. Only one live attenuated influenza vaccine (LAIV) is nasal-spray flu vaccine. The inactivated influenza vaccine is safer but induces lower level of immune response in parental route. Therefore, new vaccine delivery systems or adjuvants are needed to elicit better immune responses.

Nasal route is very attractive as a suitable method for vaccination or systemic drug delivery (Ugwoke, Verbeke and Kinget, 2001). It is easy to use, needle-free, painless and usually well accepted by patients. Moreover, nasal route can avoid hepatic first-pass metabolism. The nasal vaccination can induce strong systemic and mucosal immune responses (Kyd et al., 2001), because the mucosa surfaces are the first line of defense against the infection, this makes the nasal route an ideal for vaccination. Even nasal vaccination has diverse advantages, this mucosal vaccination

has important limitations; rapid mucociliary clearance and low permeability of macromolecule formulations (Arora, Sharma and Garg, 2002). Therefore, novel delivery system and effective adjuvant are needed to facilitate the permeation of antigens through nasal mucosa and to potentiate the immunogenicity.

Chitosan, a mucoadhesive polymer, is the most widely used natural polymer for mucosal vaccine delivery. It is an interesting biopolymer because of its nontoxicity, polycationic, biocompatible and biodegradable properties. Chitosan nanoparticles have studied widely as potential application in nasal drug delivery systems (Krauland et al., 2006; Kang et al., 2007; Jiang et al., 2008) because they can be used to control release of drugs, improve the bioavailability of substances and enhance membrane permeability. The other important property is to increase the residence time of vaccines at the mucosal surface compared to solutions. The microspheres can enhance the mucoadhesive property and help to prolong residence time and improve uptake of vaccines incorporated with them (Chowdary and Rao, 2004). Several studies try to enhance their bioavailability and membrane permeability or improve their sustained drug release properties by chemical modification (Krauland et al., 2006; Mokarram and Alonso, 2006; Lim et al., 2001; Kang et al., 2007) or by coating with other polymer (Borges et al, 2008). Moreover, to improve efficacy of vaccine, targeting the antigens in the mannose receptor onto antigen-presenting cells by the mannosylation of chitosan nanoparticles was studied (Jiang et al., 2008). The application of chitosan nanoparticles together with other adjuvant is very interesting. It has been reported that the application of chitosan nanoparticles together with the potent mucosal adjuvant, LTK63, enhanced the efficacy of nasal vaccines through their synergistic effect (Baudner, 2003). Aluminium hydroxide, licensed adjuvant in USA and Europe, has been widely used as human adjuvant in many vaccines for more than 80 years, which is considered as safe and effective adjuvant. Thus the concomitant application of chitosan nanoparticles and aluminium hydroxide gel may results the good immunostimulating property and can induce high level of humoral and mucosal immune response.

The objectives of this study were:

1. To study the effects of various preparation conditions on particle size and surface charge of the resulted chitosan nanoparticles to get the suitable size for nasal delivery.

2. To develop bovine serum albumin (BSA), as model antigen, loaded chitosan nanoparticles conjugated with aluminium hydroxide gel as nasal vaccine delivery system and evaluate their physicochemical properties, mucoadhesive property, cellular uptake and permeability through nasal cell line.

3. To evaluate the immunostimulating effect of the influenza antigen loaded chitosan nanoparticles conjugated with aluminium hydroxide gel in mice on humoral and mucosal immune responses.

CHAPTER II

LITERATURE REVIEW

Influenza

Influenza virus infection is one of major health and economic burdens worldwide. It spreads around the world in seasonal epidemics, resulting in about 3 to 5 million yearly cases of severe illness and about 300,000 to 500,000 yearly deaths (WHO, 2005: online). Among the 90 million influenza cases in the younger 5-years-old children in 2008, approximately 28,000 to 111,500 children died of lower respiratory tract infection (Nair et al., 2011). The influenza still spread around the world via movement of infected individuals and the updated situation is shown in figure 2-1.
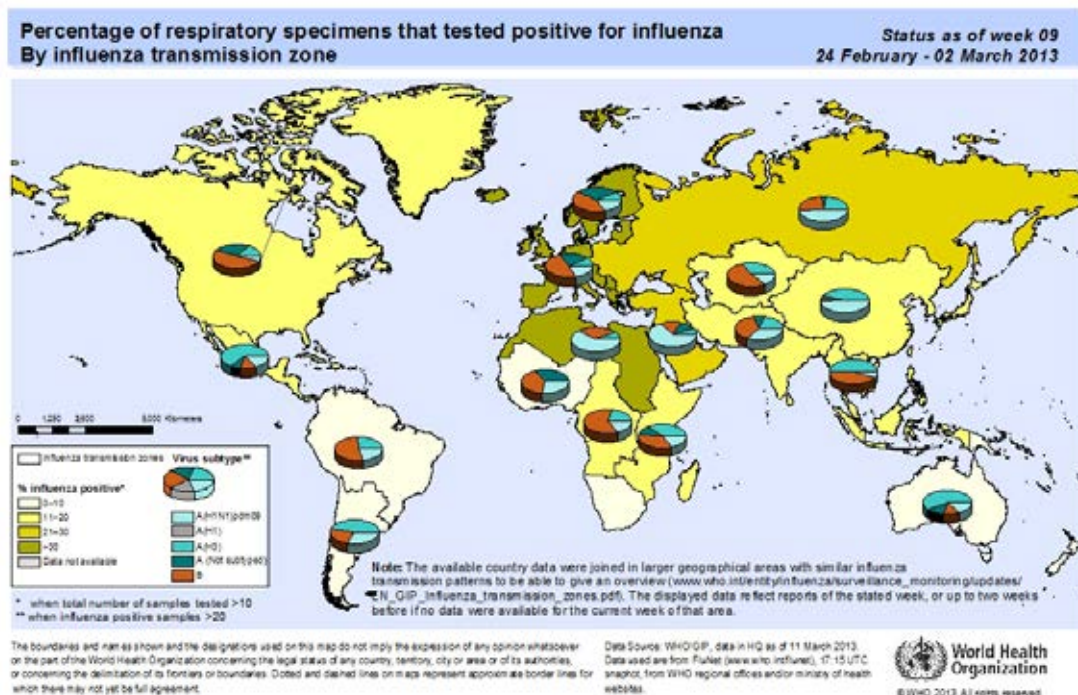
Figure 2-1 Percentage of respiratory specimens that test positive for influenza by influenza transmission zone (WHO, 2013: online)

Yearly, influenza epidemics can seriously affect all age groups, but the highest risk of complications occurs among children younger than age two, adults age 65 years or older, and people of any age with certain medical conditions, such as chronic heart, lung, kidney, liver, blood or metabolic diseases (such as diabetes), or weakened immune systems. Typically, influenza is transmitted through the air by coughing or sneezing which creates aerosols containing the virus. Influenza can also be transmitted by direct contact with contaminated surfaces.

The common symptoms of influenza infection are fever, chills, sore throat, headache, muscle pains, coughing and weakness/fatigue. Influenza infection can sometimes lead to pneumonia, either direct viral pneumonia or secondary bacterial pneumonia (Jain et al., 2009). Each year, the emergence of influenza viruses is different, and the infection can affect people differently. Even healthy people can get very sick and spread it to others. Especially, the children younger than 2 years, adults age 65 years or older, and people with certain medical conditions, which are at high risk of developing serious complications (WHO, 2009: online).

Influenza virus

The influenza viruses are RNA viruses which are in *Orthomyxoviridae* family. The virus particle is 80–120 nanometers in diameter and usually roughly spherical objects or long spaghetti like filaments (Fujiyoshi et al., 1994). The viral envelope consists of a lipid bilayer with three transmembrane proteins; HA (hemagglutinin), NA (neuraminidase) and M2 (ion channel) on the outside and M1 (matrix protein) underneath the membrane. The influenza virus lipid bilayer is a mosaic structure which contains both cholesterol-enriched lipid rafts and nonraft lipids derived from the host plasma membrane (Scheiffele et al., 1999; Zhang et al., 2000). The glycoproteins, HA and NA, are anchored in the lipid raft domain of the viral envelope, while M2 is not tightly associated with lipid rafts (Schroeder et al., 2005). HA is the major envelope protein (~80%) and cleavage of HA into HA1 and HA2 is critical for virus infectivity. NA is the second most (~17%) envelope protein. NA removes the cell surface receptor; sialic acid, and plays an important role in the release of progeny virus from infected cells as well as the spread and transmission of virus from host to host. The third envelope protein, M2 (~16–20 molecules/virion) is

functions as an ion channel (Lear, 2003) which plays a critical role in the early phase of infection leading to the uncoating and release of the viral ribonucleoprotein (vRNPs) from M1 matrix. The central core consists of helical vRNPs containing negative stranded viral ribonucleic acid (vRNAs) and nucleocapsid protein (NP) along with nuclear export protein (NEP) and three polymerase (3P) proteins (PB1, PB2, PA) forming the viral RNA polymerase complex.
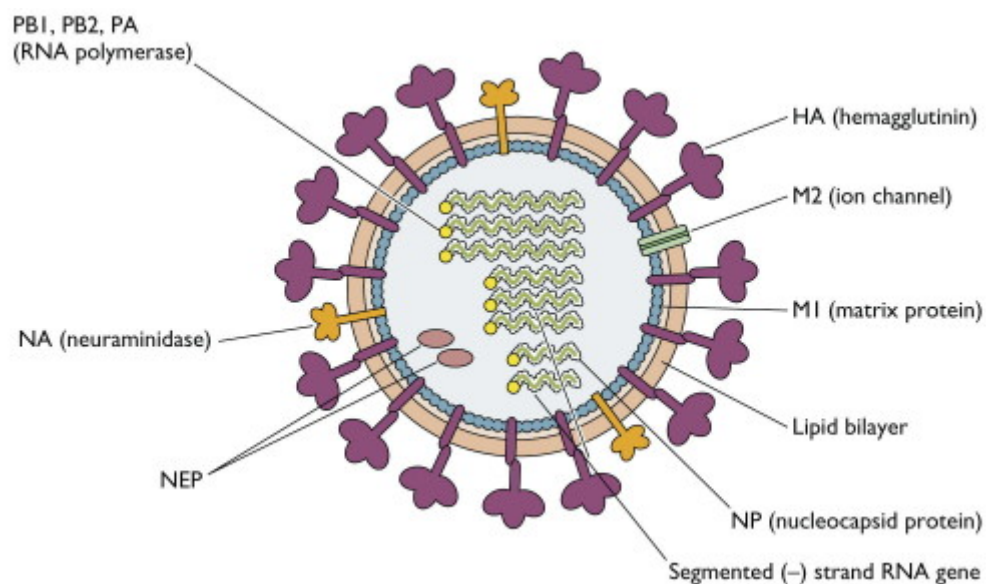
Figure 2-2 Structure of influenza virus. (Virology, 2009: online)

The influenza viruses are classified into 3 types, A, B and C. Type A influenza viruses are further subtyped according to different kinds and combinations of virus surface glycoproteins, HA and NA. 16 HA and 9 NA subtypes have been identified in the wild bird, and various combinations of HA and NA can occur. Among many subtypes of influenza A viruses, currently influenza A, H1N1 and H3N2 subtypes are circulating among humans. The type C influenza cases found much less than type A and B. Therefore, the seasonal influenza vaccines are composed of only influenza A and B viruses. (Karlsson Hedestam et al., 2008; WHO, 2009: online)

Influenza virus infection

When the influenza virus gets into the respiratory tract, it binds to the surface of cells. Then, the virus opens and releases its genetic information, vRNA, into the cell's nucleus which contain the cell's genetic information, DNA and RNA. The virus then replicates and takes over the functions of the cell. The copies of the virus move to the cell membrane and wait until the cell finally dies and releases them out into the body and go on to infect other cells. Because of movement of the virus through the respiratory tract and into the bloodstream, the respiratory tissues swell up and become inflamed as the first symptoms of infection. The viral replication process continues for several days, until the body's immune system responses to the infection and fights the virus off.
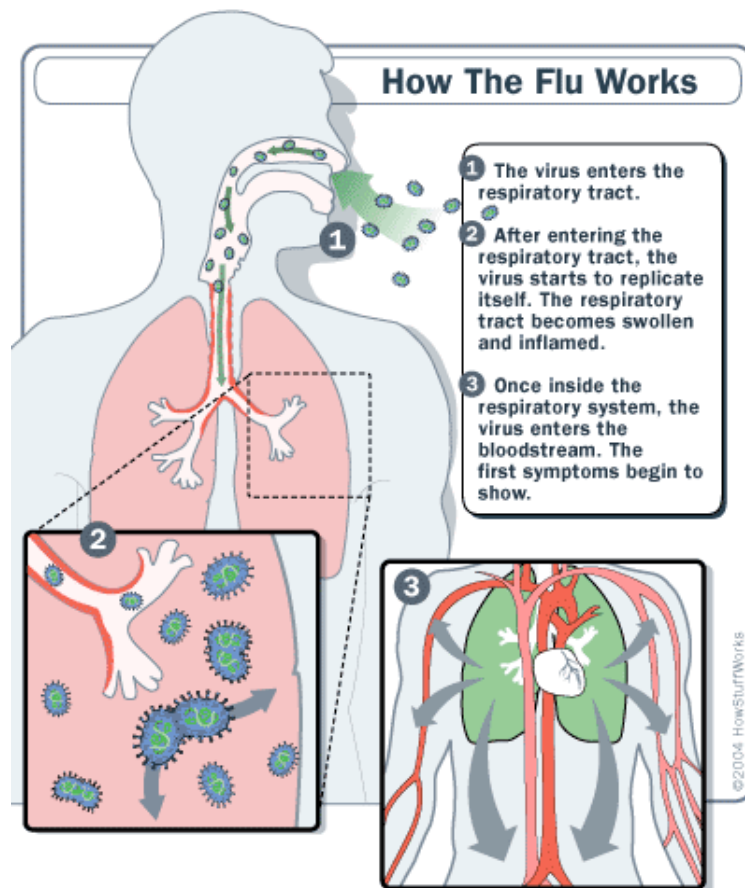
Figure 2-3 The infection process of influenza virus. (Watson, 2004: online)

Treatment of influenza

The antiviral drugs for influenza can effectively prevent and treat the illness by reduce signs and symptoms and also prevent the death in patients with severe disease. However, they are available only in some countries. There are two classes of the medicines, the first is the adamantanes, M2 ion channel inhibitors, such as amantadine and rimantadine and the other class is the neuraminidase inhibitors, such as oseltamivir and zanamavir. The adamantanes group is used only for influenza A viruses while the neuraminidase inhibitors group is used for both influenza A and B. In recent years, the influenza viruses that are resistant to adamantanes have emerged and oseltamivir resistance has also appeared in the A (H1N1) subtype (Hsu et al., 2012; Barr et al., 2010; WHO, 2009: online).

Influenza vaccination

Prophylactic vaccination is an effective method to prevent the infection. The annual seasonal flu vaccine is the best way to reduce the chances to be infected with seasonal flu and lessen the chance to spread it to others. However, the Influenza vaccination will be most effective when circulating viruses are well-matched with vaccine viruses. Moreover, the seasonal influenza viruses efficiently escape from acquired immunity in the human population through antigenic drift. As a result, a new influenza vaccine must be produced every year to match the predicted predominant circulating strains of the next season. The WHO Global Influenza Surveillance Network (GISN), a partnership of National Influenza Centers around the world, is responsible for monitor the influenza viruses circulating in humans and annually recommends the antigenic variants that will be included in the coming year's vaccine. The current seasonal influenza vaccine is a trivalent vaccine that consists of two subtypes of influenza A virus (H1N1 and H3N2) and one influenza B virus.

There are two types of influenza vaccines.

1. Injectable vaccines or called "flu shot"

An inactivated vaccine composed of 3 strains of influenza virus or also called "Trivalent inactivated influenza virus vaccine" (TIV). It is given with a needle. The flu shot is approved for use in people older than 6

months, including healthy people and people with chronic medical conditions. There are three different flu shots available:

- Regular flu shot approved for people ages 6 months and older, for example; Agriflu®, Fluarix® and Fluvirin®
- High-dose flu shot approved for people 65 years and older, for example; Fluzone® High-Dose
- Intradermal flu shot approved for people 18 to 64 years of age, for example; Fluzone® Intradermal

2. Intranasal vaccine

The nasal-spray flu vaccine made with live, weakened flu viruses. It is also called LAIV for "Live Attenuated Influenza Vaccine". The viruses in the nasal spray vaccine do not cause the flu. LAIV is approved for use in healthy people, 2 through 49 years of age who are not pregnant and do not have certain health conditions. The trade name of LAIV is FluMist®.

Until recently, almost all influenza vaccines available are TIV. The inactivated influenza virus vaccines cannot cause influenza and causes few side effects, including fever and reactions at the injection site. Only one live, attenuated, cold adapted, temperature sensitive, trivalent influenza virus vaccine or LAIV was licensed in the United States since 2003. This intranasally administered vaccine is based on virus that is adapted to replicate efficiently only at 25°C in the nasal passages, but does not replicate at the high temperatures that occur deeper in the lower respiratory tract (Abramson, 1999). The LAIV induces a higher level of protection than the TIV (Mendelman et al., 2001), possibly because the replicating viruses express the antigens for longer time and also stimulate T-cell responses that contribute to the protection. However, the LAIV has more limitations than TIV, such as; it cannot give to the asthma or immunocompromised patients (Kelso, 2012). Moreover, the attenuated viruses in the vaccine could mutate and regain the ability to cause the disease.

Anatomy and physiology of nasal cavity

The nasal passage is the first part of the respiratory tract where the respiratory airflow begins. Therefore, nasal functions are warming, moisturizing and filtering the air before it reaches the lungs. The total surface area of nasal cavity in the human adult is about 150 cm^2 (Illum, 2007). The cavity is divided by the nasal septum into two halves and posteriorly extends to the nasopharynx, while the nasal vestibule, the most anterior part of the nasal cavity, opens to the face through the nostril (Fig. 2-4). The nasal cavities are subdivided into three regions, the nasal vestibule and atrium, the respiratory region, and the olfactory region. It also contains the nasal associated lymphoid tissue (NALT) which is situated in the nasopharynx.
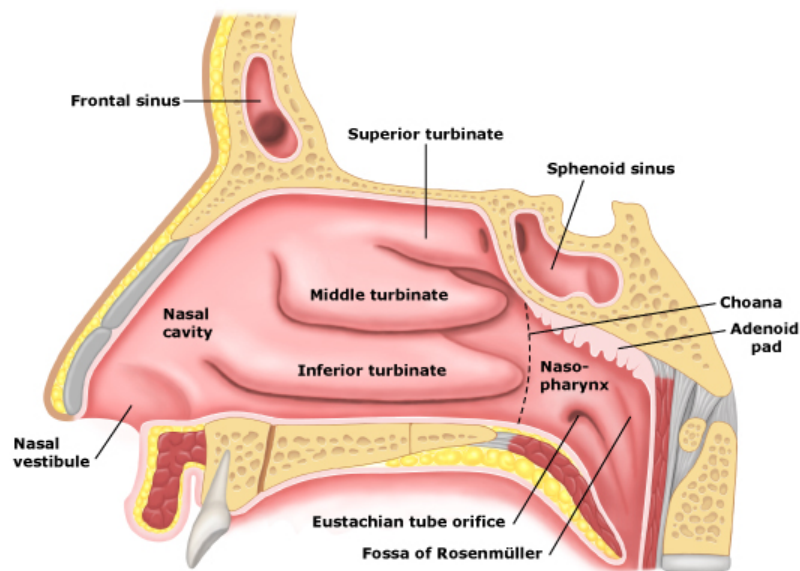
Figure 2-4 Anatomy of nasal cavity. (Neck Pain Blog, 2011: online)

The respiratory region is the major part of the nasal cavity which composes of the nasal conchae or turbinates. The nasal turbinates are shelf-like structures, divided into 3 sections: the superior, middle and inferior nasal turbinates. These shelf-like structures provide the nasal cavity with a very high surface area (Dahl and Mygind, 1998). Moreover, with the vascularized epithelium, these provide the respiratory region with high permeability, which is related to nasal drug delivery (Arora et al.,

2002). The main part of nasal tissue is covered by pseudostratified columnar epithelium which interspersed with goblet cells, seromucus ducts and the openings of subepithelial seromucus glands. This cell layer composes mostly of ciliated and nonciliated columnar cells and also goblet cells and basal cells (Figure 2-5) (Ugwoke et al., 2001). The ciliated cell contains approximately 100 cilia and both ciliated and nonciliated cells possess approximately 300 microvilli each. The basal cells, act as stem cells, are differentiated to replace other epithelium cells.
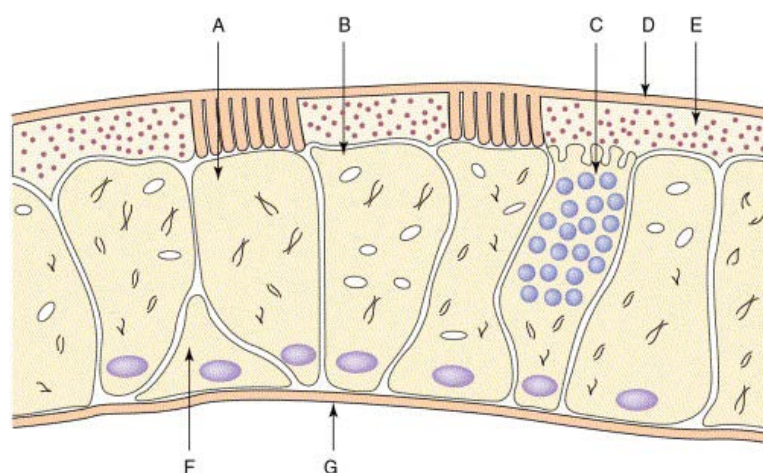
Figure 2-5 Cell types of the nasal epithelium showing ciliated cells (A), non-ciliated cells (B), goblet cells (C), gel mucus layer (D), sol layer (E), basal cells (F) and basement membrane (G). (Ugwoke et al., 2001)

The olfactory region constitutes only about 5% of the total area of nasal cavity in human. However, it is very interesting in drug delivery because it provides a direct pathway from this area in nasal cavity to the brain (Illum, 2004). The olfactory epithelium comprises of sustentacular cells supporting by ensheathing neuronal receptor cells and basal cells that can differentiate into neuronal receptor cells.

Altogether, the epithelium and lamina propria are called respiratory mucus membrane or respiratory mucosa (Burkitt, Young and Heath, 1993). The respiratory mucosa is the region where drug absorption is optimal. A thin sheet of mucus produced from the seromucus glands and goblet cells covers the nasal turbinates and the atrium (Ugwoke et al., 2001). Nasal mucus is mainly released by the goblet cells

as mucus granule and swells in the nasal fluids to conduce to mucus layer. Mucus secretion is a complex mixture of many substances and composes of approximately 95% water, 2% mucin, 1% salts, 1% other proteins and 1% lipids (Kaliner et al., 1984). Mucin is a high molecular mass glycoprotein (2,000-4,000 kDa) crosslinked with disulphide bridges, ionic bonds and physical entanglements. The carbohydrate side groups attach to the protein backbone including with galactose, L-fucose, *N*-acetylglucosamine, *N*-acetylgalactosamine and *N*-acetylneuraminic acid (sialic acid). The carbohydrate side chains terminate with an L-fucose group or sialic acid make mucin an anionic polyelectrolyte at neutral pH. Because of the multiplicity of hydroxyl groups of the carbohydrate side chains, mucin forms hydrogen bonds with suitable polymers easily (Kamath and Park, 1994). About 1.5–2 litres of nasal mucus is produced daily. This mucous layer, about 5 μm thick, covers the epithelial cells with two layers of an upper viscous layer and a lower sol layer with low viscosity where the cilia move. The viscosity of both layers affects the beating of cilia and the efficiency of mucus transport, the mucociliary clearance. When materials adhere to the mucus layer in the nasal cavity, the cilia beat and move mucous layer, the materials then transported towards the nasopharynx and discharge into the throat with a half time of clearance of 15–20 minutes and the mucous layer is continuously renewed (Illum, 2007).

Figure 2-6 Micrograph showing a cell junction in epithelial cells with the tight junction area enlarged in the insert. (Illum, 2007)

Nasal epithelial cells are interconnected on the apical side of the membrane by narrow beltlike structures that totally surround the cells as the junctional complexes. These complexes compose of zona occludens, zona adherens and macula adherens and form a dynamic regulatable semi-permeable diffusion barrier between the epithelial cells (Madara, 2000). The zona occludens is also called as the tight junction (Figure 2-6). Normally, the diameter of the tight junctions of the nasal epithelium is considered to be 3.9–8.4 A° (Hayashi et al., 1985). Absorption enhancers can induce the opening of tight junctions, but it is seem be able to increase the diameter not more than 10-15 times the normal diameter.

Intranasal drug delivery

Intranasal (i.n.) administration offers many advantages for the local and systemic delivery of therapeutic compounds. The intranasal delivery is needle-free, non-invasive, painless and can be self intranasal administration. The large surface area of the nasal mucosa presents a large number of microvilli, a porous endothelial membrane, and a highly vascularized epithelium serves a rapid onset of therapeutic effect. Moreover, it has a potential for target drugs across the blood-brain barrier (BBB), directed to central nervous system, and no hepatic first-pass metabolism (Ugwoke et al., 2001). The good results in intranasal administration were obtained with small organic molecules, which led to the successful development of many products currently on the market (Behl et al., 1998).

In the immunological perspectives, these mucosal surfaces are the first line of defense against the infection. Therefore, the mucosal route is ideal for vaccination. In addition, the nasal cavity shows relatively low enzymatic activity (Sarkar, 1992), which the vaccine can avoid from enzymatic degradation in the nasal cavity and will allow smaller doses. The nasal tissue has a high density of APCs, dendritic cells, which can induce strong systemic and mucosal immune responses (Kyd et al., 2001). Especially, the adaptive humoral immune prevents the entry of pathogens across the mucosal surfaces by secretory IgA (s-IgA) antibodies (Neutra and Kozlowski, 2006).

Although intranasal administration has diverse advantages, it also has several limitations. One of the most important limitations is the short residence time within the nasal cavity due to the rapid mucociliary clearance and also the low permeability of the macromolecule formulations which play significant roles in obstructing nasal delivery (Arora et al., 2002).

Therefore, the development of novel nasal vaccines depends on the improvement of the vaccine delivery system. Increasing the residence time of vaccines in the nasal passages can prolong the time of their contact with the nasal mucosa, including with enhancing of vaccine permeation, consequently improving their efficacy.

Permeation of the mucous membrane

The transportation of substrate across the mucous membrane to the inner cell layers or bloodstream starts from diffusion of the substances through mucus or unstirred water layer to the apical membrane, then transport across the epithelial cells. The transportations are mainly classified into two pathways.

1. Transcellular pathway

The transcellular pathway involves the transportation of substrate across the apical cell membrane surface into the intracellular space and across the basolateral membrane to the blood stream or extracellular fluid. The transcellular transportation includes transcellular diffusion, active carrier mediated transportation, and transcytosis. The transcellular diffusion generally involves the movement of solutes based on a diffusion gradient moving from high concentration area to low concentration area. However, the cell membrane is a hydrophobic environment and does not allow the passive diffusion of charged, hydrophilic or zwitterion molecules. Active transport involves the usage of energy to transport specific substrates across barriers, even against the concentration gradient. Macromolecules can sometimes be transported through transcytosis or endocytosis.

2. Paracellular pathway

The paracellular pathway involves transportation of substances across an epithelium by passing through the intercellular space or across the tight junction between the cells. It is contrast to transcellular transport, where the substances pass

through the cell, passing through both the apical membrane and basolateral membrane and more likely to involve energy comsumption than paracellular transport.

The transcellular and paracellular pathways are all important for the absorption of drugs within the nasal cavity. The paracellular pathway allows the permeation of hydrophilic molecules which cannot permeate through the lipid membrane for the transcellular pathway of absorption. However, it is only possible for small molecules, but larger molecules cannot pass through the pores in the tight junctions. The tight junctions have negative charge and believed to preferentially transport positively-charged molecules. The most of drug molecules are transported through the transcellular pathway, only the few rely on the paracellular pathway typically have much lower bioavilability.

Paracellular transportation can be enhanced by removing the zona occludens proteins from the junctional complex by permeation enhancers, such as; medium chain fatty acids, chitosan, zona occludens toxin, etc.
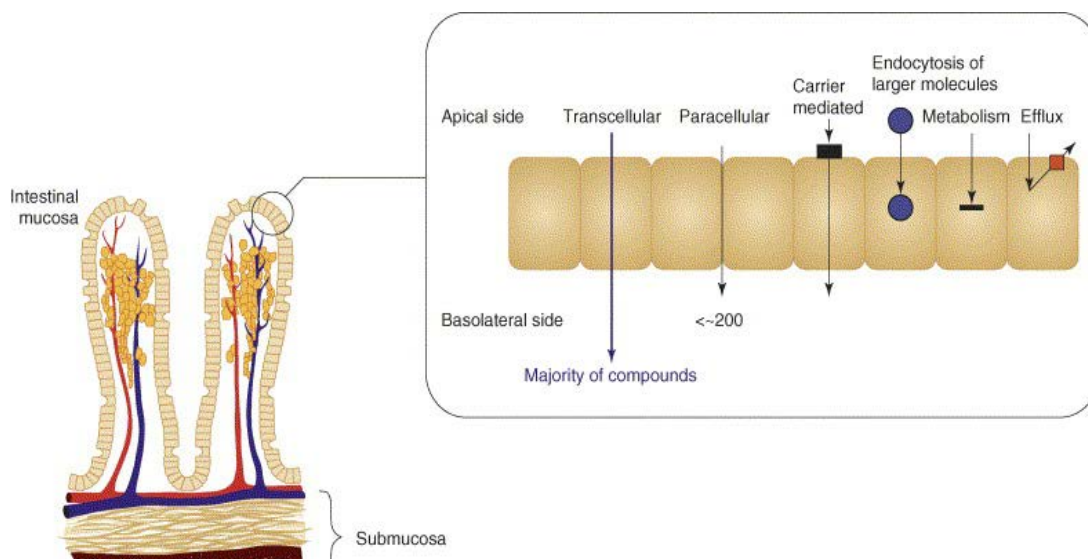
Figure 2-7 Transportation of substrates through mucous membrane. (Hamalainen and Frostell-Karlsson, 2004)

Mucosal immune system

The mucosal immune system is divided into two parts which are inductive and effector sites (Figure 2-8). Inductive sites are the areas where antigen sampling leads to initiation of immune cells activation, while effector sites are the areas where antibodies and cells of the immune system perform their specific function upon activation (Cesta, 2006). In the mucosal immune system, the inductive sites consist of region specific lymphoid tissues, which called as mucosa-associated lymphoid tissue (MALT), and also the surrounding lymph nodes. The inductive sites are composed of B-cell follicles which contain various other immune cells, including antigen presenting cells and T lymphocytes (Brandtzaeg et al., 2008). The follicles can be found singularly or in clusters, such as in Peyer's patch regions in small intestines (Clark, Jepson and Hirst, 2001).
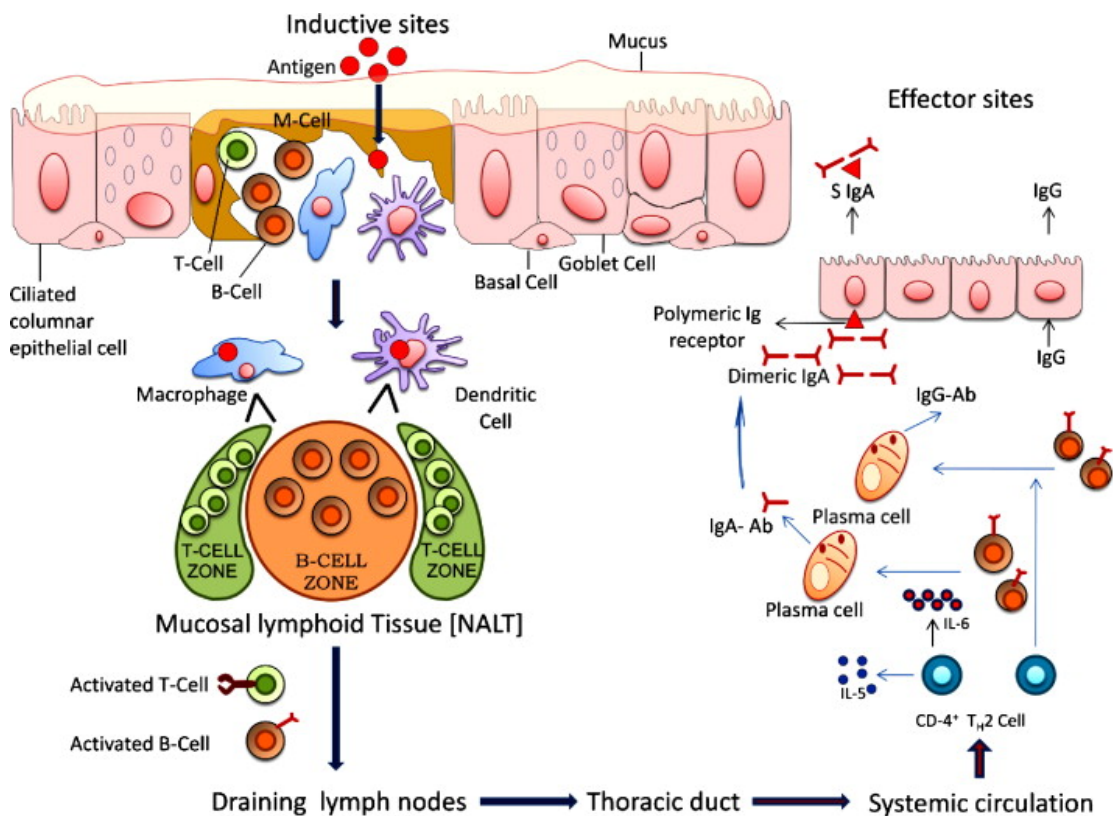
Figure 2-8 The common mucosal immune system. (Gupta et al., 2011)

In nasal cavity, the MALT is called NALT or nasal-associated lymphoid tissue, which also composes of organized lymphoid aggregates and covered with a particular overlying epithelium (Debertin et al., 2003). The organized lymphoid tissues are located in the human nasopharynx and oropharynx, incorporating the lingual, palatine and nasopharyngeal tonsils (adenoids). This assembly of lymphoid tissues is named as Waldeyer's ring which plays an important role in respiratory immune defense (Goeringer and Vidic, 1987). Actually, most particles are trapped in the mucus layer and carried to this region by the mucociliar clearance mechanism (Dahl and Mygind, 1998).

The NALT has many kinds of immunocompetent cells, including subepithelial B-lymphocytes, CD4+ and CD8+ T-lymphocytes and APCs such as macrophages and dendritic cells (DCs) (Bienenstock and McDermott, 2005). Moreover, the overlying epithelium forms a follicle associated epithelium (FAE) that allows transfer of antigenic materials from the mucosa into the lymphoid follicles which enables the contact between antigens and immune cells (Clark, Jepson and Hirst, 2001). In addition, the FAE also incorporates microfold cells (M cells) to forms an intraepithelial pocket which contains lymphocytes and some phagocytic cells (Neutra, 1999). The M cells can efficiently transport a variety of materials by transcellular vesicular transport to the underlying intraepithelial cells. It was reported that the particulates, compared to soluble antigens, could be preferentially taken up by M cells following nasal administration (Illum, 2007).

After contact with pathogens, the APCs can stimulate local adaptive immune responses by presenting the antigen to lymphocytes through the major histocompatibility complex (MHC). Furthermore, dendritic cells can also migrate and carry the antigens to nearby draining lymph nodes and circulate immune responses to distant sites of the body, result in the production of serum IgA and serum IgG antibodies (Iwasaki, 2007). The adaptive immune responses comprise of cellular and humoral immune responses against the pathogens. Cellular immune response comprises of cytotoxic T lymphocytes (CTL) and antibody dependent cell-mediated cytotoxicity through natural killer cells, which can directly destroy specific cells that crucial for the clearance of viruses and intracellular parasites (Neutra and Kozlowski, 2006; Storni et al., 2005). The humoral immune response at mucosal surface is the

production of immunoglobulin A (IgA) following activation of B cells. Dimeric IgA is found in mucosal secretions in human, which so-called secretory IgA. It plays an important role to inhibit invasion and colonization of pathogens, together with the innate immune system (Neutra and Kozlowski, 2006).

Chitosan nanoparticles

Chitosan

Chitosan is a natural linear biopolyaminosaccharide, copolymers of glucosamine and N-acetylglucosamine (Kato, Onishi, and Machida, 2003). It can be derived by the partial deacetylation of chitin, the major component of protective cuticles of crustaceans such as crabs, shrimps, prawns, and lobsters. One molecular unit of chitosan comprises of one amino group and two hydroxyl groups which are potentially reacting with acidic medium. The amino group in chitosan has a pKa value approximately of 6.5, this make chitosan has positively charged and is soluble in an acidic solution. An amino group in chitosan can chemically react with anionic systems, resulting in the modification of the physicochemical characteristics (Illum, 1998). Moreover, the free amino group in chitosan is able to reacts with negatively charged polymers.

Chitosan is one of the most interesting polymers because of its properties, such as nontoxicity, polycationic, biocompatible and biodegradable nature, and especially its mucoadhesive and permeation-enhancing properties. The strong mucoadhesive property is most important for drug delivery through the mucosal delivery. In addition, the interaction of the positive charge of chitosan with the negative charge of mucin layer and the tight junctions enhances the paracellular transport of hydrophilic macromolecules through the mucosal barriers by opening the tight junctions (Borchard et al., 1996; Dodane, Khan and Merwin, 1999). The strong mucoadhesive properties of chitosan reflex its potential of permeation enhancer for mucosal drug delivery. The reasons of the permeation enhancing effect of chitosan have been reported as the combination of improved mucoadhesion of the formulation and the nasal tissues and the transient effect of chitosan on the paracellular transport (Dodane et al., 1999).
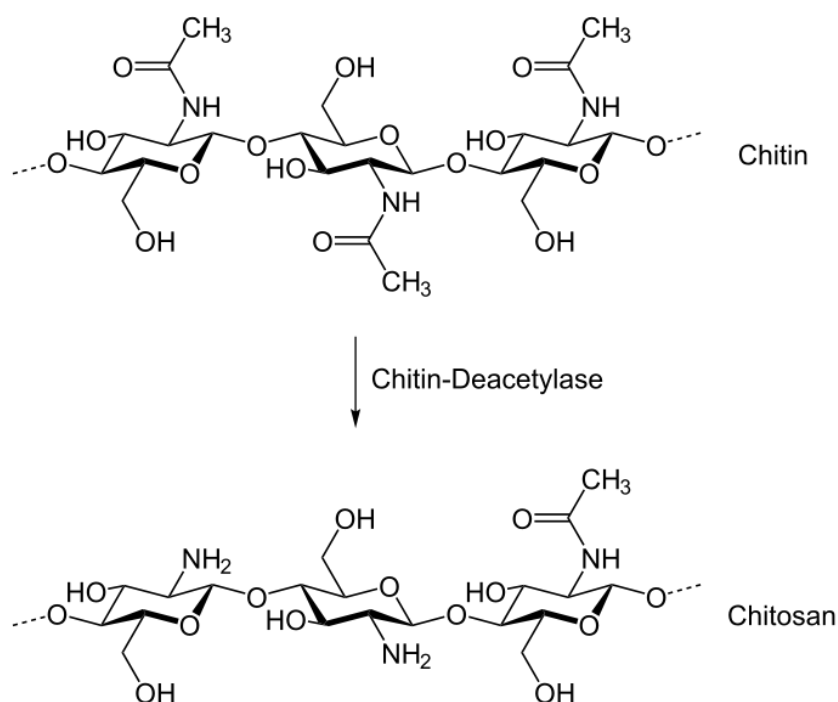
Figure 2-9 Chemical structures of chitin and chitosan (Center for Chitin - Chitosan Biomaterials, 2009: online).

The efficacy of chitosan as an adjuvant and delivery system for mucosal vaccines has been reported. The bordetella pertusis filamentous haemagglutinin and recombinant pertusis toxins were able to induce strong systemic and mucosal immune responses after intranasal administration with chitosan (Jabbal-Gill et al., 1998). Diphtheria toxin induced systemic and local immune responses after nasally co-administrated with chitosan (McNeela et al., 2000). Moreover, the chitosan-diphtheria intranasally vaccination in primed animals was shown to induce a mixed Th1/Th2 response, that showed the induction of both humoral and cellular immune responses (Illum et al., 2001). The mucociliary clearance rate can be decreased by the use of mucoadhesive polymers. There are many studies showed that chitosan can prolong the residence time of nasally delivered drugs at the absorption site (Soane et al., 2001).

Chitosan microspheres

Particulate carrier technology are used in offers vaccine delivery systems by the introduction of vaccines to the carriers such as nano/microspheres, emulsions, liposomes, virosomes, immune stimulating complex (ISCOM), virus like particles (VLPs), etc. Microspheres of the particulate vaccine delivery systems have several useful attributes to stimulate host immune system.

The most useful property of microspheres, as vaccine delivery systems, is to offer an optimum particle size for delivery into the body and also uptake by APCs. The appropriate particle size can induce internalization by APCs, and then easily transport the vaccine formulations across the cell membrane (Desai et al., 1997). The other important property is to increase the residence time of vaccines at the mucosal surface compared to solutions. The microspheres can enhance the mucoadhesive property and offer additional advantages which help to prolong residence time and improve uptake of vaccines incorporated with them (Chowdary and Rao, 2004). Chitosan, a mucoadhesive polymer, is the most widely used natural polymer for mucosal vaccine delivery. The chitosan microspheres as a delivery system were evaluated in several researches. The oral vaccination in fish with a plasmid DNA (pDNA) containing major capsid protein gene of lymphocystis disease virus encapsulated in chitosan microspheres showed significantly enhanced systemic immune responses, comparison with fish vaccinated with naked pDNA (Tian et al., 2008). The chitosan encapsulated tetanus toxoid microparticles induced antigen specific IgA in intestinal lavage, faeces, intestinal washings and elicited strong antigen specific IgG in blood circulation after oral immunization (Ahire et al., 2007).

Chitosan nanoparticles for nasal delivery of vaccines

Chitosan nanoparticles have a potential for application in drug delivery systems because they can be used to control the release of drugs and to improve the bioavailability of degradable substances or to enhance membrane permeability. There are many studies on the chitosan nanoparticles as a nasal drug delivery system in a variety of drugs, such as proteins, peptides, and vaccines (Alpar et al., 2005; Gavini et al., 2006; Kang et al., 2006; van der Lubben et al., 2003; Varshosaz, Sadrai and

Alinagari, 2004). Several studies try to enhance their bioavailability and membrane permeability or improve their sustained drug release properties by chemical modification through the thiolation of chitosan 2-iminothilane (Krauland, Guggi and Bernkop-Schnurch, 2006) or PEGylation of chitosan (Mokarram and Alonso, 2006) and through their composition with hyaluronan (Lim et al., 2001) or pluronic F127® (Kang et al., 2007) and by coating with sodium alginate (Borges et al., 2008) and even through the formation with low molecular weight chitosan (Vila et al., 2004) or N-Trimethyl chitosan (TMC) (Amidi et al., 2007). The other strategy to improve efficacy of vaccine is to target the antigens in the mannose receptor onto APCs by the mannosylation of chitosan nanoparticles (Jiang et al., 2008). The application of chitosan nanoparticles together with the potent mucosal adjuvant, LTK63, is an effective method to enhance the efficacy of nasal vaccines through their synergistic effect (Baudner et al., 2003).

Licensed vaccine adjuvants

While the developments of prophylactic vaccine are continuously progressive, another challenge is to improve the effectiveness of vaccines. Subunit vaccines are normally safer than inactivated or live-attenuated vaccines but they usually have less immunogenicity and often require the additional adjuvant to achieve protective immunity. The development of new adjuvants is necessary because only few adjuvants have been licensed for prophylatic vaccine in human now a day. Among these few adjuvants, aluminium salts have been widely used for more than 80 years and still recently be the only adjuvant approved in the USA. MF59® and AS03, oil in water emulsions, are licensed adjuvants for influenza vaccines in Europe. Moreover, a combination adjuvant composed of monophosphoryl lipid A (MPL) adsorbed to aluminium salts, called as AS04, was approved for adjuvanted human papilloma-viruses (HPV) and hepatitis B virus (HBV) vaccines in Europe and also has been recently licensed in the USA. The licensed vaccine adjuvants are all described in table 2-1.

Table 2-1 Licensed adjuvants. (adapted from O'Hagan and De Gregorio, 2009)

Name	Company	Class	Indications
Alum	Various	Mineral salts	Various
MF59	Novartis	O/W emulsion	Influenza (Fluad) / pandemic flu
AS03	GSK	O/W emulsion + a tocopherol	Pandemic Flu (Pandemrix)
AS04	GSK	MPL + alum	HBV (Fendrix), HPV (Cervarix)
Liposomes	Crucell	O/W emulsion	HAV, Flu (EU)

The adjuvant for nasal vaccine is still in the clinical trial stage. LTK63 or non-toxic mutants of heat labile *Escherichia coli* enterotoxin (LT) are known as a potent mucosal adjuvant. It was conducted in the clinical trial phase I with tuberculosis nasal subunit vaccine and intranasal trivalent inactivated influenza vaccine (Stephenson et al., 2006).

In this study, the synergistic effect of chitosan nanoparticles with other adjuvants is attractive. Among these licensed adjuvants, aluminium hydroxide gel is interesting to combine with the chitosan nanoparticles. It is the most commonly used in human vaccination in many kind of vaccine and considered as effective and safe adjuvant.

Aluminium hydroxide gel

Aluminium compounds have been widely used as human vaccine adjuvants for more than 80 years. Even there are many different aluminium compositions, aluminium hydroxide and aluminium phosphate are the most commonly used adjuvants at present (Lindblad, 2004). It was found in numerous vaccines, including hepatitis, diphtheria-tetanus-pertussis and human papillomavirus vaccine.

The immuno-stimulating and immuno-modulating effects of aluminium compounds arise from several mechanisms. The basic effect is the absorption of the antigen by electrostatic and hydrophobic attraction, and ligand exchange as the major

force (Iyer et al., 2004). Therefore, the complexed antigen is cleared slowly from the injection site by building a depot and lets the antigen released very slowly (Gupta et al., 1995). The high local concentration of the antigen sequentially stimulates the uptake by APCs (HogenEsch, 2002). Moreover, the absorption to aluminium compound potentiates the immune response by direct stimulation of immune cells. For example, macrophages are directly activated by the foreign particulate character of the aluminium hydroxide and thereby adapt to a mature dendritic cell-like phenotype with an improved ability to present the concomitantly applied antigen to Th cells (Rimaniol et al., 2004). The direct stimulation of macrophages may depend on the intracellular innate immune response system called NALP3 inflammasome (Eisenbarth et al., 2008). On the other hand, the too-strong absorbance, to the adjuvant, may negatively interfere with the antigen processing and lead to an impaired presentation to T cells and results in a weaker immune response (Hansen et al., 2007).

Aluminium hydroxide is considered as effective adjuvant for induction of Th2 responses in mice, therefore it can induce IgE and IgG1 antibodies. One of the drawbacks of aluminium is weak stimulation of cellular immune responses (Agger et al., 2008), needed for clearing of intracellular pathogens, such as *Mycobacterium tuberculosis*, plasmodia and HIV.

Although aluminium compounds are considered as safe adjuvant, they still have some potential side effects. There are reports about severe local effects including sterile abscesses, myofasciitis, eosinophilia and granuloma formation (Brunner et al., 2007; Schoell et al., 2006) and also Th2 immune response induction in allergy treatment in humans (Spazierer et al., 2009). Moreover, there is evidence that the aluminium compounds may have an influence on the incidence of Alzheimer's disease (Martyn et al., 1989). In animal studies, aluminium compounds act as Th2 adjuvant not only when applied parenterally (Brunner et al., 2007), but also when given orally (Brunner et al., 2009; Schoell et al., 2007).

CHAPTER III

METHODOLOGY

Materials

1. **Influenza antigen**
   - Influenza A (H1N1) Virus, strain A/Taiwan/1/86 antigen, Lot No.12/07-8IN73, MyBiosource Inc., San Diego, California, USA

2. **Cell lines**
   - RPMI 2650 cells (ATCC$^®$ CCL-30) originated from a human nasal septum with squamous cell carcinoma, American Type Culture Collection (ATCC), Manassas, VA, USA
   - Raji cells (ATCC$^®$ CCL-86) originated from a human Burkitt's lymphoma, Lot No.4123444, ATCC, Manassas, VA, USA

3. **Cell culture media**
   - Minimum Essential Medium (MEM) Alpha (1X) + GlutaMAX^{TM}-I, Lot no.1158265, Cat.No.32561-036, Gibco$^®$, Invitrogen, USA
   - RPMI Medium 1640 (1X) , Lot No.1016438, Cat.No.11875, Gibco$^®$, Invitrogen, USA
   - Fetal Bovine Serum (FBS) , Lot No.41G8397K, Cat.No.10270, Gibco$^®$, Invitrogen, USA
   - Antibiotic-Antimycotic 100X, Lot No.1092593, Cat.No.15240, Gibco$^®$, Invitrogen, USA
   - Penicillin-Streptomycin, Lot No.1092592, Cat.No.15140, Gibco$^®$, Invitrogen, USA
   - 0.25% Trypsin-EDTA (1X), Lot No.1000187, Cat.No.25200, Gibco$^®$, Invitrogen, USA

4. **Secondary antibodies**

- Goat polyclonal Secondary Antibody to Mouse IgG - H&L (HRP), Lot No.GR23382-11, Abcam, Bristol, UK

- Goat polyclonal Secondary Antibody to Mouse IgG1 - heavy chain (HRP), Lot No.GR97653-1, Abcam, Bristol, UK

- Goat anti-Mouse IgG2a heavy chain (HRP) secondary antibody, Lot No.GR57724-4, Abcam, Bristol, UK

- Goat anti-Mouse IgA alpha chain (HRP) secondary antibody, Lot No.GR97652-3, Abcam, Bristol, UK

5. **Chemicals**

- Chitosan (CS), Low molecular weight (8,434 Da), Lot No.61496MJ, Sigma-Aldrich, USA

- Sodium tripolyphosphate pentabasic (TPP), Lot No.0001436920, Sigma-Aldrich, Germany

- Tween 80, Lot No.809861, Srichand United Dispensary Co.Ltd, Thailand

- Bovine serum albumin (BSA) , Lot No.84H0301, Sigma-Aldrich, USA

- Aluminium hydroxide gel (Rehydragel HPA) , Control No.4122401, Reheis Inc., USA

- Sodium dodecyl sulfate, Lot No.59H03281, Sigma-Aldrich, Japan

- Acrylamide, Batch No.036K0195, Sigma-Aldrich, China

- N,N'-Methylenebis (acrylamide), Lot No.84F-0282, Sigma-Aldrich, USA

- N,N,N',N'-Tetramethylethylenediamine (TEMED), Lot No.STBB5825, Sigma-Aldrich, Germany

- Precision Plus Protein Standard, Control No. 350000889, Bio-Rad Laboratories, Inc., USA

- Coomassie$^®$ Brilliant Blue, Lot No.1387240, Fluka, UK

- Tris (hydroxymethyl) aminomethane, Lot No.8382B011, Merck, Germany

- Albumin–fluorescein isothiocyanate (FITC-BSA), Lot No.080M7400, Sigma-Aldrich, USA

- Fluorescein isothiocyanate conjugated dextran, molecular weight 4000 (FD-4) , Lot No.096K1729, Sigma-Aldrich, Sweden

- Trypan Blue Solution, Lot No.J157-6, Cat.No.82750, JR Scientific Inc., CA, USA
- Thiazolyl Blue Tetrazolium Bromide, Lot No.MKBD4834, Sigma-Aldrich, USA
- Hank's Balanced Salt Solution (HBSS) 1X, Lot No.1042217, Cat.No.14025, Gibco®, Invitrogen, USA
- Phenylmethanesulfonyl fluoride, Lot No.SLBD5020V, Sigma-Aldrich, Germany
- Carbonate-Bicarbonate buffer capsules, Lot No.070M8202, Sigma-Aldrich, USA
- Phosphate buffered saline (PBS) pH 7.4, Lot No.SLBD1728, Sigma-Aldrich, USA
- Tween 20, Lot No.MKBK1089V, Sigma-Aldrich, USA
- 3, 3′,5 ,5′-Tetramethylbenzidine (TMB) Liquid Substrate, Supersensitive, for ELISA, Lot No.091M1442, Sigma-Aldrich, USA
- Stop Reagent for TMB Substrate, Lot No.071M1175, Sigma-Aldrich, USA
- Dimethyl sulfoxide (DMSO), Lot No.K41067812, Merck, Germany
- Triton X-100, Batch No.1095900, Fisher Scientific, UK
- All other materials used were of analytical grade.

6. Equipment

- Magnetic stirrer, Variomag, Poly15 grau, H+P Labortechnik GmbH, Germany
- pH meter, FE20, Mettler Toledo, Switzerland
- Zetasizer ZS, Malvern Instruments, United Kingdom
- Transmission Electron Microscopy (TEM), JEM-2100, Jeol, Japan
- Fourier-transform infrared (FTIR) spectrometer, Spectrum 400, Perkin Elmer, USA
- Circular dichroism (CD) spectrometer, J-715 spectropolarimeter, Jasco, Japan
- Scanning Electron Microscope (SEM), JSM-5410LV, JEOL, Japan

- Fluorescence-Assisted Cell Sorter (FACS), BD-FACSalibur, Becton Dickinson, USA
- Ultracentrifuge, L-80, Beckman, USA
- Spectrophotometer, Microplate Reader, Victor3, Perkin Elmer, USA
- Vertical electrophoresis, SE 250 & SE 260, Hoefer Inc., USA
- Water-Jacketd Incubator (Humidified CO_2 Incubator), 3164, Forma Scientific, USA
- Bio-Freezer (-80°C), 8417, Forma Scientific, USA
- Inverted microscope, CKX31,Olympus, USA
- BS II Laminair Flow Hood, Holten LaminAir, Thermo Scientific, USA
- Epithelial Volt-Ohm Meter, Millicell® ERS-2, Millipore, USA
- Orbital Shaker, SO3, Straut Scientific, UK
- Microplate reader, Biochrom Ltd., Asys UVM340, Cambridge, UK
- Microplate washer, Biochrom Ltd., Asys Atlantis 2, Cambridge, UK

7. **Laboratory supplies**
- QuantiPro BCA Assay Kit, Sigma-Aldrich, USA
- 96 Well EIA/RIA Plate, Flat bottom without lid, Polystyrene, Non-sterile, Corning®, USA
- 25cm² Cell Culture Flask, Rectangular canted neck, with plug seal cap, Corning®, USA
- 96 Well Cell Culture plate, Flat bottom with lid, Tissue culture treated, non-pyrogenic, polystyrene, sterile, Corning®, USA
- Assay Plate, 96 Well, No lid, Flat bottom, Non-treated, Non-sterile, Black polystyrene, Corning®, USA
- Transwell® Permeable Supports, 0.4 µm Polyester Membrane 24 mm Insert, 6 Well Plate, Corning®, USA
- ELISA plate, Immunoplate (96 well), Crystal grade Polystyrene, Flat bottom, SPL Lifesciences Co.Ltd, Gyeonggi-do, Korea

Methods

1. **Preparation of blank chitosan nanoparticles with aluminium hydroxide gel**

   Chitosan nanoparticles (CSNPs) were prepared based on the ionotropic gelation of chitosan with anion of TPP. Briefly, Chitosan was dissolved in solution with 2% (v/v) acetic acid overnight. The particles were formed spontaneously upon slowly drop-wised addition of an aqueous solution of TPP to chitosan solution at ambient temperature under magnetic stirring. The effect parameters such as chitosan concentration, pH of chitosan solution and weight ratio of chitosan:TPP were investigated on particle size, zeta potential and appearance of chitosan nanoparticles. The formulations with smallest particles or opalescent suspension were further studied.

   The formulation with optimized parameters was added with Tween 80 and aluminium hydroxide gel in various amount and different order of mixing of each component. These preparations were also investigated on particle size and zeta potential of the obtained nanoparticles.

2. **Preparation of BSA loaded chitosan nanoparticles with aluminium hydroxide gel**

   The BSA loaded chitosan nanoparticles, in concentration of 30 μg/ml, were prepared, with optimized conditions, as described above. The methods to incorporate BSA into chitosan nanoparticles were investigated. The first method, BSA was dissolved in chitosan solution, after pH adjustment. The second method, BSA was dissolved in TPP solution before dropping into chitosan solution. The particle size, zeta potential and aggregation of BSA loaded chitosan nanoparticles were investigated.

   The formulations prepared by selected method were used for further studies.

3. Characterization of chitosan nanoparticles

3.1 Particle size and zeta potential

The particle sizes of samples were evaluated by a dynamic light scattering (DLS) technique with a Zetasizer ZS (Malvern Instruments, UK). Zeta potential determinations were based on electrophoretic mobility of the nanoparticles in aqueous suspensions using laser Doppler velocimetry (LDV). These measurements were performed in triplicate with independent particle batches.

3.2 Particle morphology

The morphological examination of chitosan nanoparticles was performed by transmission electron microscopy (JEM-2100, Jeol, Japan) after staining with 1% phospho-tungstic acid (PTA).

3.3 Polymeric interaction

The FTIR spectra of raw materials, chitosan nanoparticles and chitosan nanoparticles with aluminium hydroxide gel (with or without BSA) were investigated by Fourier-transform infrared (FTIR) spectrometer (Spectrum 400, Perkin Elmer, USA). The samples were freezed below -20ºC and dried by gradually increasing of temperature until reach 20ºC under vacuum condition and keep drying for 1 hour. Then freeze dried sample was placed on IR crystal window and subjected to light within the infrared region. The instrument was operated with resolution of 1 cm^{-1} and scaned with frequency range of 400-4000 cm^{-1}.

3.4 Loading efficacy of BSA in chitosan nanoparticles

BSA loaded chitosan nanoparticles with aluminium hydroxide gel were prepared as described before. The amount of protein entrapped in the nanoparticles was calculated from the difference between the total amount added to the loading

solution and the amount of non-encapsulated protein remaining in the supernatant. BSA concentrations in the supernatants were measured by the QuantiPro BCA Assay (Sigma-Aldrich, USA). Since Tween 80 in the supernatant interfered with the protein assay, for this study the BSA-loaded chitosan nanoparticles with aluminium hydroxide gel were prepared without Tween 80. Aliquots of the resulting nanoparticle suspension were centrifuged by ultracentrifuge (Beckman, L-80, USA) for 30 minutes at 60,000 rpm and 8^OC and the supernatants were then separated from the nanoparticles. The amount of non-encapsulated protein remaining in the supernatant was measured. A supernatant from non-loaded chitosan nanoparticle suspension without Tween 80 was used as a blank to correct for interference by chitosan. Loading efficiency (LE) was calculated as follows.

$$LE = \frac{(\text{Total amount of BSA} - \text{Free BSA}) \times 100\%}{\text{Total amount of BSA}}$$

3.5 Particle aggregation study

BSA-loaded chitosan nanoparticles without and with aluminium hydroxide gel in various concentrations were prepared as described before. The formulations were kept in refrigerator (2-8^OC) without stirring and sampled at day 0, 2, 5, 10, 21 and 150. The samples were investigated on particle size, size distribution and zeta potential.

4. Protein properties

4.1 Sodium Dodecyl Sulphate-Polyacrylamide Gel Electrophoresis (SDS-PAGE)

SDS-PAGE was done to evaluate the effect of the preparation process on protein integrity. BSA-loaded chitosan nanoparticles were destabilized by adding 1 ml of 10% NaCl to 5 ml of nanoparticle suspension, resulting protein concentration of 50 µg/ml in solution. The samples were mixed with SDS-PAGE loading buffer

containing bromophenol blue before electrophoresed in 10% SDS-polyacrylamide gel with 30 mA for 3.5 hours. After electrophoresis, the protein bands were strained with Coomassie® brilliant blue R250 and destrained with destrain solution.

4.2 Circular dichroism (CD) measurements

CD spectrometer (J-715 spectropolarimeter, Jasco, Japan) was used to measure the conformational change of the encapsulated BSA compared with the native one. Solution of the native BSA or the encapsulated BSA was prepared to 30 and 60 μg/ml. Supernatant of CSNPs was used as solvent and blank. The ellipticity of samples was recorded by scanning over the wavelength range 200-250 nm, using a 1-mm quartz cylindrical cell. The CD spectra were obtained by plotting molar ellipticity against wavelength.

5. Mucoadhesive evaluation

Mucoadhesive property of the formulations was evaluated by adaptive method described by Harikarnpakdee et al. (2006). The porcine intestinal tissue was used for testing model and conducted as stated in protocol approved from Chulalongkorn University Animal Care and Use Committee, Approval No. 12-33-015. The intestine was obtained from a local abattoir and delivered with ice pack to laboratory within 1 hour from killing. The intestine was cut in pieces of 5 centimeters long, then incised along and cleaned by PBS buffer, pH 7.4. After that the tissue was attached on glass Petri dish and applied 0.5 ml of sample on the tissue. Then the Petri dish was installed in the funnel, in an angle of 40° relative to the horizontal plane. PBS buffer, pH 7.4, was dropped over the surface of the tissue in the rate of 5 ml/min. The washed was collected at 5, 10, 15, 30, 45 and 60 minutes and determined by fluorometry at excitation of 485 nm and emission of 535 nm (Microplate Reader, Victor3, Perkin Elmer, USA)

The formulations were prepared with FITC-BSA instead of BSA. The cleaned tissue was kept in refrigerator, 2-8°C, not more than 8 hours after killing slaughter until the experiment.

6. *In vitro* study in cell culture

6.1 Cell cultures

Culturing of RPMI 2650 cells

RPMI 2650 cells (ATCC® CCL-30) originated from a human nasal septum with squamous cell carcinoma (ATCC, Manassas, VA, USA), passage 37-50, were grown in horizontal plastic cultural flask. Briefly, cells were maintained in Minimum Essential Medium (MEM) Alpha (1X) + GlutaMAX™-I (Gibco® Cat.No.32561-036 supplemented with 10% fetal bovine serum (FBS) and 1% antibiotic-antimycotic solution as culture medium and incubated in humidified 5% CO_2 incubator at 37ºC until reached 70-80% confluence. These cells were then trypsinized and seeded in 96-well plates for cytotoxicity study and in 6-well plates for cellular uptake study.

Culturing of Raji cells

Raji cells (ATCC® CCL-86) originated from a human lymphoblast with Burkitt's lymphoma (ATCC, Manassas, VA, USA), passage 12-15, were grown in horizontal flask. Briefly, cells were maintained in RPMI 1640 with L-Glutamine (GIBCO Cat. No.11875) supplemented with 10% FBS and 1% antibiotic-antimycotic as culture medium and incubated in humidified 5% CO_2 incubator at 37ºC. The medium was added every 2-3 day until reached a density of 2-3 x 10^6 viable cells/ml. Then they were splitted into new culture flasks and added fresh medium at 3-5 x 10^5 viable cells/ml.

Culturing of nasal M-cells model

Nasal M-cells model was prepared by co-culturing of RPMI 2650 cells and Raji cells as described by Pichayakorn et al., (2008). The RPMI cells were trypsinized and seeded on polycarbonate filters, 3 μm pore size, of 6 wells Transwell® at a density of 4.0 x 10^5 cells/cm². The Raji cells were centrifuged, resuspended in MEM and

added basolaterally at a density of 4 x 10^5 cells/ml. The apical and basolateral compartments received 1.5 and 2.6 ml of cultural media respectively. Every two days, the medium in basolateral compartment was changed by replacing 1.5 ml of the resuspended cells in MEM, while apical compartment was changed by fresh MEM.

6.2 Cytotoxicity study

RPMI 2650 cells were cultured in 96-well plate at a density of 1 x 10^5 cells/ml, 100 µl/well. In the next two days, 10 µl of samples, the same volume and concentration in immunization study, were each added in 16 wells and incubated for 2 hours. Control group consisted of cell in culture medium was processed identically and incubated simultaneously as treated groups. The 50 µl of MTT solution (1 mg/ml in PBS) was added into each well after all liquid was removed. The plates were incubated for 3 hours, then MTT solution was replaced with 100 µl DMSO and agitated by orbital shaker for 20 minutes. The absorbance was read at 560 nm on microplate reader (Victor3, Perkin Elmer, USA). The relative cell viability was expressed as a percentage relative to the control group.

6.3 Cellular uptake study

The RPMI 2650 cells were cultured in 6-wells plate at a density of 1 x 10^6 cells/3 ml. In the next day, samples, prepared with FITC-BSA, were incubated for 2 hours in each well. Then, RPMI 2650 cells were washed 3 times with PBS, trypsinized, and resuspended in fresh medium. After that they were centrifuged and resuspended in PBS. Fluorescein uptake was analysed by fluorescence-assisted cell sorter (FACS, BD-FACSalibur, Becton Dickinson, USA) equipped with argon laser and detected with G1 detector (excitation of 485 nm and emission of 525 nm). The number of fluorescent events was counted which correlated to the particles taken up in cells. The data were calculated using the instrument software and showed as mean of particle fluorescent.

6.4 Permeation Study

Nasal M-cell model was used for permeation study. After the RPMI 2650 and Raji cells were seeded in 6 wells Transwell®, culture medium was changed regularly until 100% confluence was reached. The monolayer integrity was firstly assessed by the inverted microscope and confirmed before permeation study by measurement of trans-epithelial electrical resistance (TEER).

Permeation of fluorescein isothiocyanate–dextran, MW 4,000, (FD-4) as model substance, through the Nasal M-cell model in comparison to blank filter was to qualify the barrier function of the cultivated human cell monolayer. The FD-4 in Hank's balance salt solution (HBSS) at concentration of 100 μg/ml was added to the apical compartment of 6 wells Transwell®. At different time intervals, 1-ml samples were withdrawn from the basolateral compartment and replaced by fresh HBSS. The amounts of permeated FD-4 were determine by fluorometry at the excitation of 485 nm and emission of 535 nm (microplate reader, Victor3, Perkin Elmer, USA).

For the permeation study, the confluent cell monolayers were rinsed 3 times and filled with HBSS into apical and basolateral compartments. Samples, prepared with FITC-BSA, were incubated in apical compartments for 3 hours. At different time interval, 1 ml basolateral buffers were withdrawn and replaced by fresh HBSS. The TEER of culturing cell monolayer was measured by using an electrode (Millicell ERS-2 meter, Millipore, USA) at the beginning and before withdrawal of samples. After termination of permeation study, the filter were rinsed with PBS and digested with 1% triton-X100 solution and centrifuged. The amounts of permeated and cell lysated fluorescein were determined by fluorometry at the excitation of 485 nm and emission of 535 nm (microplate reader, Victor[3], Perkin Elmer, USA).

7. Immunization studies

7.1 Preparation of formulations for immunization

Influenza A (H1N1) virus, strain A/Taiwan/1/86 antigen (Lot no.12/07-8IN73, MyBiosource Inc., San Diego, California, USA) was used for preparation of

formulations for immunization. Each dose contained 10 µg of the antigen. For antigen solution, the antigen was dissolved in PBS, pH 7.4, in concentration of 10 µg/50 µl and 10 µg/10 µl for intramuscular (i.m.) and intranasal (i.n.) administration respectively. The antigen loaded chitosan nanoparticle with and without aluminium hydroxide gel were prepared as previous study. Briefly, the antigen was dissolved in TPP solution and added dropwise to the chitosan solution in 2% w/v acetic acid (adjusted to pH 4.5), while stirring, obtained final concentration of antigen 10 µg/10 µl formulation. Tween 80 was added and then aluminium hydroxide gel was suspended in formulation with aluminium hydroxide gel, resulted in 0.1% (w/v) and 0.1 mg/ml concentration respectively.

7.2 Experimental animals

Female ICR mice, 6–8 weeks old (Horse Farm and Laboratory Animal Breeding Center, Queen Saovabha Memorial Institute, Thai Red Cross Society, Thailand), were housed in groups of eight mice and maintained in the animal facility of research and development department of Queen Saovabha Memorial Institute with a 12 hours day and night schedule, while food and water were ad libitum. The experiments were approved by the Animal Care and Use Committee of Queen Saovabha Memorial Institute (QSMI-ACUC), protocol number 4/2012.

7.3 Immunization

Five groups of ICR mice (eight per group) were either intramuscularly vaccinated or intranasally immunized with different formulations. Before each immunization, the mice were lightly anesthetized with an inhaled gaseous of diethyl ether and then immunized with different formulations (Table 3-1).

For intramuscular (i.m.) immunization, one group of mice received 50 µl of the antigen solution by injection into their hind leg. The blood samples were taken from tail vein before and 3 weeks after immunization.

The intranasal (i.n.) administered formulations were given 3 successive in 3 weeks interval, excepted for PBS, in a total volume of 10 µl (5 µl in each nostril) with

a 10-µl micropipette tip. The blood samples were taken from tail vein before each administration and 2 weeks after the last immunization. Only in PBS group, the blood samples were taken as in i.m. immunization.

Individual blood samples were centrifuged for 10 min at 4,000 rpm at 4 ∘C, and then serum samples were separated from blood cells, coagulated proteins and stored at −80 ∘C.

After the last blood sampling, mice were sacrificed by intraperitoneal injection of thiopental sodium (100 mg/kg). The trachea of each mouse was opened and then a volume of 500 µl of PBS containing 0.1% (w/v) BSA and 1mM phenylmethylsulfonyl fluoride (PMSF) was flushed through the nasal cavity and collected from the nostrils. The nasal lavages were stored at −80 ∘C until the day of analysis.

Table 3-1 Immunization design

Sample	Route of administration	Immunization (day)	Blood Sampling (day)	Nasal washes (day)
1. PBS	i.n.	0	0, 21	21
2. Antigen solution	i.n.	0, 21, 42	0, 21, 42, 56	56
3. Antigen-CSNP	i.n.	0, 21, 42	0, 21, 42, 56	56
4. Antigen-CSNP-Al	i.n.	0, 21, 42	0, 21, 42, 56	56
5. Antigen solution	i.m.	0	0, 21	21

7.4 Antibody assessment

To determine the influenza antigen-specific antibody responses, the enzyme-linked immunoabsorbent assay (ELISA) was conducted. Briefly, ELISA plates (SPL Life Science, Korea) were coated overnight at 37 ∘C with 100 µl of 200 ng influenza antigen (H1N1) per well in coating buffer (0.05M carbonate-bicarbonate, pH 9.6). Plates were thoroughly washed 3 times with 300 µl of washing buffer (PBS containing 0.05% (v/v) Tween 20, pH 7.4) per well and blocked by incubation with 150 µl of 1% (w/v) BSA in coating buffer for 1 hour at 37 ∘C. Subsequently, the

plates were thoroughly washed 3 times. Appropriate dilutions of samples with diluting buffer (PBS containing 0.05% (v/v), Tween 20 and 0.1% (w/v) BSA of each individual mouse were added to the plates and incubated for 2 hours at 37∘C. The plates were then thoroughly washed 3 times and incubated with 100 µl horseradish peroxidase-conjugated goat anti-mouse IgG, IgG1, IgG2a or IgA antibodies (IgG diluted 1:100,000 and 1:50,000 for the rest in diluting buffer) for 1 hour at 37 ∘C. Then, the plates were thoroughly washed 3 times and stained the specific antibodies by adding 3,3',5,5'-tetramethylbenzidine (TMB) solution, 100 µl per well. The plates were placed in the dark for 10 minutes at room temperature. Then the reaction was stopped with an equal volume of stop reagent and optical density (OD) was read at 450 nm using microplate reader (Biochrom Ltd., Asys UVM340, Cambridge, UK). Antibody titers are expressed as the reciprocal of the calculated sample dilution corresponding with an A_{450} of 0.2 above the background. Comparison of antibody titers between groups was made by a one-way ANOVA program.

CHAPTER IV

RESULTS AND DISCUSSION

1. **Preparation of blank chitosan nanoparticles with aluminium hydroxide gel**

1.1 Influence of chitosan solution concentrataion

Chitosan nanoparticles were prepared based upon the ionotropic gelation of chitosan contact with the TPP anions. In order to study the appropriate conditions for encapsulation of BSA, it was firstly evaluated the influence of critical formulation parameters such as concentration and pH of chitosan solution, weight ratio of chitosan : TPP, order of mixing and mixing time, amount of surfactant and aluminium hydroxide gel and incorporation methods of BSA into chitosan nanoparticles. These parameters were discussed and chosen.

The appearances of resulting chitosan nanoparticles is shown in table 4-1. The preliminary weight ratios of chitosan : TPP showed that the opalescent suspension was formed from 2:1 to 3:1 in 0.1 % (w/v) chitosan solution and from 2.5:1 to 3:1 in 0.2 % (w/v) chitosan solution.

Table 4-1 The appearance of chitosan nanoparticle suspension

Weight ratio of CS:TPP	0.1% (w/v) chitosan	0.2% (w/v) chitosan
1.0 : 1	Turbid and precipitated	Turbid and precipitated
1.5 : 1	Turbid and precipitated	Turbid and precipitated
2.0 : 1	Opalescent	Turbid
2.5 : 1	Opalescent	Opalescent
3.0 : 1	Opalescent	Opalescent

The particle size and zeta potential of 0.1% and 0.2% chitosan solution with TPP solution in chitosan : TPP weight ratio of 2:1, 2.5:1 and 3:1 were 104.5±4.7,

103.6±4.6, 109.3±3.1 nm / +20.9±0.84, +31.1±2.25, +35.1±3.97 mV (0.1% (w/v) chitosan) and 679.1±122.3, 115.3±2.2, 121.6±1.7 nm / +17.5±0.31, +27.2±0.42, +33.2±1.47 mV, (0.2% (w/v) chitosan), respectively, as shown in figures 4-1 and 4-2.
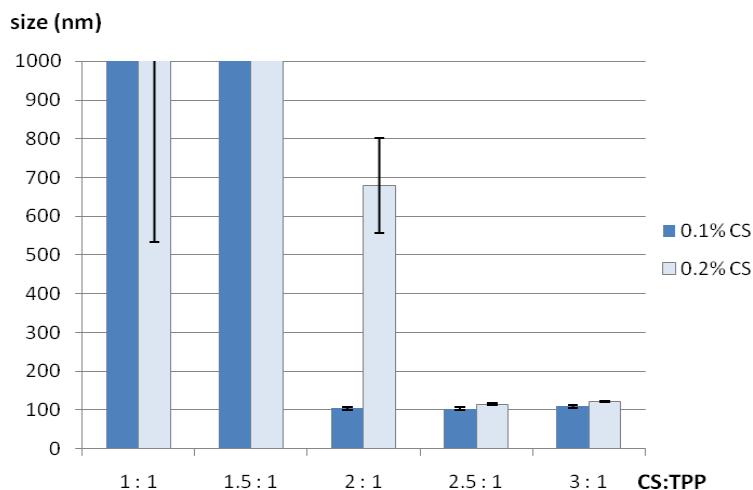
Figure 4-1 Effects of concentration of chitosan solution and weight ratio of chitosan : TPP on nanoparticles formation.
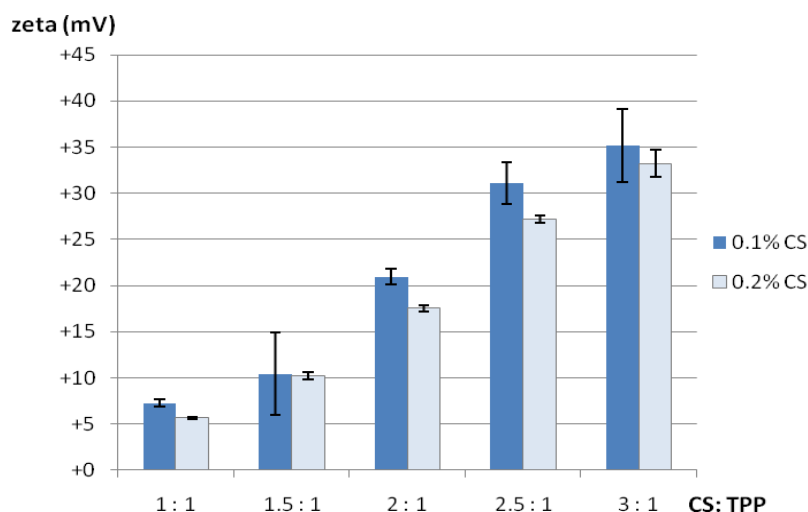
Figure 4-2 Effects of concentration of chitosan solution and weight ratio of chitosan : TPP on zeta potential.

The results of concentration of chitosan solution showed that lower concentration promoted formation of smaller particles while zeta potentials were not significantly different ($p > 0.05$). Moreover, it was supposed that a relatively lower viscosity of

chitosan with lower concentration promoted the formation of nanoparticles of chitosan and TPP (Tang, Qian and Shi, 2007). The effect of weight ratios of chitosan : TPP on particle size was prominent. Increasing of the ratio provoked a decreasing of turbidity to opalescent, which mean decreasing of particle size. The adding of excess TPP to the formulation showed a tendency of aggregation and caused the decreasing of zeta potential because of the excess poly anion.

1.2 Influence of pH of chitosan solution and weight ratio

The 0.1% (w/v) of chitosan solution was chosen to study on effect of pH of chitosan solution (initial pH of 3.11 and adjusted to 4.5, 5.5 and 6.5 by 3N NaoH) and the optimized weight ratio (from 2:1 to 6:1). Figure 4-3 presents the mean diameter of chitosan nanoparticles which was slightly decreased when increasing the pH to 4.5 but increased significantly with pH of 5.5 and 6.5 ($p<0.05$). The increase in pH, positive charges would be neutralized with deprotonation of amino groups. It might change the conformation of the chitosan molecules and decreased the solubility, therefore, increasing tendency to nanoaggregate (Mokarram & Alonso, 2006). Moreover, the zeta potential decreased when pH increased as shown in figure 4-4, which implies that the number of activated amine groups in the chitosan chain decreased when pH increased.
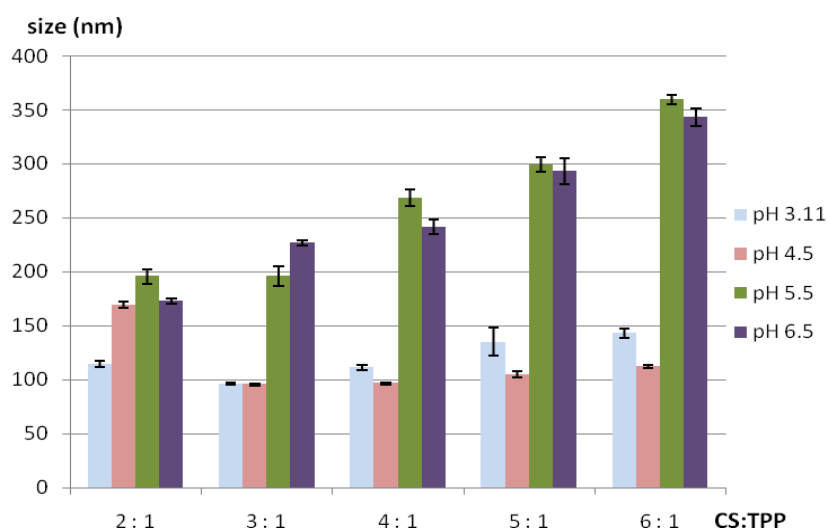
Figure 4-3 Effects of pH of chitosan solution and weight ratio of chitosan : TPP on nanoparticles formation.

The optimum weight ratio of chitosan : TPP resulted in smallest particle size as shown in figures 4-1 and 4-3, which related to the suitable ratio of cation and anion. In addition, the positive charge of particles was desired for adhesion to mucous membrane. The more ratio of chitosan showed the more positive zeta potential value. However, to choose the conditions for preparation, all parameters had to be considered.

The pH of nasal cavity varied between 5.5-6.5 in adults. The ideal pH of a formulation should be within 4.5-6.5 because the pH of nasal cavity can alter the pH of formulation (Arora et al., 2002). Especially, the formulation with out of range pH may cause irritation of nasal mucosa. Thus the pH of initial chitosan solution for preparation of the nasal formulation should be 4.5 with chitosan : TPP weight ratio of 3:1which resulting the smallest particle size.
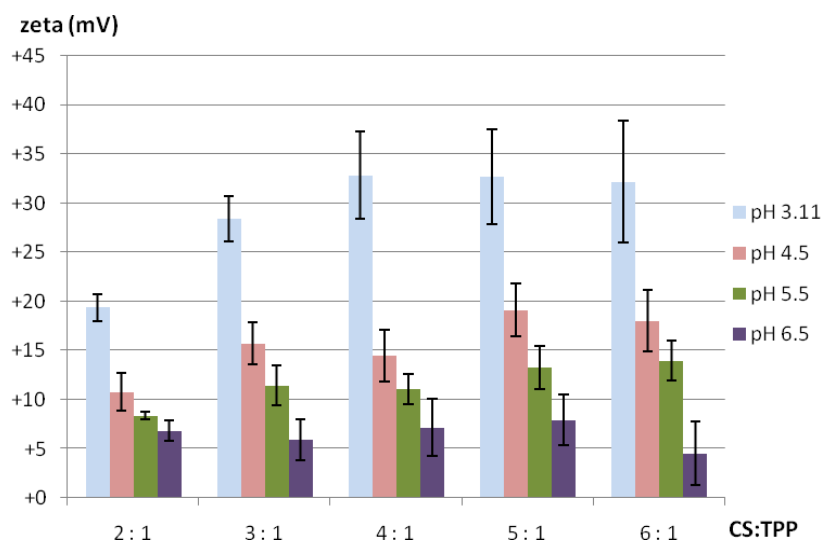
Figure 4-4 Effects of pH of chitosan solution and weight ratio of chitosan : TPP on zeta potential.

1.3 Influence of order of mixing, mixing time and amount of Tween 80

After weight ratio of chitosan : TPP and pH of the initial chitosan solution were defined, other components such as Tween 80, for reducing particles aggregation and aluminium hydroxide gel, or called alum, were added. The order of mixing of each component seemed to influence on the nanoparticles formation. In formulation
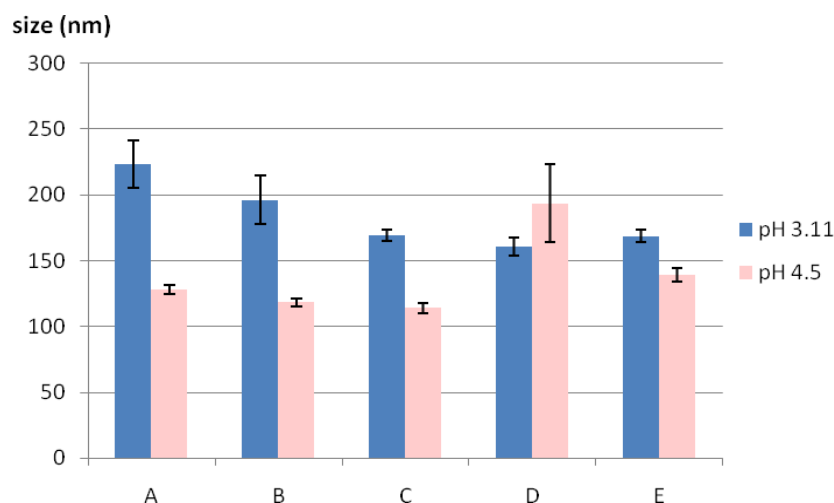
Figure 4-5 The influence of order of mixing on particle size.

A: mixed chitosan solution with Tween 80, then added alum, and TPP lastly.

B: mixed chitosan solution with alum, then add Tween 80, and TPP lastly.

C: mixed chitosan solution with TPP, then added Tween 80, and alum lastly.

D: mixed chitosan solution with Tween 80, then added TPP, and alum lastly.

E: mixed chitosan solution with TPP, then added Tween 80, and alum with tween 80 lastly.
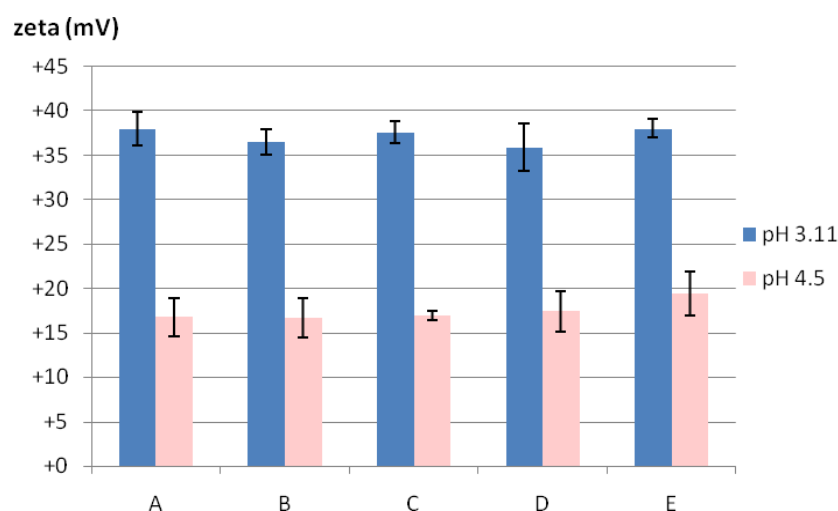
Figure 4-6 The influence of order of mixing on zeta potential.

A: mixed chitosan solution with Tween 80, then added alum, and TPP lastly.

B: mixed chitosan solution with alum, then add Tween 80, and TPP lastly.

C: mixed chitosan solution with TPP, then added Tween 80, and alum lastly.

D: mixed chitosan solution with Tween 80, then added TPP, and alum lastly.

E: mixed chitosan solution with TPP, then added Tween 80, and alum with tween 80 lastly.

with chitosan solution pH of 3.11 (unadjusted), each order of mixing caused different sizes of nanoparticles. The formulation D that initially mixed Tween 80 into chitosan solution, then dropped with TPP and suspended lastly with aluminium hydroxide gel resulted the smallest particle size (160.9 ±0.9 nm). While the formulation with chitosan solution pH of 4.5, the formulation C that initially dropped TPP into chitosan solution, then mixed with Tween 80 and suspended lastly with aluminium hydroxide gel resulted the smallest particle size (114.1 ±4.1 nm). It seemed that the order of mixing of each component caused the different order of interaction that might effect on the particle size. On the other hand, the order of mixing might have no effect on zeta potential ($p>0.05$) as the results shown in figure 4-6.

With the optimized order of mixing, method C, the formulations were prepared with different amount of Tween 80 and mixing time after adding all components. Briefly, TPP solution was added into chitosan solution, pH 4.5 as the chosen pH. After 15 minutes, Tween 80 was added into the suspension in concentrations of 0.05, 0.1 and 0.15% (w/v), continuously stirred for 5 minutes. Then aluminium hydroxide gel suspension was suspended in the formulations in the concentration of 0.05% (w/v) and continued stirring for 30 and 60 minutes for formulation A and B respectively. The whole preparation was performed at stirring condition of 600 rpm.
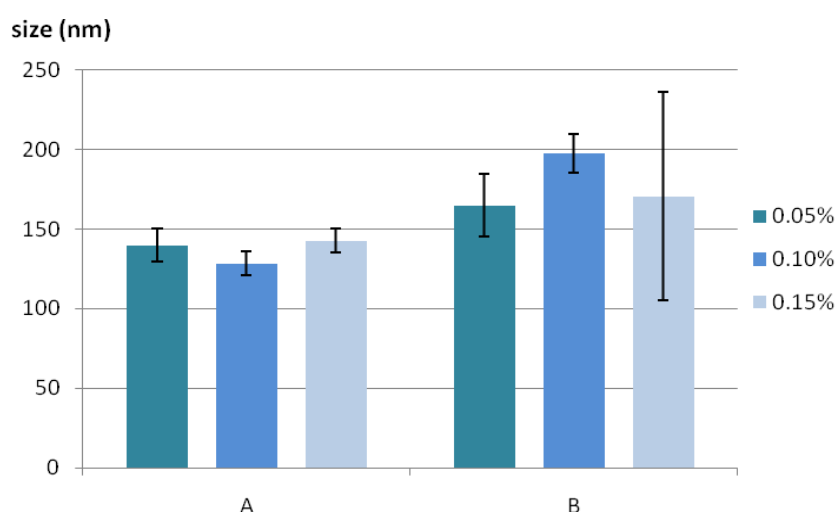
Figure 4-7 Effects of mixing time and amount of Tween 80 on nanoparticle formation. A and B were 30 and 60 minutes mixing time, respectively.

zeta (mV)
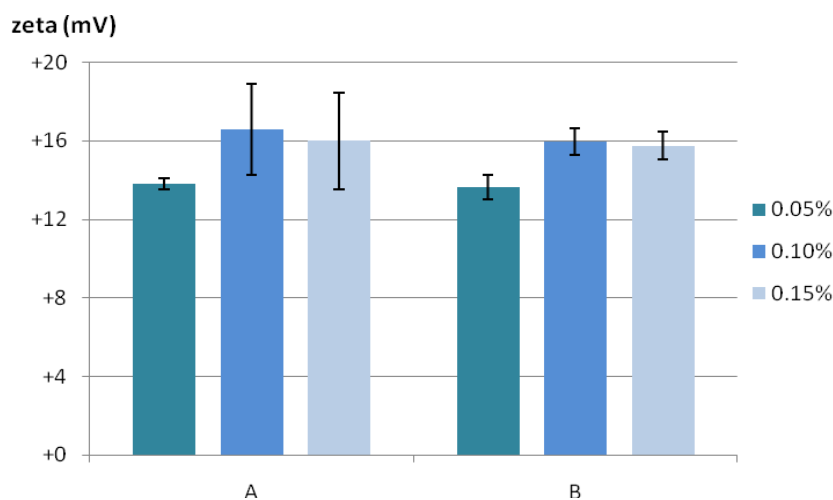
Figure 4-8 Effects of mixing time and amount of Tween 80 on zeta potential. A and B were 30 and 60 minutes mixing time, respectively.

From figure 4-7, the particle sizes of formulation A were 139.9±10.2, 128.3±7.6 and 142.6±7.3 nm and those of formulation B were 164.9±19.6, 197.6±12.1 and 170.6±65.3 nm for 0.05, 0.1 and 0.15% (w/v) Tween 80, respectively. While the zeta potentials of them, figure 4-8, were +13.8±0.3, +16.6±0.6 and +16.0±2.6 mV and +13.6±2.3, +15.9±0.7 and +15.7±0.4 mV, respectively. The results reflected that the suitable mixing time was 30 minutes and the further mixing promoted its tendency to nanoaggregate, especially in 0.1% (w/v) Tween 80 ($p<0.05$). Therefore, the 0.1% (w/v) Tween 80 and 30 minutes mixing time were chosen for further study. However, the mixing time might not affect on zeta potential ($p>005$).

1.4 Influence of amount of aluminium hydroxide gel

Before adding of the BSA as model antigen, the suitable amount of aluminium hydroxide gel had to be studied. The formulations were prepared with various concentrations of aluminium hydroxide gel with optimized condition as aforementioned study. The final concentrations of aluminium hydroxide gel in the formulations were 0.15, 0.4, 0.8, 1.2 and 1.6 mg/ml following the regulation of US code of federal regulation (610.15(a)) that the amount of aluminium in the recommended individual dose of a biological product shall not exceed 0.85 mg (Baylor, Egan and Richman, 2002), or 1.7 mg/ml for dosage of 0.5 ml.
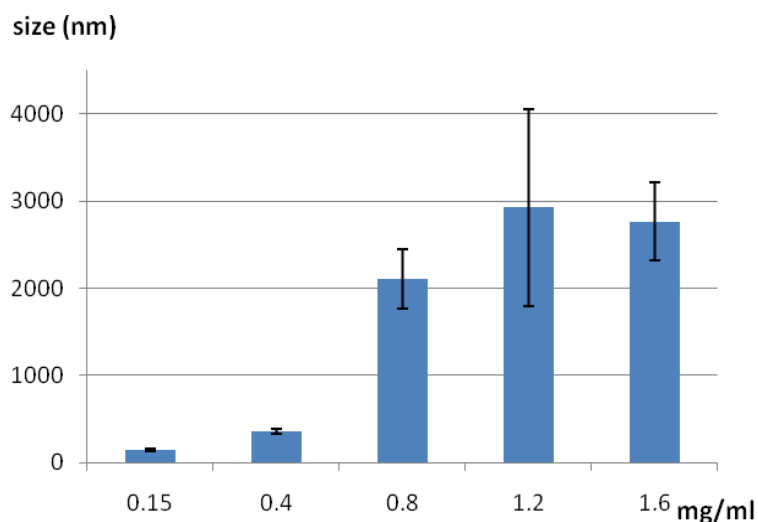
Figure 4-9 Effects of aluminium hydroxide gel concentration on particle size.

The particle sizes and zeta potential tended to increase when increasing the aluminium hydroxide gel concentration as shown in figures 4-9 and 4-10. The aluminium hydroxide gel may cover on the chitosan nanoparticles caused increasing of the particle size. But the excess amount might cause particles agglomeration as in the concentration of 0.8, 1.2 and 1.6 mg/ml which showed increased numbers of the particle sizes ($p < 0.05$). Thus the concentration of aluminium hydroxide gel for preparation of the formulation with BSA should not more than 0.4 mg/ml.
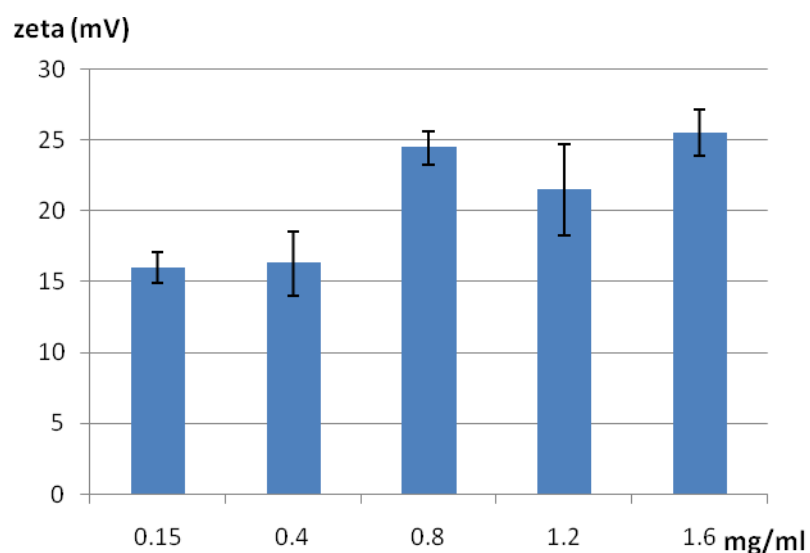
Figure 4-10 Effects of aluminium hydroxide gel concentration on zeta potential.

2. Preparation of BSA loaded chitosan nanoparticles with aluminium hydroxide gel

The BSA loaded chitosan nanoparticles with aluminium hydroxide gel were prepared as optimized conditions with 2 methods of BSA incorporation. Method A was dissolving BSA in pH4.5-adjusted chitosan solution. While BSA was dissolved in TPP solution before adding in pH4.5-adjusted chitosan solution in method B. The final concentrations of aluminium hydroxide gel in formulation were 0.1, 0.2 and 0.4 mg/ml. The formulations were kept in refrigerator (2-8°C) and sampled on day 0, 2, 4 and 9 for investigation of particle size and zeta potential.
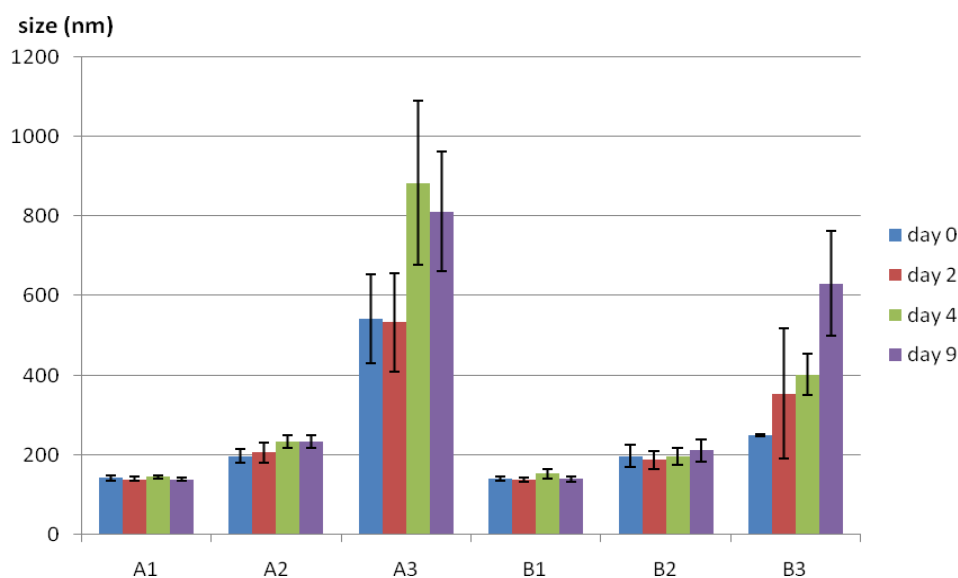
Figure 4-11 Effects of method to incorporate BSA into chitosan nanoparticles on particle size. The number 1, 2 and 3 represented 0.1, 0.2 and 0.4 mg/ml of aluminium hydroxide gel in formulations with method A (dissolved BSA in chitosan solution) or B (dissolved BSA in TPP solution).

The results reflected that method A tended to form bigger particle size than method B, especially in concentration of 0.4 mg/ml aluminium hydroxide gel. As shown in figure 4-11, the particle size was the smallest at the aluminium hydroxide gel concentration of 0.1% and increased with increasing aluminium hydroxide gel concentration. However, even a slight increase in zeta potential when increasing the concentration of aluminium hydroxide gel, the aggregation tended to take place.
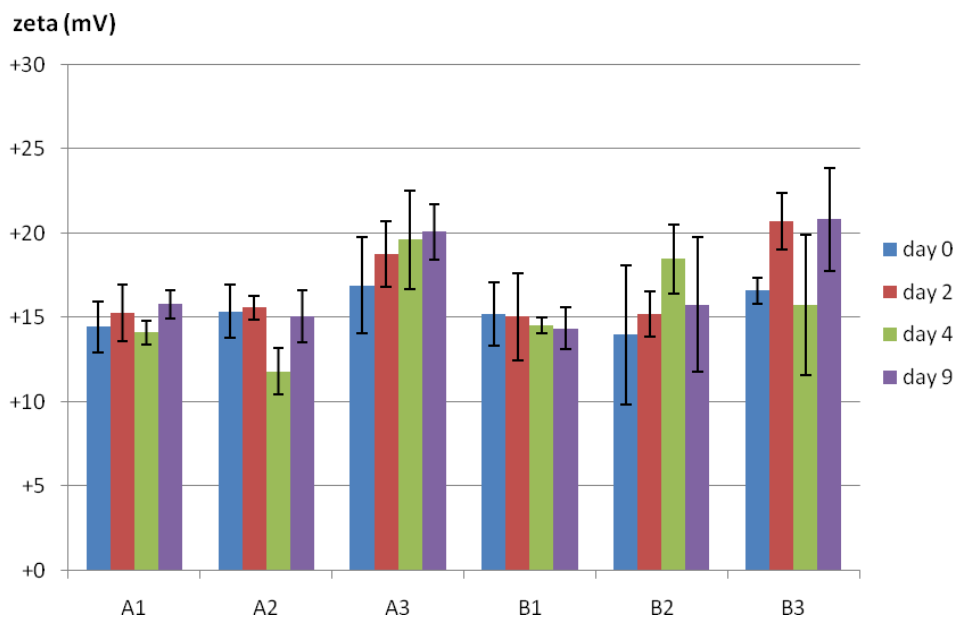
Figure 4-12 Effects of method to incorporate BSA into chitosan nanoparticles on zeta potential. The number 1, 2 and 3 represented 0.1, 0.2 and 0.4 mg/ml of aluminium hydroxide gel in formulations with method A (dissolved BSA in chitosan solution) or B (dissolved BSA in TPP solution).

Then BSA loaded chitosan nanoparticles with aluminium hydroxide gel were prepared with optimized conditions and BSA incorporation by dropping BSA-TPP solution into chitosan solution, pH 4.5, while stirring.

3. Characterization of chitosan nanoparticles

3.1 Morphology of chitosan nanoparticles

The shape of nanoparticles was examined by TEM. Figure 4-13 shows the physical appearance of chitosan nanoparticles in spherical structure, while chitosan nanoparticles with aluminium hydroxide gel had slightly bigger size as a compact core surrounded by a fluffy coat of aluminium hydroxide gel. Their average particle size and zeta potential, measured by Zetasizer ZS, were 117.1 ± 0.6, 130.0 ± 5.5, 187.6 ± 21.3 and 402.8 ± 67.9 nm and $+15.5\pm3.3$, $+14.8\pm1.2$, $+15.3\pm2.5$ and $+17.6\pm2.3$ mV for chitosan nanoparticles and chitosan nanoparticles with 0.1, 0.2 and 0.4 mg/ml of aluminium hydroxide gel, respectively.

From figure 4-14, the TEM photograph of BSA loaded chitosan nanoparticles (a) showed spherical shape with small white dots as of BSA spreaded all over the surface of the particles. While the formulations with aluminium hydroxide gel shown only the fluffy coat on the surface. Their average particle size and zeta potential, measured by Zetasizer ZS, were 118.9 ± 4.4, 135.4 ± 4.5, 191.4 ± 28.6 and 414.7 ± 50.4 nm and 17.7 ± 0.3, 18.5 ± 0.4, 17.4 ± 3.4 and 18.1 ± 2.8 mV for chitosan nanoparticles and chitosan nanoparticles with 0.1, 0.2 and 0.4 mg/ml of aluminium hydroxide gel, respectively.

The obtained chitosan nanoparticles did not show significantly change in size or surface potential according to the BSA addition which might due to small amount of BSA loaded in the particles.
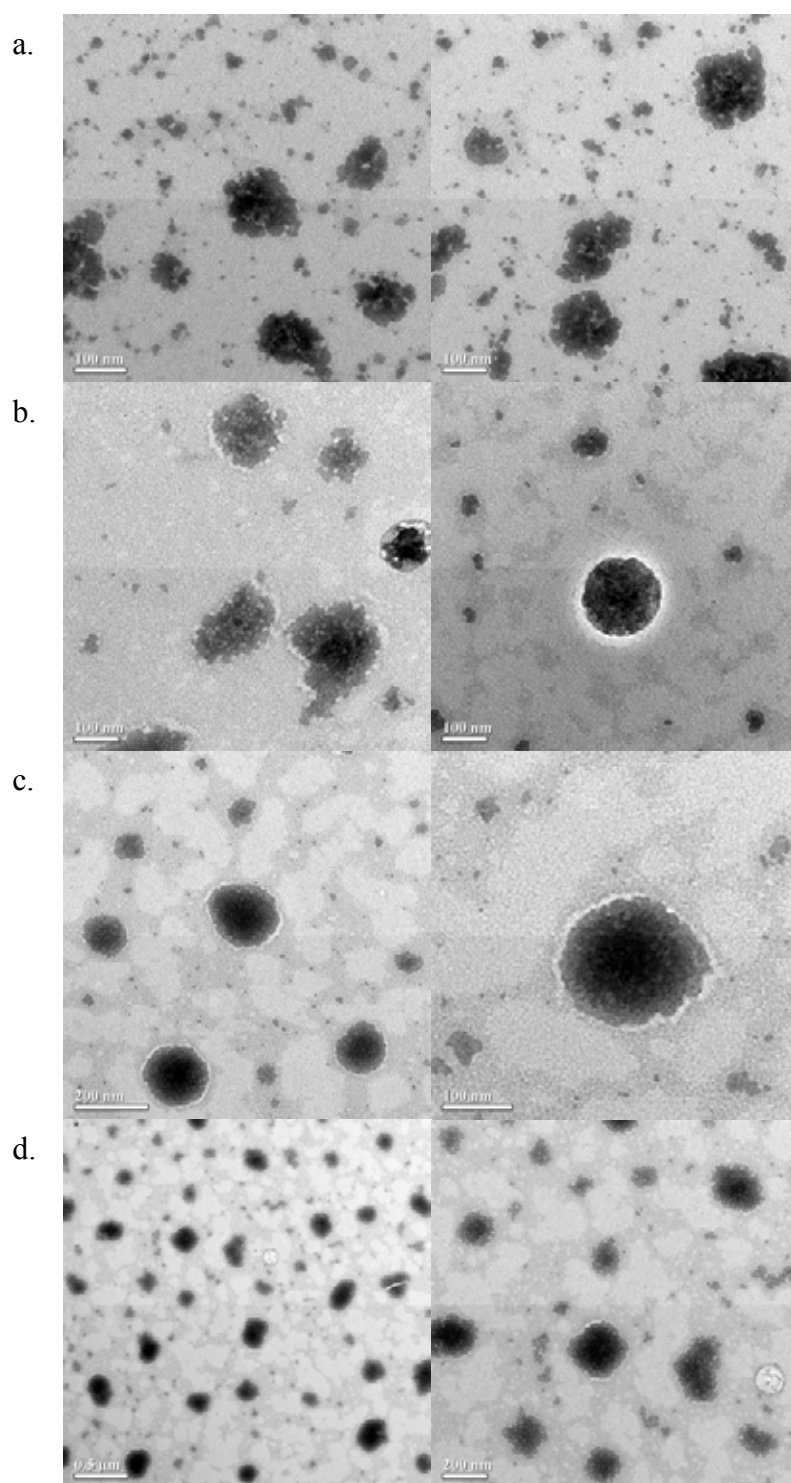
Figure 4-13 TEM photographs of chitosan nanoparticles (a) and chitosan nanoparticles with aluminium hydroxide gel at concentration of 0.1, 0.2 and 0.4 mg/ml (b, c and d, respectively).
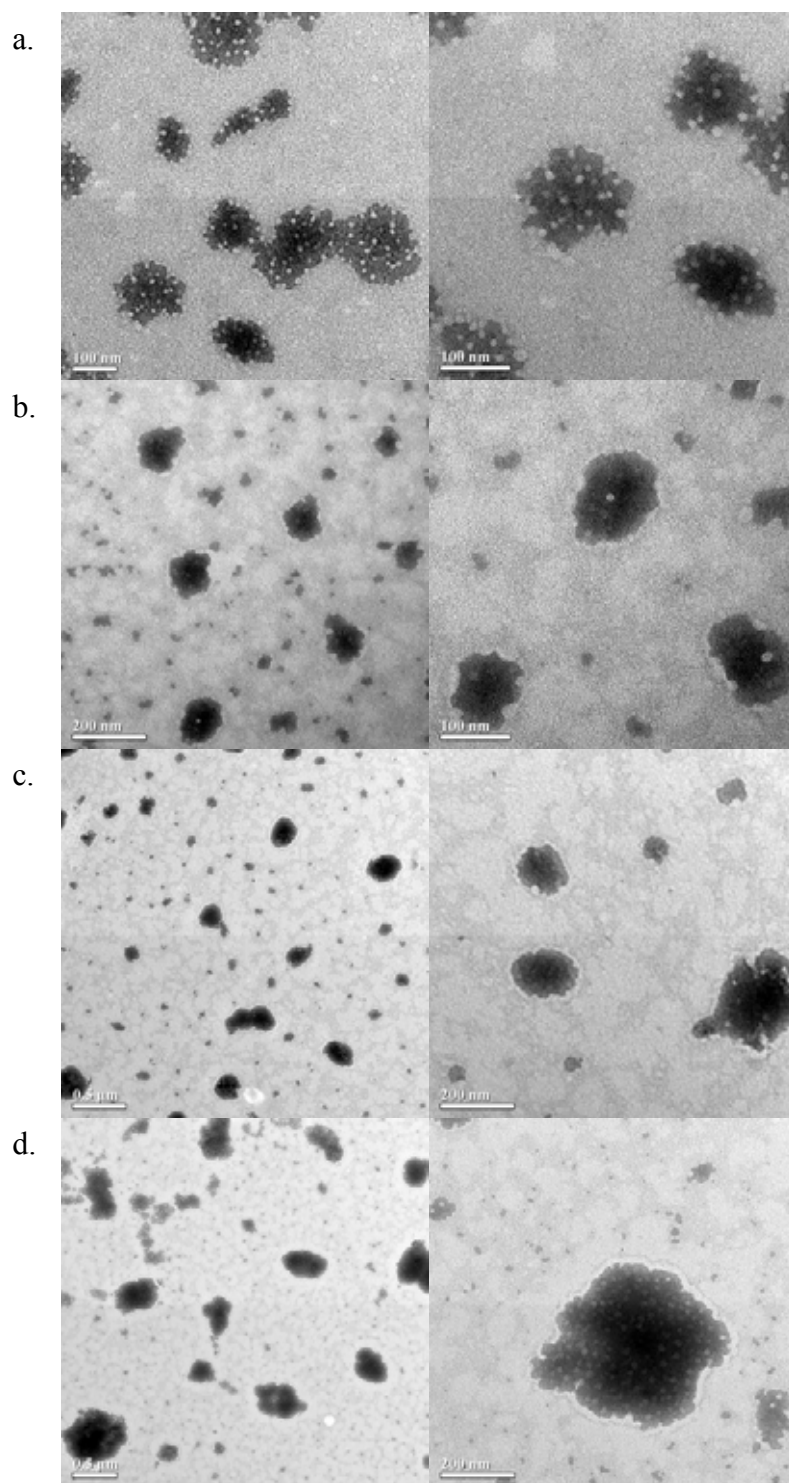
Figure 4-14 TEM photographs of BSA loaded chitosan nanoparticles (a) and BSA loaded chitosan nanoparticles with aluminium hydroxide gel at concentration of 0.1, 0.2 and 0.4 mg/ml (b, c and d, respectively).

3.2 Polymeric interaction

Figure 4-15 shows FTIR spectra of chitosan, chitosan nanoparticles, BSA loaded chitosan nanoparticles and BSA. Three characteristic absorption bands observed in chitosan, at 3435, 1650 and 1321 cm^{-1} are due to the N-H, amide I and amide III groups present in chitosan respectively. According to Yuan et al. (2010), the peak of 3435 cm^{-1} corresponded to stretching vibration of N-H in chitosan but it had shifted to lower wave numbers, 3412 cm^{-1} and widened in chitosan nanoparticles indicating enhanced hydrogen bonding (Wu et al., 2005). Primary amines also showed peak between 3500 and 3400 cm^{-1} which could be attributed to the asymmetric and symmetric stretching of the N-H bonds (Yuan et al., 2010). The peaks in chitosan and chitosan nanoparticles appeared broad in this region due to the contribution of O-H stretching peaks and hydrogen bonding (Zhang and Kosaraju, 2007). FTIR spectrum of BSA showed peaks around 1656, 1534 and 3314 cm^{-1}, reflecting the acetylamino I, acetylamino II and (NH$_2$) groups respectively (Zhang and Kosaraju, 2007). Theoretically, 1656 cm^{-1} as acetylamino I and 1534 cm^{-1} as acetylamino II in BSA should overlap 1650 cm^{-1} of amide I and 1602 cm^{-1} in chitosan, and showed higher intensive peaks for the BSA loaded chitosan nanoparticles. But, because of the low concentration of BSA in the formulation, those peaks of BSA had no effect on FTIR spectrum of chitosan nanoparticles.

Figure 4-16 show FTIR spectra of BSA loaded chitosan nanoparticles without and with aluminium hydroxide gel at different concentrationss. In term of aluminium hydroxide gel, the absorption spectrum could be classified into; region of 3,800-2,400 cm^{-1} as O-H stretching vibration by the absorption of water, 1,200-1,000 cm^{-1} as O-H bending vibration and region of 1,000-400 cm^{-1} as Al-O vibration (Park, Lee and Koo, 2010).

The FTIR spectrum of BSA loaded chitosan nanoparticles with 0.1 mg/ml of aluminium hydroxide gel showed no difference to those without aluninium hydroxide gel due to the small amount. However, the absorption bands observed in BSA loaded chitosan nanoparticles, at 1571 and 1410 cm^{-1}, reflecting the amide II and amide III, showed decreasing of intensity with the appearance of peak 734 and 623 cm^{-1}, refering
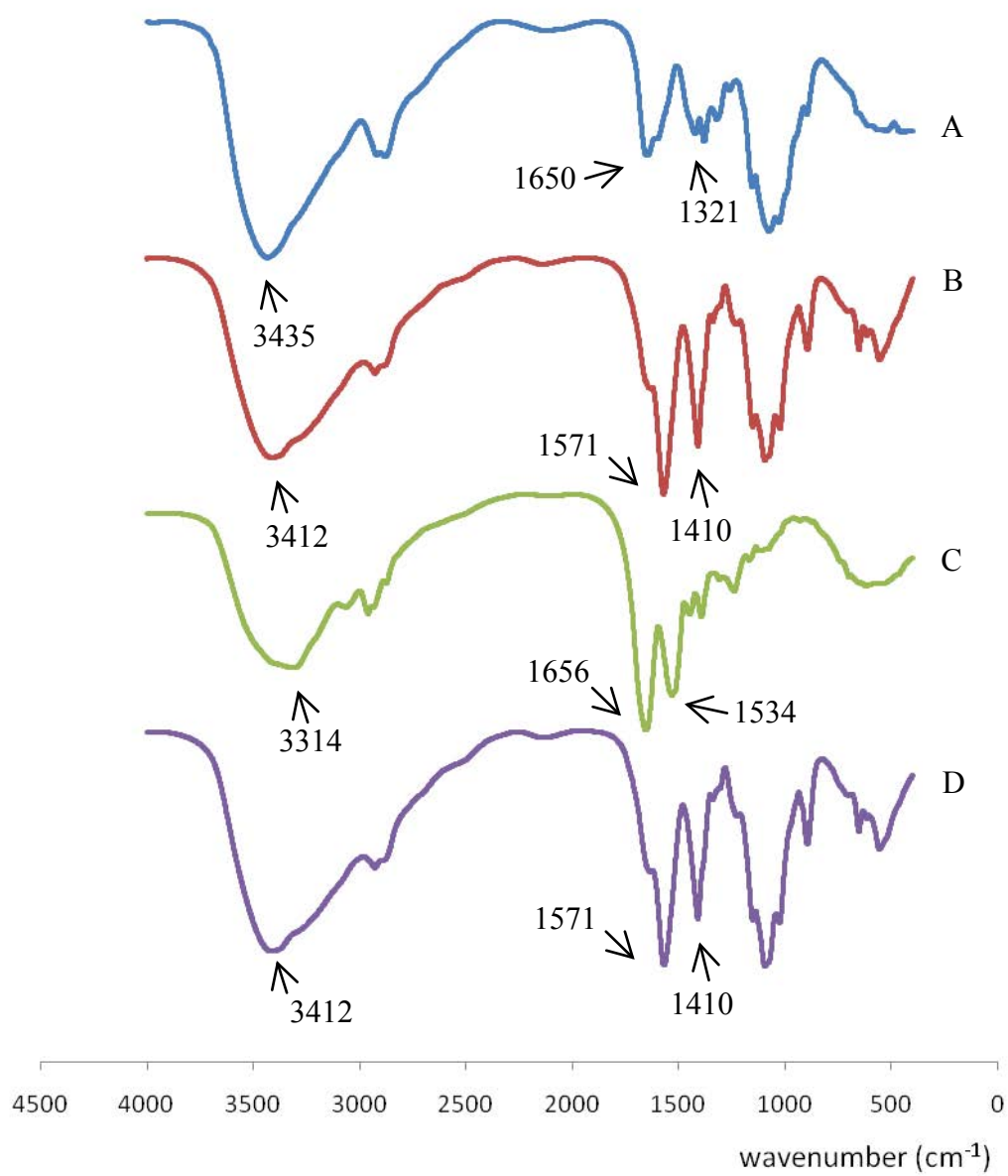
Figure 4-15 FTIR spectra of chitosan (A), chitosan nanoparticles (B), BSA (C) and BSA loaded chitosan nanoparticles (D).
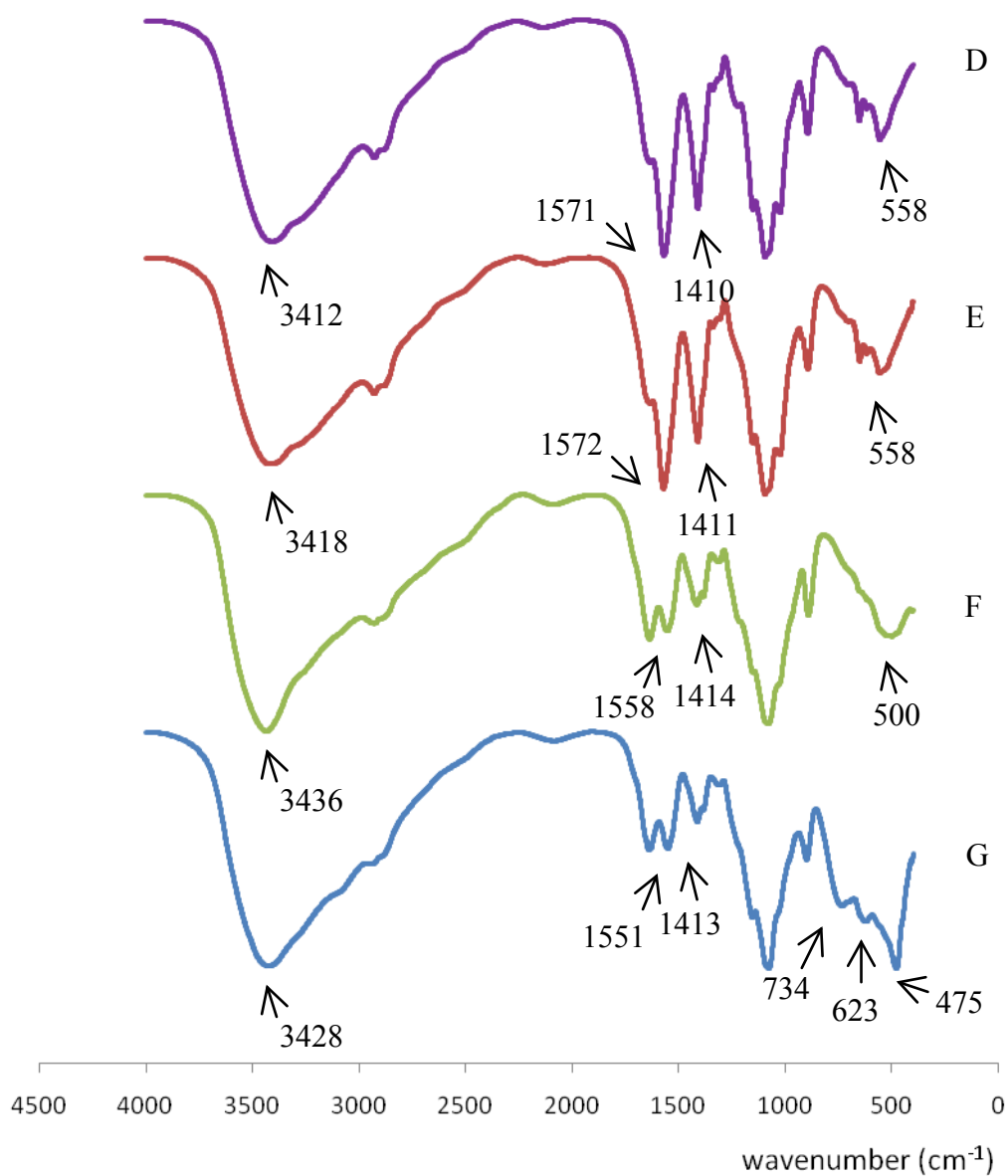
Figure 4-16 FTIR spectra of BSA loaded chitosan nanoparticles (D) and BSA loaded chitosan nanoparticles with aluminium hydroxide at concentration of 0.1, 0.2 and 0.4 mg/ml. (E, F and G, respectively).

to stretching mode of Al-NH$_2$ bond (Himmel, Downs and Greene, 2000) and symmetric stretching mode of Al-OH bond (Tzoupanos and Zouboulis, 2010), respectively, when added with 0.4 mg/ml of aluminium hydroxide gel. These provided the indication that there was an interaction or conjugation between aluninium hydroxide gel and chitosan nanoparticles (Ng et al., 2012).

3.3 Loading efficacy of BSA from chitosan nanoparticles

There are two phenomena of BSA loading in nanoparticles; entrapment into nanoparticles and adsorption on the nanoparticle surface. BSA was entrapped into nanoparticles by interactions between opposite charge of chitosan and BSA and formation of hydrogen bonds between the TPP and BSA (Kafshgari et al., 2011).

The BSA loaded chitosan nanoparticles with 0.1, 0.2 and 0.4 mg/ml of aluminium hydroxide gel displayed loading efficiency of 52.47±2.99%, 55.65±0.56%, 56.56±0.66%, and 49.79±4.98%, 50.34 ±4.77%, 50.67±2.22% for 30 and 60 μg/ml BSA, respectively, while showed 47.92±3.66% and 47.35±4.47% for samples without aluminium hydroxide gel.

From the results, the formulations loading with 30 μg/ml BSA showed more loading efficiency than the formulations loading with 60 μg/ml BSA. It might attributed to the saturated absorption was achieved and the more addition of BSA was seldom absorbed onto the nanoparticles (Xing et al., 2008).

Moreover, some of BSA might be adsorbed onto the aluminium hydroxide gel layer on the surface of the particles leading to the increase in loading efficiency when increasing amount of aluminium hydroxide gel.

3.4 Particle aggregation study

The aggregation study of BSA loaded chitosan nanoparticles was conducted to evaluate the stability of the nanoparticles because the usages of chitosan nanoparticles with consistent characteristics, such as the size of nanoparticles in suspension over long periods of time, was very important (Tsai et al., 2011). Lopez-Leon et al. (2005) reported that the chitosan/TPP nanogel particles, stored at 5 and 20$^{\text{O}}$C in non-buffer solution (pH 5-6) containing 1 mM of KBr, resulted the increasing average diameter and standard deviation of chitosan nanoparticles with time.

In this study, the formulations of chitosan nanoparticles loaded with 30 and 60 mg/ml of BSA both unconjugated and conjugated with aluminium hydroxide gel, 0.1, 0.2 and 0.4 mg/ml, were prepared and stored in refrigerator (2-8$^{\text{o}}$C). The figure 4-17 showed the average particle size of the formulation at different time interval. The particle sizes of BSA loaded chitosan nanoparticles and chitosan nanoparticles conjugated with 0.1 and 0.2 mg/ml of aluminium hydroxide gel did not show any trend of increase or decrease on particle sizes. The standard deviations were very small in the formulations, unconjugated and conjugated with 0.1 mg/ml of aluminium hydroxide gel but much wider in formulation with 0.2 mg/ml. On the other hand, the formulations conjugated with 0.4 mg/ml of aluminium hydroxide gel showed a trend of changing in particle sizes. The average particle sizes were fluctuated and the standard deviation shown large numbers. It might due to the excess aluminium hydroxide gel loosely attached the particles together, including with collision and adhesion, leading to the particles aggregation. The zeta potentials gradually increased with time as shown in figure 4-18.
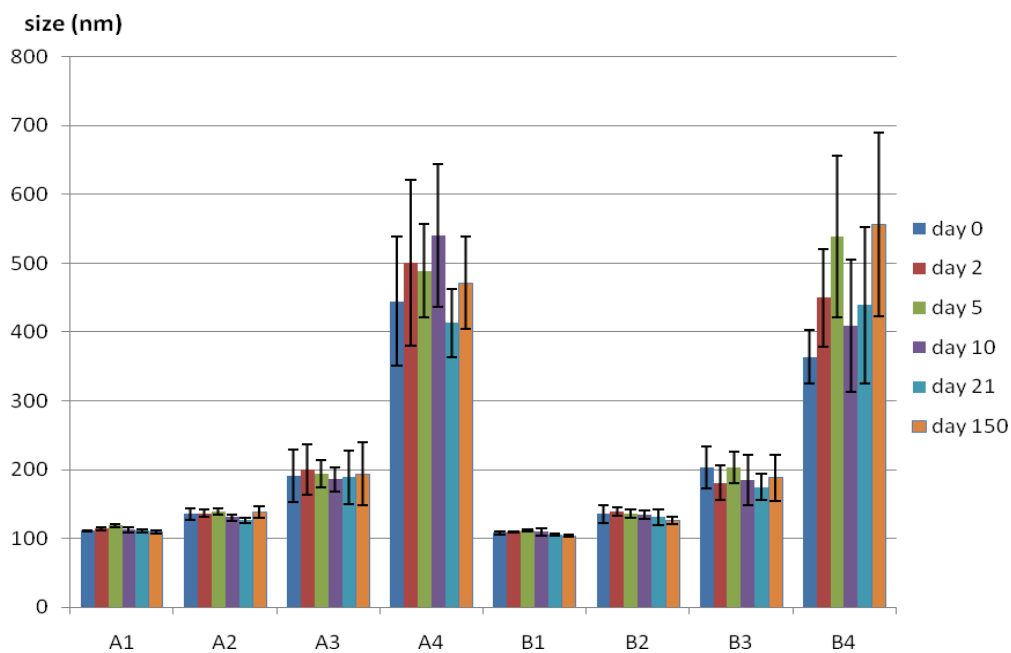
Figure 4-17 The aggregation study on particle sizes of chitosan nanoparticles loaded with 30 and 60 mg/ml of BSA (A and B, respectively) and conjugated with 0.0, 0.1, 0.2 and 0.4 mg/ml of aluminium hydroxide gel (as 1, 2, 3 and 4, respectively).
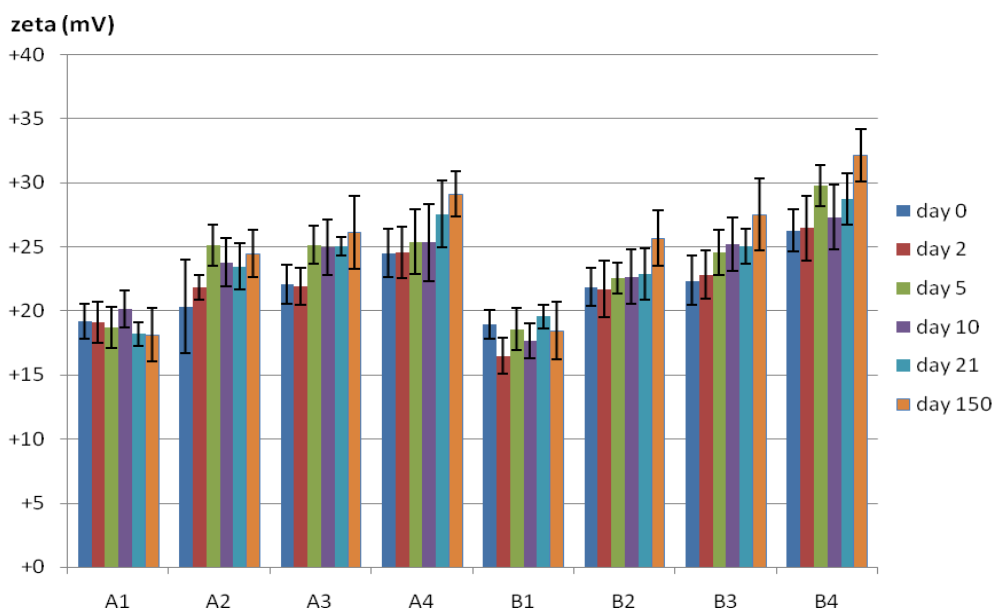
Figure 4-18 The aggregation study on zeta potentials of chitosan nanoparticles loaded with 30 and 60 mg/ml of BSA (A and B, respectively) and conjugated with 0.0, 0.1, 0.2 and 0.4 mg/ml of aluminium hydroxide gel (as 1, 2, 3 and 4, respectively).

4. Protein properties

Proteins are highly complex biomolecules with specific functions. Their biological functions depend on the protein structures. When the structure was changed or denatured, the proteins might not function properly. So the integrity of the protein structure was very important. In the process of loading BSA or any protein in the particles, such as coacervation (de Kruif, Weinbreck and de Vries, 2004), freeze drying (Zijlstra et al., 2009), spray drying (Benchabane, Subirade and Vandenberg, 2007) or even mild method as ionotropic gelation, there were many factors which might affect the protein stability. In the preparation, the protein was exposed to mechanical force as magnetic stirring and also the acidic condition. These factors might cause denaturation and loss of protein activity. Therefore, protein integrity was necessary to be evaluated after the manufacturing.

4.1 Sodium Dodecyl Sulphate-Polyacrylamide Gel Electrophoresis

The SDS-PAGE was the technique to evaluate the primary structure of protein. It can provide information about the molecular weights, charges of proteins and purity of protein preparation. The different protein molecular weight or sizes were separated by different moving rate in polyacrylamide gel. The protein with lower molecular weight can move faster than higher molecular weight.

SDS-PAGE revealed both native and extracted BSA as shown in figure 4-19. The BSA, molecular weight of 66.4 kDa (Determan et al., 2004), in PBS buffer was seen as lane 2. It showed no difference to others with different solvents as lanes 3 and 4. Moreover, the SDS-PAGE bands of the extracted BSA from chitosan nanoparticles, without or with aluminium hydroxide gel in different concentrations, showed no additional bands that would indicate the aggregation or fragmentation was visible. These indicated that the primary structure of BSA loaded in chitosan nanoparticles, prepared as optimized conditions, was generally conserved.
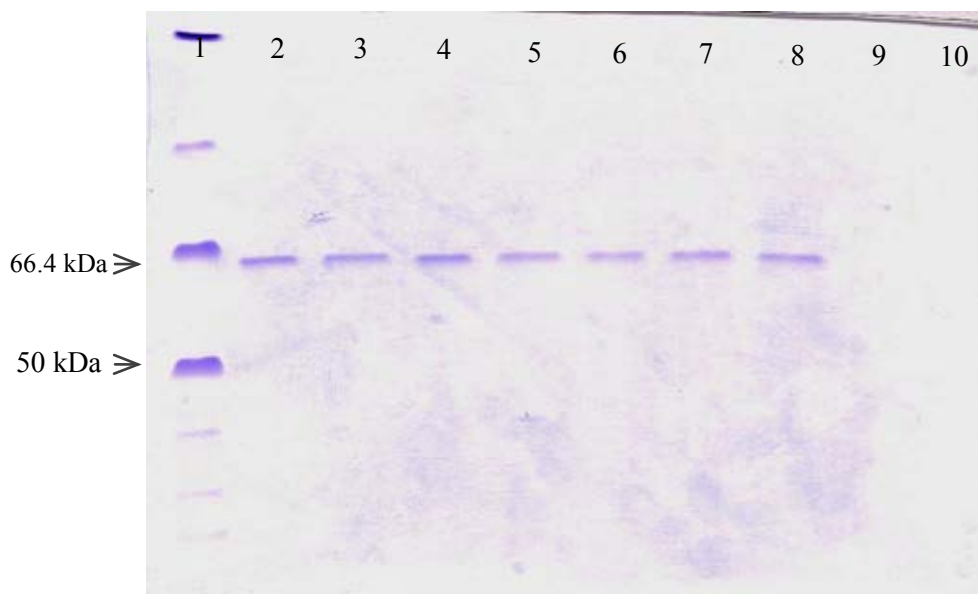
Figure 4-19 SDS-PAGE bands of native BSA and extracted BSA from the chitosan nanoparticles.

Lane 1: molecular weight markers

Lane 2: native BSA in PBS

Lane 3: native BSA in PBS + 10% (w/v) NaCl

Lane 4: native BSA in 2% (v/v) acetic acid

Lane 5: BSA loaded CSNPs + 10% (w/v) NaCl

Lane 6: BSA loaded CSNPs with 0.1 mg/ml $Al(OH)_3$ + 10% (w/v) NaCl

Lane 7: BSA loaded CSNPs with 0.2 mg/ml $Al(OH)_3$ + 10% (w/v) NaCl

Lane 8: BSA loaded CSNPs with 0.4 mg/ml $Al(OH)_3$ + 10% (w/v) NaCl

Lane 9: CSNPs

Lane 10: CSNPs + 10% (w/v) NaCl

4.2 Circular dichroism (CD) measurement

CD spectroscopy is used to examine the secondary and tertiary structure of protein release from the formulations. CD spectroscopy can determine the protein secondary structure in the far-UV spectral region (190-250 nm), while observe the tertiary structure in the near-UV spectral region (250-320 nm) (Ranjbar and Gill, 2009).

However, the tertiary structure could not be observed in this study because of the very low concentration of BSA in the formulations.
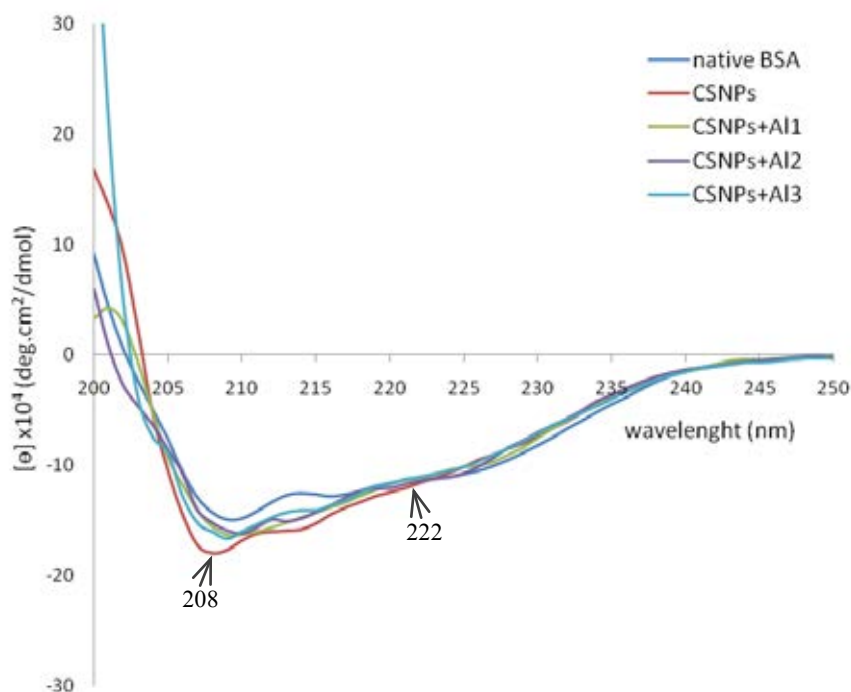
Figure 4-20 CD spectra of native BSA, BSA extracted from chitosan nanoparticles (CSNPs), chitosan nanoparticles with 0.1, 0.2 and 0.4 mg/ml aluminium hydroxide gel (CSNPs+Al1, CSNPs+Al2 and CSNPs+Al3, respectively).

CD spectroscopy measured the conformational change of the encapsulated BSA compared with the native one. The native BSA had two extreme valleys at 208 and 222 nm and the CD spectra might change after formulation processes. There were many stresses affected to protein integrity, such as high temperature or acidic condition. Kusonwiriyawong et al. (2009) reported that molar ellipticity decreased when dissolved protein in acidic solution. Figure 4-20 shows CD spectra of native BSA and BSA extracted from chitosan nanoparticles without or with aluminium hydroxide gel in concentration of 0.1, 0.2 and 0.4 mg/mL. Even the formulations were prepared in acidic condition but with pH adjusting before cross-linking and other optimized conditions, the CD spectra of native BSA and released BSA from the formulations showed not much difference on the shape of spectra and molar ellipticities. The results indicated

that there was no significant conformational change in BSA encapsulated in chitosan nanoparticles with aluminium hydroxide gel.

5. Mucoadhesive evaluation

The mucoadhesive property of the formulations was determined by the percentage of washed FITC-BSA from the tissue surface over time. The high percentage of washed FITC-BSA represented the low efficiency of mucoadhesive property. The results showed that the control, FITC-BSA in PBS buffer, was washed out about 75% instantaneously from the mucous tissue and reached 100% within 15 minutes. While the washed out patterns of FITC-BSA from the particulate formulations were not different among each other. As shown in figure 4-21, the FITC-BSA in the particulate formulations were washed out about 40% at first 5 minutes and 60% in 15 minutes, then gradually increased to 70% approximately at 60 minutes. Regarding to the loading efficiency of the particulate formulations which were around 50 - 56%, thus the 44 - 50 % of non-entrapped FITC-BSA was washed out immediately in the first period then the loaded FITC-BSA nanoparticles were washed out from time to time. The results indicated that the particulate formulations had similar mucoadhesive property but dramatically higher compared to control.
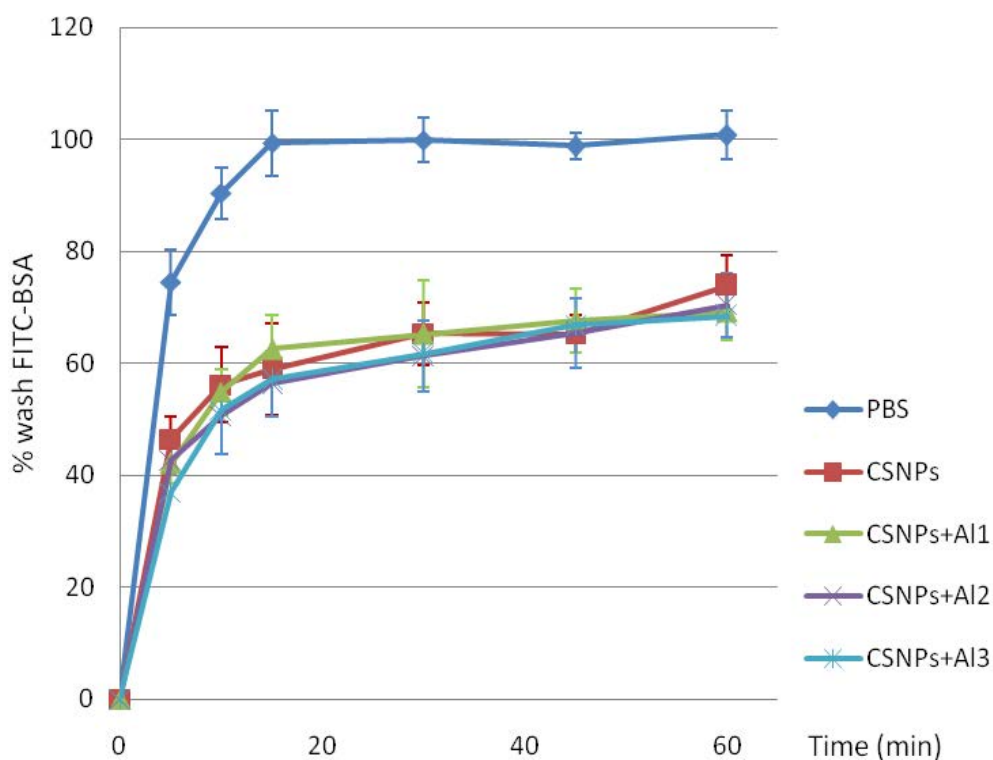
Figure 4-21 The percentage of washed FITC-BSA representing the mucoadhesive property on mucous tissue of FITC-BSA in PBS buffer (control), chitosan nanoparticles (CSNPs) and chitosan nanoparticles conjugated with 0.1, 0.2 and 0.4 mg/ml of aluminium hydroxide gel (CSNPs+Al1, CSNPs+Al2 and CSNPs+Al3, respectively).

6. *In vitro* study in cell culture

6.1 Cytotoxicity study

The cytotoxicity of BSA loaded chitosan nanoparticles without and with aluminium hydroxide gel at concentration of 0.1, 0.2 and 0.4 mg/ml was investigated by MTT assay as an indicator of cellular mitochondrial dehydrogenase activity. The MTT assay measures the cell metabolic activity by mitochondrial dehydrogenase enzyme in the viable cells. The enzyme oxidizes the yellow tetrazolium salt, 3-[4,5-dimethylthiazol-2-yl]-3,5-diphenyl tetrazolium bromide dye, to a purple formazan crystals (Nasti et al., 2009). Thus the dead or damaged cells show no or reduced dehydrogenase activity. The optical density of the dissolved formazan from the cell lysate is linear correlated with the dehydrogenase activity and reflects the cell viability.

In this study, the MTT assay was performed in RPMI 2650 cells (passage 37) to evaluate the effect of the formulations on cell viability before animal testing. Thus the formulations were prepared with the same concentration and applied the same volume as applied in animal. Figure 4-22 shows the percentage of nasal cell viability after incubated with the formulations compared to cell culture medium (100%). The BSA loaded chitosan nanoparticles showed the highest percentage as 102.97±7.37% viability while the other formulations were relatively non-toxic to nasal cell. The lowest percentage of cell viability was 84.76±8.60% derived from BSA loaded chitosan nanoparticles conjugated with 0.4 mg/ml of aluminium hydroxide gel. However, the percentage of cell viability tended to decrease with increasing of aluminium hydroxide gel. It might due to the increasing of aluminium hydroxide gel leaded to increasing of zeta potential as shown in figure 4-18. The higher positive charge induced stronger interference with cell membrane (negative charged), leading to increasing of cytotoxicity (Mao et al., 2007).
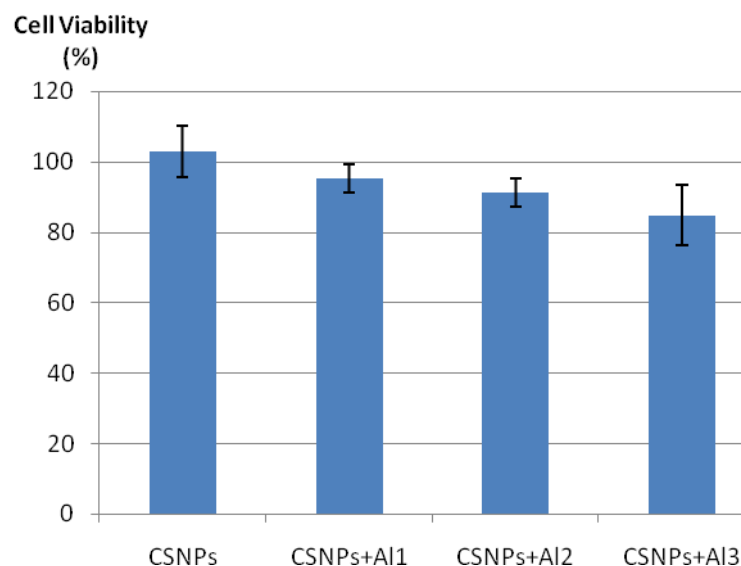
Figure 4-22 The percentage of nasal cell viability after incubated with BSA loaded chitosan nanoparticles (CSNPs) and BSA loaded chitosan nanoparticles conjugated with 0.1, 0.2 and 0.4 mg/ml of aluminium hydroxide gel (CSNPs+Al1, CSNPs+Al2 and CSNPs+Al3, respectively).

6.2 Cellular uptake study

The protein administered through the nasal cavity can permeate by both paracellular pathway and transcellular pathway. The main proposed mechanism of absorption for the macromolecular substances such as protein is endocytosis via NALTs (Wu and Russell, 1997). However, the application of monoculture of RPMI 2560 for drug transport study has been reported (Cho et al., 2010).

The cellular uptake study was conducted in RPMI 2650 cells (passage 42) to evaluate the transcellular transportation of the formulations which was expected to be enhanced by the optimized formulations. Figure 4-23 shows histograms of flow cytometry of RPMI 2650 cells before uptake study as a baseline and RPMI 2650 cells after 2 hours incubated with FITC-BSA in PBS buffer, FITC-BSA loaded chitosan nanoparticles, FITC-BSA loaded chitosan nanoparticles conjugated with 0.1, 0.2 and 0.4 mg/ml of aluminium hydroxide gel, detected with G1 detector for green fluorescence.
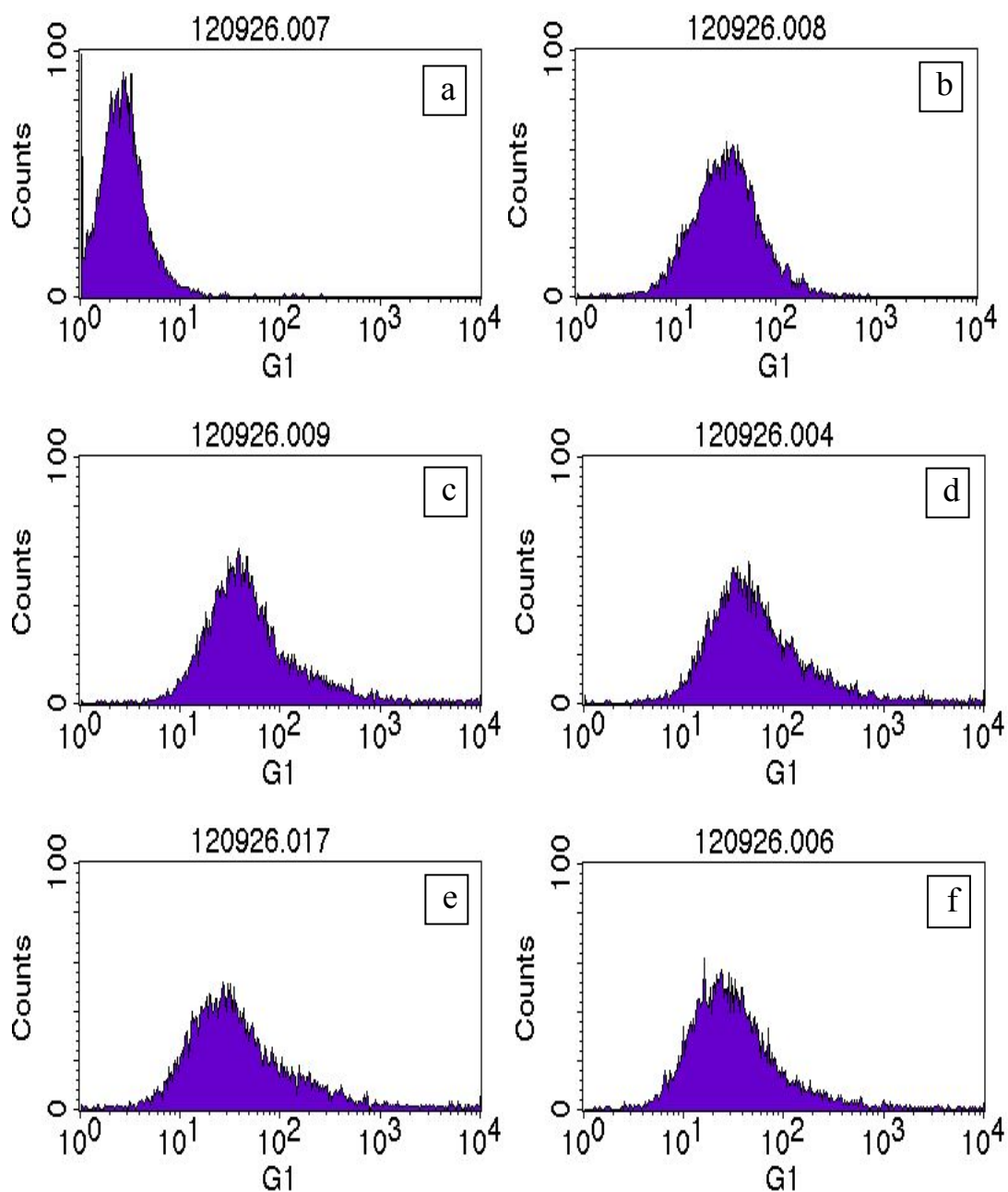
Figure 4-23 FACS of RPMI 2650 cells: before uptake study (a), after 2 hours uptake studied of FITC-BSA in PBS buffer (b), FITC-BSA loaded chitosan nanoparticles (c), FITC-BSA loaded chitosan nanoparticles conjugated with 0.1, 0.2 and 0.4 mg/ml of aluminium hydroxide gel (d, e and f, respectively).
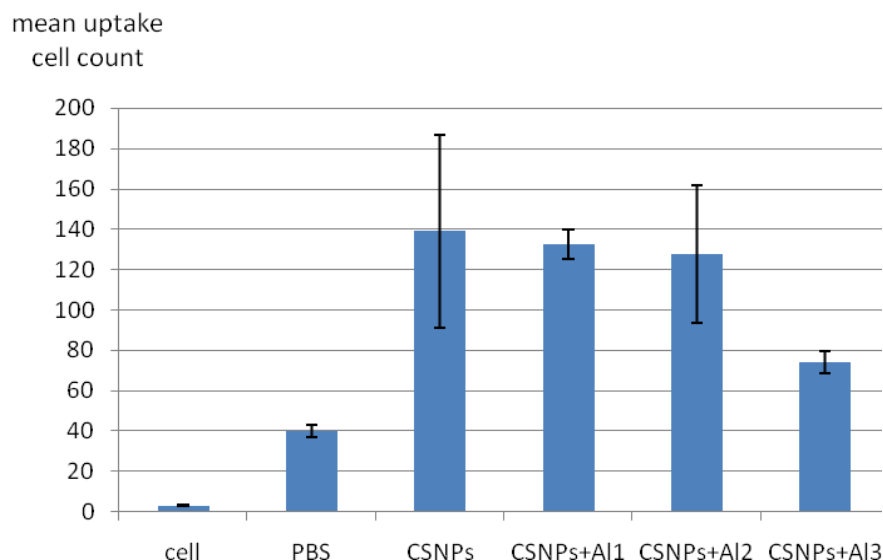
Figure 4-24 The mean uptake cell count of RPMI 2650 cells, before uptake study and after 2 hours uptake studied of FITC-BSA in PBS buffer (PBS), FITC-BSA loaded chitosan nanoparticles (CSNPs), FITC-BSA loaded chitosan nanoparticles conjugated with 0.1, 0.2 and 0.4 mg/ml of aluminium hydroxide gel (CSNPs+Al1, CSNPs+Al2 and CSNPs+Al3, respectively).

Various intensities of positive event as fluorescence-assisted cell or uptake cell were shown in figure 4-23. The data from the histograms could be analysed as shown in figure 4-24. The mean uptake cell count of RPMI 2650 incubated with FITC-BSA in PBS was very small while the cells incubated with nanoparticle formulations were higher. It may due to the nanoparticle formulations had mucoadhesive property which provided an intimate contact of particles with cells, prolonged residence time and also provided higher drug concentration at absorption sites which facilitated drug transport (Yin et al., 2009).

The averages of mean uptake cell count of RPMI 2650 incubated with the nanoparticles formulations were not obviously different (p>0.05), excepted the cells incubated with FITC-BSA loaded chitosan nanoparticles conjugated with 0.4 mg/ml of aluminium hydroxide gel showed dramatically lower than the others. It might due to the excess of aluminium hydroxide gel attach the particles together, leading to the particles aggregation. The relative large particle size might be less preferable for cell uptake (Desai et al., 1997).

6.3 Permeation Study

Nasal M-cell model was used for permeation study. The nasal M-cell is composed of RPMI 2650 and Raji cells coculture, figures 4-25 a. and b., respectively. After the RPMI 2650 cells (passage 50) and Raji cells (passage 15) were seeded in 6 wells Transwell®, culture medium was changed regularly until 100% confluence was reached. The monolayer integrity was firstly assessed by the inverted microscope and confirmed before permeation study by measurement of TEER value.

a.

b.
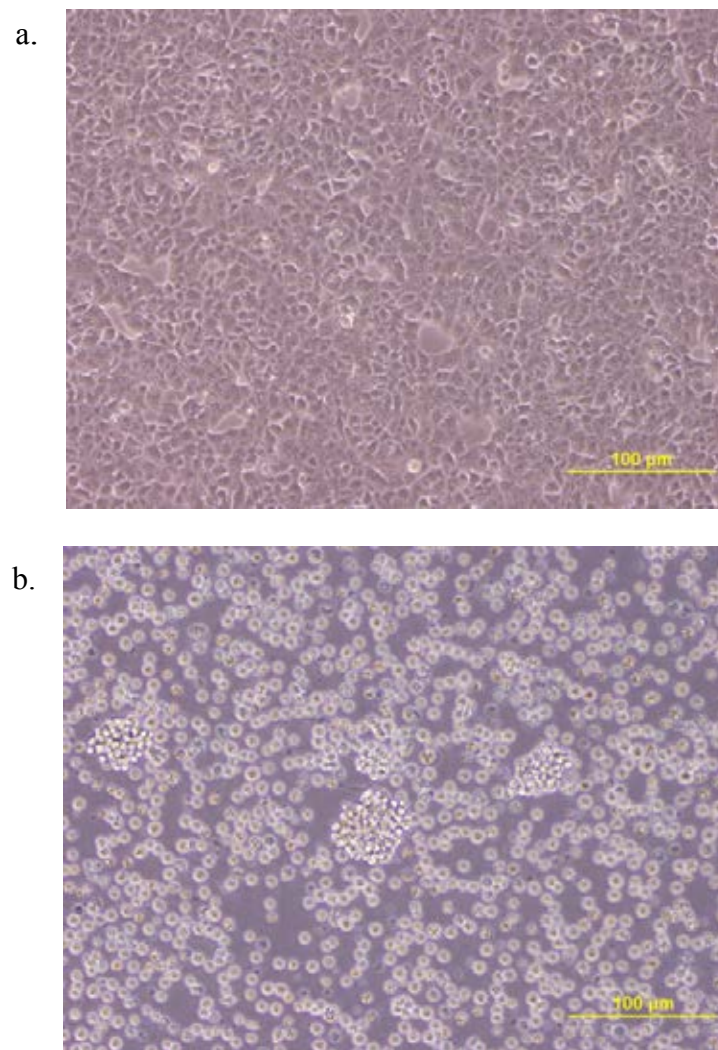
Figure 4-25 Optical micrographs of RPMI 2650 cells at 80% confluence (a) and Raji cells (b).
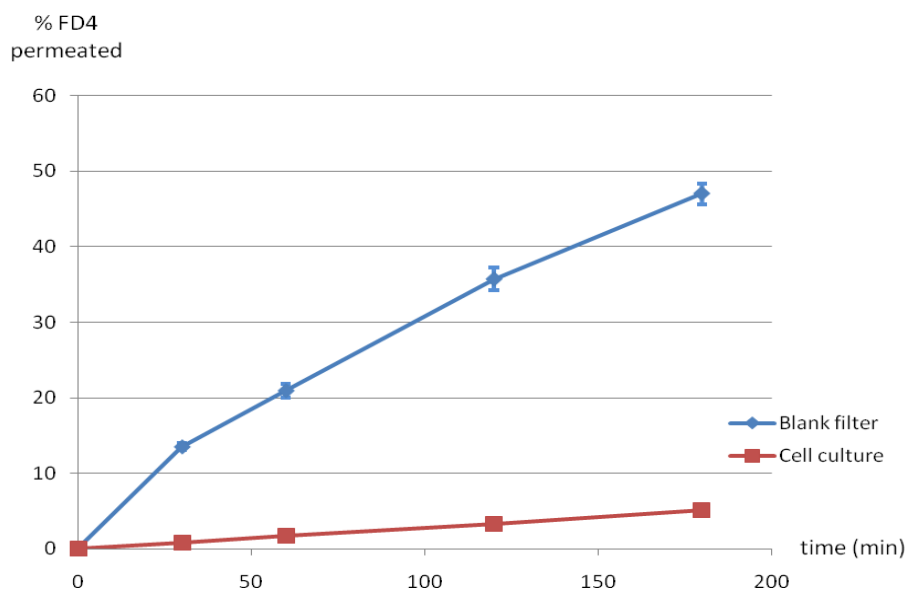
Figure 4-26 The permeation profile of FD-4 in PBS though cell culture and blank filter.

The integrity of epithelial monolayer was determined by Fluorescein isothiocyanate conjugated dextran, molecular weight 4000 Da (FD-4) which molecular weight was larger than normal tight junction of epithelial monolayer. From figure 4-26, the permeation profiles across the cell monolayer showed much lower permeation of FD-4 through the cell monolayer than through blank filter which confirmed the barrier function of cell monolayer model.

The TEER values of the confluent monolayers, before study, reached 130.87±5.72 $\Omega \cdot cm^2$, 129.36±9.82 $\Omega \cdot cm^2$, 130.36±4.36 $\Omega \cdot cm^2$, 134.39±9.82 $\Omega \cdot cm^2$, and 130.36±9.82 $\Omega \cdot cm^2$ for FITC-BSA in PBS, FITC-BSA loaded chitosan nanoparticles and FITC-BSA loaded chitosan nanoparticles conjugated with 0.1, 0.2 and 0.4 mg/ml of aluminium hydroxide gel, respectively. During permeation study, incubation of cell monolayers with formulations showed slightly reduction in the resistance in similar profile as shown in figure 4-27. It indicated that the formulations could not open the tight junction. This contrasts to the report that chitosan, a cationic polysaccharide, can adhere to the epithelial surface to impart transient opening of the tight junctions (Smith, Wood and Dornish, 2004). It might be because of the low concentration of chitosan in the formulations that not enough to induce transient

loosening of tight junction through electrostatic interaction (van der Merwe, S.M. et al., 2004). Vllasaliu et al. (2010) reported that the minimum concentrations of chitosan nanoparticle which able to decrease TEER values of Caco-2 cells and Calu-3 cells were 0.0125 and 0.003% (w/v), respectively. In this study, the chitosan nanoparticle concentration was 0.0047% (w/v) but could not obviously decrease the TEER values. It might due to the different kinds of cell cultures needed different concentrations of chitosan nanoparticles to loose the tight junction.
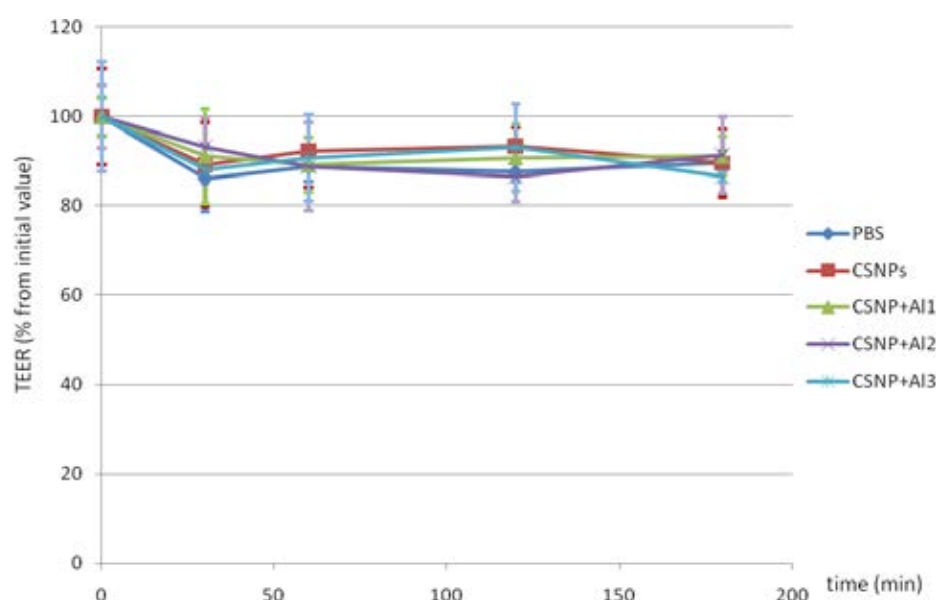
Figure 4-27 Effect of formulations on the TEER value during permeation study. FITC-BSA in PBS (PBS), FITC-BSA loaded chitosan nanoparticles (CSNPs), FITC-BSA loaded chitosan nanoparticles conjugated with 0.1, 0.2 and 0.4 mg/ml of aluminium hydroxide gel (CSNPs+Al1, CSNPs+Al2 and CSNPs+Al3, respectively).

Figure 4-28 shows the permeation profiles of the formulations. The FITC-BSA in PBS revealed higher permeation than the nanoparticle formulations. While the profiles were not different among nanoparticle formulations. There were reported that ovalbumin in PBS showed higher permeation than ovalbumin in chitosan nanoparticles in mono-culture model but showed a lot lower permeation in co-culture model (Slütter et al., 2009). The correlate results also reported by Pichayakorn et al. (2008). Therefore the results rather correlated to the permeation in mono-culture model than co-culture model.
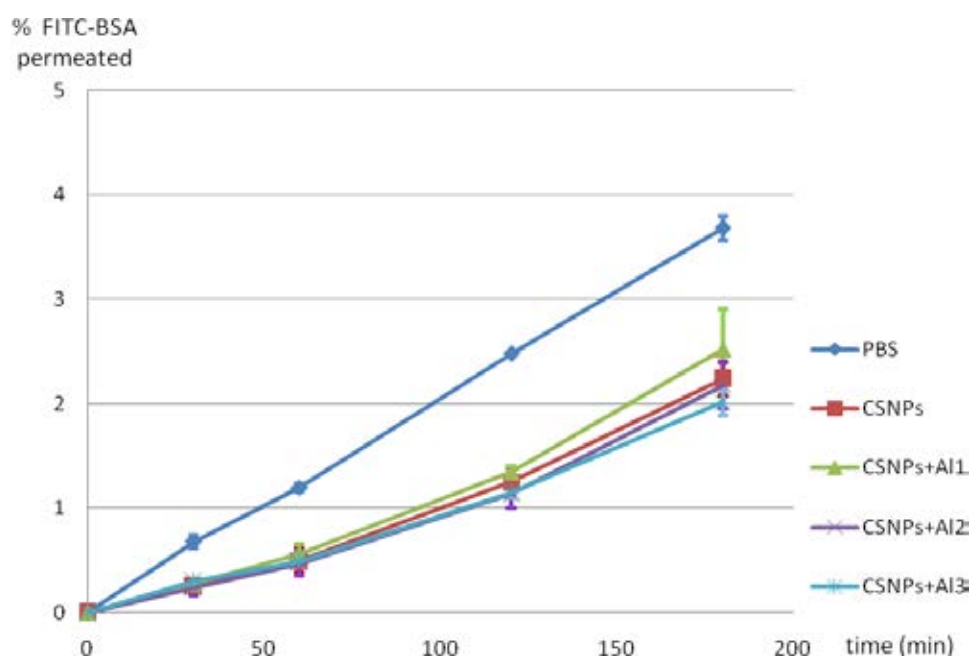
Figure 4-28 The permeation profile of FITC-BSA in PBS (PBS), FITC-BSA loaded chitosan nanoparticles (CSNPs), FITC-BSA loaded chitosan nanoparticles conjugated with 0.1, 0.2 and 0.4 mg/ml of aluminium hydroxide gel (CSNPs+Al1, CSNPs+Al2 and CSNPs+Al3, respectively).

The scanning electron microscope (SEM) spectroscopy was used for examination of cell morphology. The cell models were prepared as RPMI 2650 cell monolayer and nasal M-cell model as described previously. The cell models were fixed with 2% glutaraldehyde in 0.1M PBS. Then the cell models were rinse for 5 minutes with PBS and ultrapure water, dehydrated 3 times with gradient concentrations of 30, 50, 70, 90 and 100% ethanol, respectively. Before observed under SEM, the samples had to be dried by the critical point dryer and coated with gold.

Figure 4-29 shows the SEM photomicrographs of cell models prepared as RPMI 2650 cell monolayer (a) and nasal M-cell model (b). The nasal M-cell model was expected to show the area with less microvilli than normal monoculture of RPMI 2650 as described by Pichayakorn et al. (2008). However, the pictures showed no difference, without the expected area, which indicates that the cell model possibly established only monoculture of RPMI 2650.
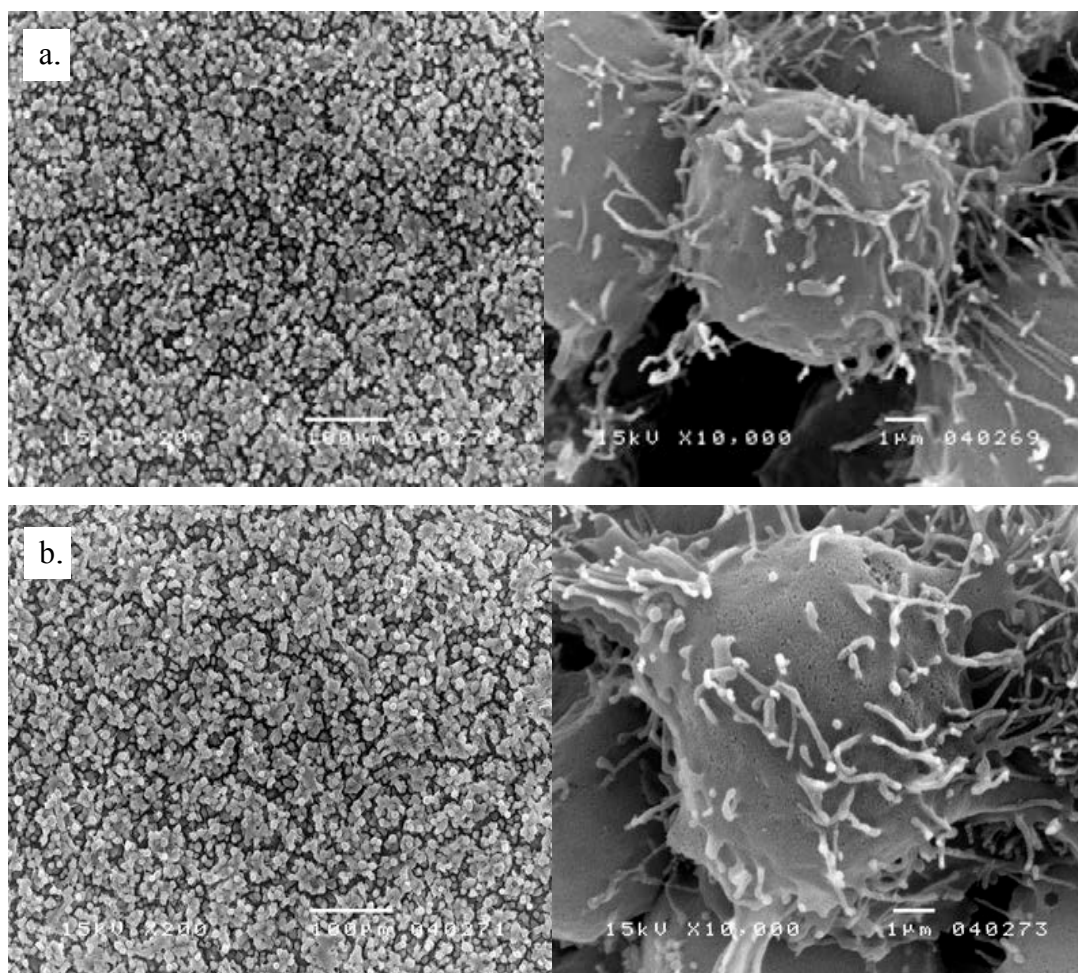
Figure 4-29 The SEM photomicrographs, at 200x and 10,000x, of cell models, prepared as RPMI 2650 cell monolayer (a) and nasal M-cell model (b).

Even the nasal M-cell model could not be established, but the monoculture RPMI 2650 cells monolayer was also used for the permeation study. Bai et al. (2008) reported that RPMI 2650 cells could form confluent cell monolayer and developed enough TEER values under air-liquid interface culture condition. Moreover, the RPMI 2650 cell monolayer was used for evaluation of spray-dried mucoadhesive microspheres permeation (Harikarnpakdee et al., 2006).

As figure 4-28, the FITC-BSA in PBS revealed higher concentration in basolateral compartments than the nanoparticle formulations. But the figure 4-30 revealed high level of FITC-BSA remained in the cell monolayer after the permeation study. The PBS formulation showed very low amount of FITC-BSA remained in the

cells, while the nanoparticle formulations showed dramatically higher amount of FITC-BSA (p<0.05, excepted the 0.4-mg/ml conjugated formulation). The maximum FITC-BSA concentration was derived from FITC-BSA loaded chitosan nanoparticles conjugated with 0.1mg/ml of aluminium hydroxide gel and decreased with increasing of aluminium hydroxide gel concentration which correlated to the results from the cellular uptake study.
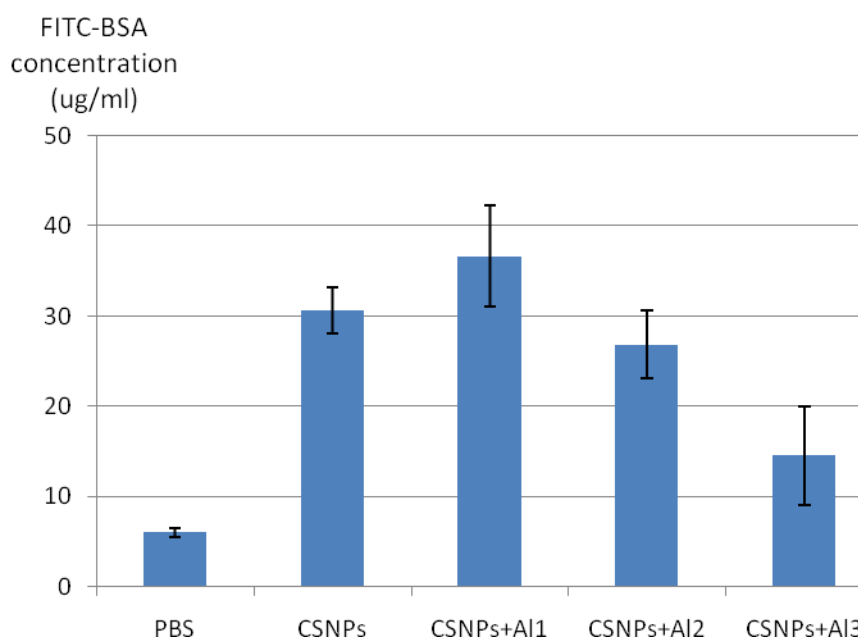
Figure 4-30 The amount of lysated BSA-FITC from each formulation after permeation study. FITC-BSA in PBS buffer (PBS), FITC-BSA loaded chitosan nanoparticles (CSNPs), FITC-BSA loaded chitosan nanoparticles conjugated with 0.1, 0.2 and 0.4 mg/ml of aluminium hydroxide gel (CSNPs+Al1, CSNPs+Al2 and CSNPs+Al3, respectively).

With the result from permeation study and all previous studies, the BSA loaded chitosan nanoparticles conjugated with 0.1 mg/ml of aluminium hydroxide gel was used to prepare influenza vaccine formulation for testing in animals.

7. Immunization studies

The aim of this study was to evaluate the immunogenicity of the optimized chitosan nanoparticles conjugated with aluminium hydroxide gel administrated intranasally. The whole inactivated Influenza A (H1N1) virus, strain A/Taiwan/1/86 antigen, was used as the vaccine antigen and immunized in mice model. The serum immune responses of mice after intranasal vaccination with the antigen solution, antigen loaded chitosan nanoparticles, antigen loaded chitosan nanoparticles conjugated with aluminium hydroxide gel and intramuscular vaccination with antigen solution, as positive control, were compared. The anti-influenza (H1N1) antigen-specific total serum IgG responses of vaccinated mice were showed in figure 4-31. After single vaccination, antigen solution, antigen loaded chitosan nanoparticles showed poor immune response of having low serum IgG titers only in 2/8 (2 responded mice from 8 immunized mice) and 3/8 mice respectively. While antigen loaded chitosan nanoparticles conjugated with aluminium hydroxide gel showed dramatically higher serum IgG titer but also showed only in some mice (4/8). In contrast, the intramuscular vaccination of antigen solution was able to generate significantly higher IgG antibody titers in all mice ($p<0.05$).

Because intranasal immunization usually requires booster vaccination to induce strong immune responses (de Haan et al., 2001; van der Lubben et al., 2003), thus 2 boosters of additional formulations, excepted PBS buffer, were nasally vaccinated. The mice nasally administrated with antigen solution showed no increasing of serum IgG antibody titers but increased the number of responded mice to 3 and 4 mice for the first and second booster. While the serum IgG titers of mice vaccinated with antigen loaded chitosan nanoparticles and antigen loaded chitosan nanoparticles conjugated with aluminium hydroxide gel were gradually increased with the increased number of responded mice. After the second booster, the serum IgG titers of the latter showed higher than the first. Moreover, both IgG and number of responded mice (8/8) were not different from the intramuscular vaccinated mice ($p>0.05$). This indicated that antigen loaded chitosan nanoparticles conjugated with aluminium hydroxide gel administrated intranasally could induce serum IgG immune response better than the unconjugated.
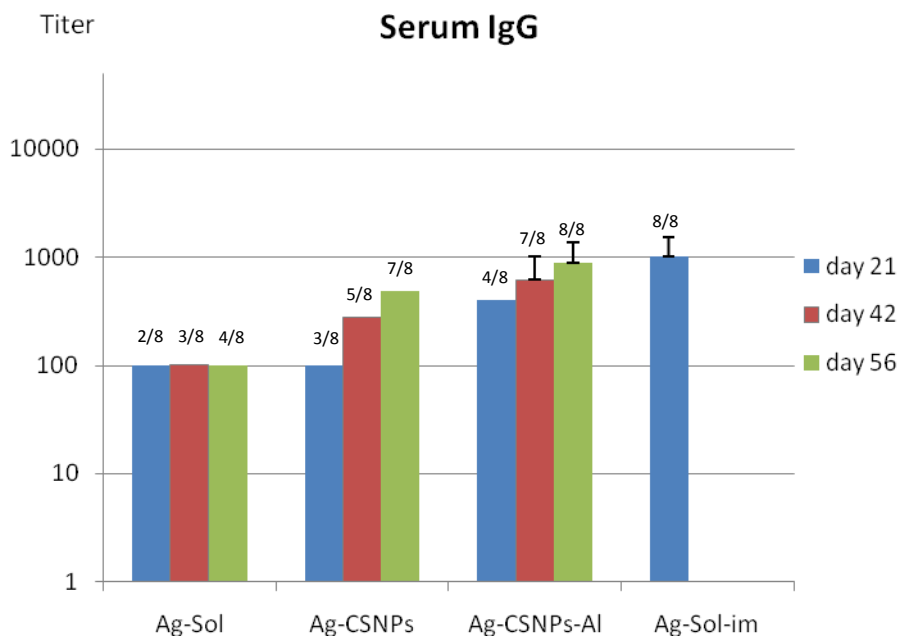
Figure 4-31 Anti-influenza (H1N1) antigen-specific total serum IgG responses in mice after intranasal vaccination with the antigen solution, antigen loaded chitosan nanoparticles, antigen loaded chitosan nanoparticles conjugated with aluminium hydroxide gel, and intramuscular vaccination with antigen solution.

The IgG subtype (IgG1 and IgG2a) profiles of the influenza-specific antibodies are shown in figures 4-32 and 4-33. The subtype profile of intramuscular immunization with antigen solution resulted in predominant serum IgG2a responses and also high level of serum IgG1 in all mice. While the intranasal administration with antigen solution induced significantly lower serum IgG1 and IgG2a titers (p<0.05) compared to intramuscular vaccination with only 2/8 responded mice in the first vaccination. The antigen loaded chitosan nanoparticles conjugated with aluminium hydroxide gel triggered lower level of both serum IgG1 and IgG2a titers, with 4 and all responders respectively, in the first vaccination. The titers gradually increased with slow kinetics after booster immunizations and elicited to the same level as responded to intramuscular immunization after the second boosters. Even the intranasally administration of antigen loaded chitosan nanoparticles induced serum IgG1 and IgG2a titers as the same profile as induced with the conjugated formulation but lower titers and less amount of responders (7/8) were notified. This indicated that
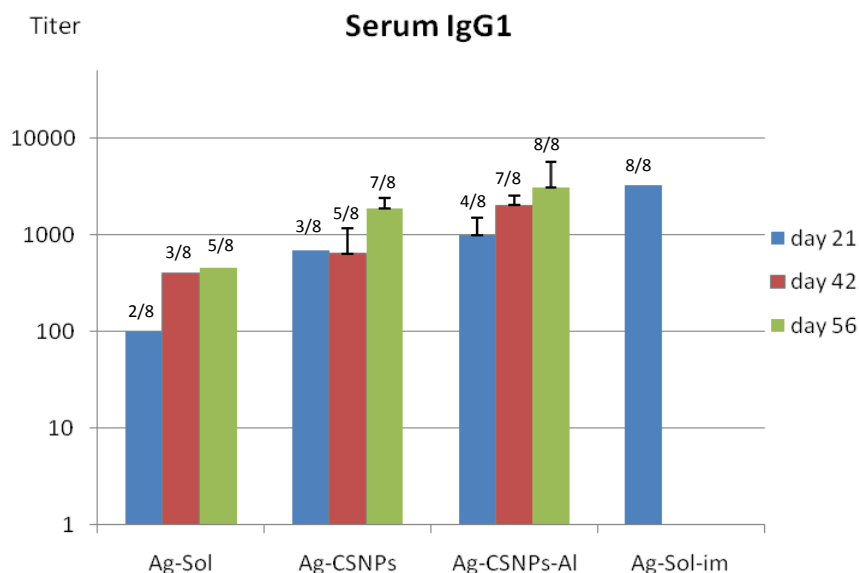
Figure 4-32 Anti-influenza (H1N1) antigen-specific serum IgG1 responses in mice after intranasal vaccination with the antigen solution, antigen loaded chitosan nanoparticles, antigen loaded chitosan nanoparticles conjugated with aluminium hydroxide gel, and intramuscular vaccination with antigen solution.
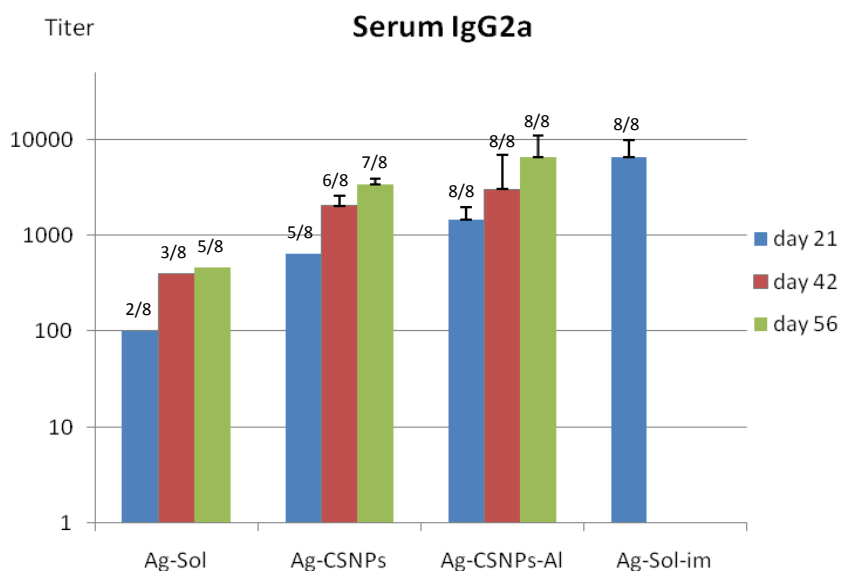
Figure 4-33 Anti-influenza (H1N1) antigen-specific serum IgG2a responses in mice after intranasal vaccination with the antigen solution, antigen loaded chitosan nanoparticles, antigen loaded chitosan nanoparticles conjugated with aluminium hydroxide gel, and intramuscular vaccination with antigen solution.
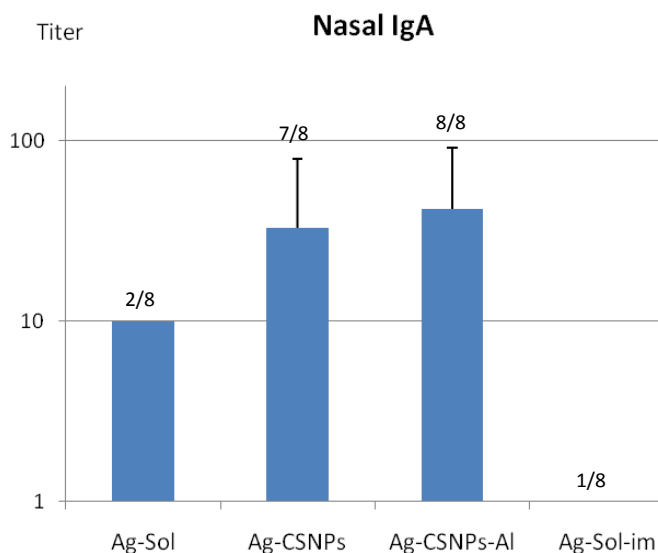
Figure 4-34 Anti-influenza (H1N1) antigen-specific S-IgA titers in nasal lavages of mice after intranasal vaccination with the antigen solution, antigen loaded chitosan nanoparticles, antigen loaded chitosan nanoparticles conjugated with aluminium hydroxide gel, and intramuscular vaccination with antigen solution.

the antigen loaded chitosan nanoparticles conjugated with aluminium hydroxide gel had better immunostimulating effect than the nanoparticles without conjugation and could induce no different level of serum IgG, IgG1 and IgG2a compared to intramuscular vaccination (p>0.05).

Since mucosal vaccination had a potential to induce local immune responses, especially secretory IgA (S-IgA) which was claimed to be more effective in cross protection against virus infection than systemic immuniny (Ito et al., 2003; Asahi et al., 2002). Therefore, not only the systemic immunostimulating effect but also the mucosal immune response were investigated. Figure 4-34 shows the specific anti-influenza S-IgA titer in the nasal lavage of mice vaccinated intranasally and intramuscularly with different formulations. High S-IgA titers (42) were detected in all mice after intranasal vaccination with antigen loaded chitosan nanoparticles conjugated with aluminium hydroxide gel, while antigen loaded chitosan nanoparticles elicited lower S-IgA titer (33) in 7/8 mice. However, the titers were statistically insignificantly different (p>0.05). On the other hand, mice vaccinated

intranasally with antigen solution showed low S-IgA titers in 2/8 mice. Moreover the mice immunized intramuscularly gave very low S-IgA titer (1) in 1/8 mouse. The results reflected that the intranasal vaccination with antigen loaded chitosan nanoparticles, both conjugated and unconjugated formulations, can induce the S-IgA response in the respiratory tract.

The chitosan nanoparticles were an efficient system to transport the antigen through nasal epithelium and M-cells on the NALT by cellular uptaking (Brooking, Davis, and Illum, 2001). Moreover, the positive charge on the surface and mucoadhesive property enhanced the affinity of particles to mucosal tissue increased more residential time to be up taken (Bozkir and Saka, 2004). The immune responses induced by antigen loaded chitosan nanoparticles were probably based on cellular uptake of the particles in the nasal epithelium and M-cells and delivered of the antigen to the lymphoid tissues. The mucoadhesive property and the particulate nature of chitosan nanoparticles were probably important for the immune-stimulating effect.

As the results, antigen loaded chitosan nanoparticles conjugated with aluminium hydroxide gel showed better immune responses than the unconjugated form. It probably dued to the adjuvant effect of aluminium hydroxide gel. It had been reported that engulfment of aluminium salt leaded to lysosomal distuption and activation of NALP3 which is a component of inflammasome complex that can induce some of proinflammatory cytokines and enhances immunogenicity (Eisenbarth et al., 2008). Moreover, the antigen absorbed on the aluminium hydroxide gel was presented in multivalent form, enhancing the internalization by antigen presenting cells (Morefield et al., 2005).

The main protection against influenza infection is neutralization with immunoglobulins that bind to viral HA (Amidi et al., 2007). There were reported that IgG1 and IgG2a antibodies are contributed to virus neutralization. IgG1 has been shown to be very effective in neutralizing virus as humoral immune response while IgG2a has been reported to play a role in antibody-dependent cell-mediated immune response and also complement activation (Hocart, Mackenzie and Stewart, 1989) which facilitates the clearance of influenza virus from the infected host (Huber et al., 2006). It enhances antibodies responses by increasing of antigen uptaking by APCs, therefore, enhances presentation of antigen to Th cells (Getahun et al., 2004). Thus,

the induction of serum IgG1 and IgG2a responses may increase vaccine efficacy against viral infections.

From the results, the intramuscular administration with antigen solution elicited high serum IgG1 and IgG2a titers which were not different to the intranasal administration with antigen loaded chitosan nanoparticles conjugated with aluminium hydroxide gel after the third vaccination, while the lower titers and less number of responded mice were shown in the vaccination with antigen loaded chitosan nanoparticles without aluminium hydroxide gel. This shows that chitosan nanoparticles concomitant with aluminium hydroxide gel significantly enhanced the immunogenicity of vaccines given intranasally, both humoral and cell mediated immune response.

The advantage of mucosal vaccination is the induction of S-IgA antibody at the mucosal epithelium which is the first defense against influenza viruses entry in the respiratory tract. Moreover, it was reported to elicit crossprotective immunity more effectively than serum IgG (Ito et al., 2003). In this study, the S-IgA from nasal lavage indicates antigen-induced stimulation of IgA-secreting cells in the NALT. The intranasal administration of antigen loaded chitosan nanoparticles conjugated with aluminium hydroxide gel elicited the highest S-IgA titers after three vaccination in all mice. On the other hand, intramuscular administered antigen solution showed very low titer (1) in only one mouse which correlated with previous report that intramuscular administration of antigen cannot induce S-IgA response (de Haan et al., 2001).

CHAPTER V

CONCLUSIONS

This present research study was to investigate the suitability of chitosan nanoparticles conjugated with aluminium hydroxide gel for nasal antigen delivery and the potential of influenza antigen loaded chitosan nanoparticles conjugated with aluminium hydroxide gel to elicit local and systemic immune responses after nasal vaccination in mice. Chitosan nanoparticles were prepared in mild conditions based on the ionotropic gelation of chitosan with TPP. The optimal chitosan conconcentration of 0.1% (w/v) and weight ratios of chitosan : TPP of 3:1 were selected by considering the appropriate particle size and zeta potential for nasal delivery. To obtain the suitable conditions for preparation of the intranasal formulations, pH of chitosan solution, order of mixing, amount of Tween 80 and aluminium hydroxide gel were varied and considered based on the particle size and zeta potential.

In this study, the optimum pH of chitosan solution was 4.5 which resulted in a slight decrease of mean particle diameter while the pH of 5.5 and 6.5 had opposite effect. Moreover, this pH 4.5 was suitable for intranasal administration. For zeta potential, increasing the pH of chitosan solution decreased the zeta potential. The suitable order of mixing was by adding of TPP dropwise into the pH-adjusted chitosan solution while stirring, followed by adding Tween 80 in concentration of 0.1% (w/v) then suspending aluminium hydroxide gel in concentration of 0.1, 0.2 and 0.4 mg/ml and continuously stirring for 30 minutes. BSA, the model protein, was loaded in the nanoparticle formulation by dissolving in TPP solution before adding into chitosan solution which tended to form smaller particles than dissolving the protein in chitosan solution.

From TEM photographs, chitosan nanoparticles were spherical structure, while chitosan nanoparticles with aluminium hydroxide gel has slightly bigger size as a compact core surrounded by a fluffy coat of aluminium hydroxide gel. The FTIR spectra confirmed the formation of chitosan nanoparticles and revealed that the aluminum hydroxide gel could interact with chitosan nanoparticles by intermolecular

hydrogen bonding. The 30-µg/ml BSA loaded chitosan nanoparticles conjugated with 0.1, 0.2 and 0.4 mg/ml of aluminium hydroxide gel displayed loading efficiency of 52.47±2.99%, 55.65±0.56%   and 56.56±0.66%, respectively, and 47.92±3.66% for the unconjugation, which indicated the absorption of BSA on the aluminium hydroxide gel layer.

 With the optimized formulations, the particles sizes of BSA loaded chitosan nanoparticles with 0.1 and 0.2 mg/ml of aluminium hydroxide gel did not show any trend of increase or decrease on particles sizes after storage in refrigerator (2-8°C) for 150 days. On the other hand, the formulation with 0.4 mg/ml aluminium hydroxide gel showed some changes in particle sizes. SDS-PAGE revealed that the primary structure of BSA loaded in chitosan nanoparticles with and without aluminium hydroxide gel was generally conserved. Moreover, CD spectra showed no significant conformational change in BSA encapsulated in chitosan nanoparticles with aluminium hydroxide gel.

The nanoparticles formulations showed good mucoadhesive property and relatively non-toxic to nasal cell but the percentage of cell viability tended to decrease with increasing of aluminium hydroxide gel dued to increasing of zeta potential which induced stronger interference with cell membrane. The averages of mean uptake cell count of RPMI 2650 incubated with the nanoparticle formulations were not obviously different but the formulation with excess aluminium hydroxide gel tended to form particles aggregation which might be less preferable for cellular uptake. The TEER values of RPMI 2650 confluent monolayer incubated with FITC-BSA in PBS and nanoparticle formulations was slightly decreased in similar profile. While the FITC-BSA concentration in basolateral compartments relatively low in all formulations but the nanoparticle formulations showed dramatically higher amount of FITC-BSA remained in cells. These indicated that the formulations cannot open the tight junctions to induce the paracellular transportation which possibly due to the low concentration of chitosan. The main transportation was transcellular by cellular uptake.

The triple intranasal immunization with influenza antigen loaded chitosan nanoparticles conjugated with aluminium hydroxide gel elicited as high serum immune response as single intramuscular vaccination with antigen solution but

induced stronger immune response than triple intranasal administration with unconjugated formulation. Moreover, the intranasal immunization with the conjugated formulation induced slightly higher local immune response compared with the unconjugated formulation while intramuscular administration was not able to induce local immune response. Thus, chitosan nanoparticles conjugated with aluminium hydroxide gel was evident to be a promising nasal delivery system for influenza vaccine.

REFERENCES

Abramson, J.S. Intranasal, cold-adapted, live, attenuated influenza vaccine. <u>Pediatric Infectious Disease Journal</u> 18 (1999) : 1103-1104.

Agger, E.M., Cassidy, J.P., Brady, J., Korsholm, K.S., Vingsbo-Lundberg, C., and Andersen, P. Adjuvant modulation of the cytokine balance in mycobacterium tuberculosis subunit vaccines: immunity, pathology and protection. <u>Immunology</u> 124 (2008) : 175-185.

Ahire, V.J., Sawant, K.K., Doshi, J.B., and Ravetkar, S.D. Chitosan microparticles as oral delivery system for tetanus toxoid. <u>Drug Development and Industrial Pharmacy</u> 33 (2007) : 1112-1124.

Alpar, H.O., Somavarapu, S., Atuah, K.N., and Bramwell, V.W. Biodegradable mucoadhesive particulates for nasal and pulmonary antigen and DNA delivery. <u>Advanced Drug Delivery Reviews</u> 57 (2005) : 411-430.

Amidi, M., et al. N-Trimethyl chitosan (TMC) nanoparticles loaded with influenza subunit antigen for intranasal vaccination: Biological properties and immunogenicity in a mouse model. <u>Vaccine</u> 25 (1) (2007) : 144-153.

Amidi, M., et al. Preparation and characterization of protein-loaded N-trimethyl chitosan nanoparticles as nasal delivery system. <u>Journal of Controlled Release</u> 111 (1-2) (2006) : 107-116.

Arora, P., Sharma, S., and Garg, S. Permeability issues in nasal drug delivery. <u>Drug Discovery Today</u> 7 (2002) : 967-975.

Asahi, Y., et al. Protection Against Influenza Virus Infection in Polymeric Ig Receptor Knockout Mice Immunized Intranasally with Adjuvant-Combined Vaccines. Journal of Immunology 168 (2002) : 2930-2938.

Bai, S., Yang, T., Abbruscato, T.J., and Ahsan, F. Evaluation of human nasal RPMI 2650 cells grown at an air-liquid interface as a model for nasal drug transport studies. Journal of Pharmaceutical Science 97 (2008) : 1165-1178.

Barr, I.G., et al. Epidemiological, antigenic and genetic characteristics of seasonal influenza A(H1N1), A(H3N2) and B influenza viruses: Basis for the WHO recommendation on the composition of influenza vaccines for use in the 2009–2010 Northern Hemisphere season. Vaccine 28 (2010) : 1156-1167.

Baudner, B.C. The concomitant use of the LTK63 mucosal adjuvant and of chitosan-based delivery system enhances the immunogenicity and efficacy of intranasally administered vaccines. Vaccine 21 (25-26) (2003) : 3837-3844.

Baylor, N.W., Egan,W., and Richman, P. Aluminium salts in vaccine—US perspective. Vaccine 20 (3) (2002): 18-23.

Behl, C.R., Pimplaskar, H.K., Sileno, A.P., de Meireles, J., and Romeo, V.D. Effects of physicochemical properties and other factors on systemic nasal drug delivery. Advanced Drug Delivery Reviews 29 (1998) : 89-116.

Benchabane, S., Subirade, M., and Vandenberg, G.W. Production of BSA-loaded alginate microcapsules: Influence of spray dryer parameters on the microcapsule characteristics and BSA release. Journal of Microencapsulation 24 (7) (2007) : 647-658.

Bienenstock, J., and McDermott, M.R. Bronchus- and nasal-associated lymphoid tissues. Immunological Reviews 206 (2005) : 22-31.

Borchard, G., Luessen, H.L., De Boer, A.G., Verhoef, J.C., Lehr, C.M., and Junginger, H.E. The potential of mucoadhesive polymers in enhancing intestinal peptide drug absorption III: Effect of chitosan glutamate and carbomer on epithelial tight junctions in vitro. Journal of Controlled Release 39 (1996) : 131-138.

Borges, O., et al. Immune response by nasal delivery of hepatitis B surface antigen and codelivery of a CpG ODN in alginate coated chitosan nanoparticles. European Journal of Pharmaceutics and Biopharmaceutics 69 (2) (2008) : 405-416.

Bozkir, A. and Saka, O.M. Chitosan nanoparticles for plasmid DNA delivery: effect of chitosan molecular structure on formulation and release characteristics. Drug Delivery 11 (2004) : 107-112.

Brandtzaeg, P., Kiyono, H., Pabst, R., and Russell, M.W. Terminology: nomenclature of mucosa-associated lymphoid tissue. Mucosal Immunology 1 (2008) : 31-37.

Brooking, J., Davis, S.S., and Illum, L. Transport of nanoparticles across the rat nasal mucosa. Journal of Drug Targeting 9 (2001) : 267-279.

Brunner, R., et al. Aluminium per se and in the anti-acid drug sucralfate promotes sensitization via the oral route. Allergy 64 (2009) : 890-897.

Brunner, R., et al. The impact of aluminium in acid-suppressing drugs on the immune response of BALB/c mice. Clinical and Experimental Allergy 37 (2007) : 1566-1573.

Burkitt, H. G., Young, B., and Heath, J. W. Wheater's Functional Histology. A Text and Colour Atlas. London : Longman, 1993.

Center for Chitin - Chitosan Biomaterials, Chulalongkorn University. Marine waste become value added product "chitin-chitosan" [online]. 2009. Available from : http://www.material.chula.ac.th/CCB/image/712px-Chitosan_Synthese.svg.png [2013, 31 March]

Cesta, M.F. Normal structure, function, and histology of mucosa-associated lymphoid tissue. Toxicologic Pathology 34 (2006) : 599-608.

Chol, H.J., Termsarasab, U., Kim, J.S., and Kim, D.D. In Vitro Nasal Cell Culture Systems for Drug Transport Studies. Journal of Pharmaceutical Investigation 40 (6) (2010) : 321-332.

Chowdary, K.P., and Rao, Y.S. Mucoadhesive microspheres for controlled drug delivery. Biological & Pharmaceutical Bulletin 27 (2004) : 1717-1724.

Clark, M.A., Jepson, M.A., and Hirst, B.H. Exploiting M cells for drug and vaccine delivery. Advanced Drug Delivery Reviews 50 (2001) : 81-106.

Csaba, N., Garcia-Fuentes, M. and Alonso, M.J. Nanoparticles for nasal vaccination. Advanced Drug Delivery Reviews 61 (2) (2009) : 140-141.

Dahl, R., and Mygind, N. Anatomy, physiology and function of the nasal cavities in health and disease. Advanced Drug Delivery Reviews 29 (1998) : 3-12.

de Haan, L., et al. Nasal or intramuscular immunization of mice with influenza subunit antigen and the B subunit of *Escherichia coli* heat-labile toxin induces IgA- or IgG-mediated protective mucosal immunity. Vaccine 19 (2001) : 2898-2907.

de Kruif, C.G., Weinbreck, F., and de Vries, R. Complex coacervation of proteins and anionic polysaccharides. Current Opinion in Colloid & Interface Science 9 (2004) : 340-349.

Debertin, A.S., Tschernig, T., Tonjes, H., Kleemann, W.J., Troger, H.D., and Pabst, R. Nasal associated lymphoid tissue (NALT): frequency and localization in young children. Clinical & Experimental Immunology 134 (2003) : 503-507.

Desai, M.P., Labhasetwar, V., Walter , E., Levy, R.J., and Amidon, G.L. The mechanism of uptake of biodegradable microparticles in Caco-2 cells is size dependent. Pharmaceutical Research 14 (1997) : 1568-1573.

Determan, A.S., Trewyn, B.G., Lin, V.S.Y., Nilsen-Hamiltonc, M., and Narasimhana, B. Encapsulation, stabilization, and release of BSA-FITC from polyanhydride microspheres. Journal of Controlled Release 100 (2004) : 97-109.

Dodane, V., Khan, M.A., and Merwin, J.R. Effect of chitosan on epithelial permeability and structure. International Journal of Pharmaceutics 182 (1999) : 21-32.

Eisenbarth, S.C., Colegio, O.R., O'Connor, W., Sutterwala, F.S., and Flavell, R.A. Crucial role for the NALP3 inflammasome in the immunostimulatory properties of aluminium adjuvants. Nature 453 (2008) : 1122-1126.

Fujiyoshi, Y., Kume, N.P., Sakata, K., and Sato, S.B. Fine structure of influenza A virus observed by electron cryo-microscopy. European Molecular Biology Organization Journal 13 (2) (1994) : 318–326.

Gavini, E., et al. Nasal administration of carbamazepine using chitosan microspheres: in vitro/in vivo studies. International Journal of Pharmaceutics 307 (2006) : 9-15.

Getahun, A., Dahlstroem, J., Wernersson, S., and Heyman, B. IgG2a-Mediated Enhancement of Antibody and T Cell Responses and Its Relation to Inhibitory and Activating Fcɤ Receptors. The Journal of Immunology 172 (2004) : 5269-5276.

Goeringer, G.C. and Vidic, B. The embryogenesis and anatomy of Waldeyer's ring. Otolaryngologic Clinics of North America 20 (1987) 207-217.

Gupta, N.K., Tomar, P., Sharma, V., and Dixit, V.K. Development and characterization of chitosan coated poly-(ε-caprolactone) nanoparticulate system for effective immunization against influenza. Vaccine 29 (2011) : 9026– 9037.

Gupta, R.K., Rost, B.E., Relyveld, E., and Siber, G.R. Adjuvant properties of aluminum and calcium compounds. Pharmaceutical Biotechnology 6 (1995) : 229-248.

Hagenaars, N., et al. Relationship between structure and adjuvanticity of N,N,N-trimethyl chitosan (TMC) structural variants in a nasal influenza vaccine. Journal of Controlled Release 140 (2) (2009) : 126-133.

Hamalainen, M.D. and Frostell-Karlsson, A. Predicting the intestinal absorption potential of hits and leads. Drug Discovery Today : Technologies 1(4) (2004) : 397-405.

Hansen, B., Sokolovska, A., HogenEsch, H., and Hem, S.L. Relationship between the strength of antigen adsorption to an aluminum-containing adjuvant and the immune response. Vaccine 25 (2007) : 6618-6624.

Harikarnpakdee, S., Lipipun, V., Sutanthavibul, N., and Ritthidej, G.C. Spray-dried mucoadhesive microspheres: preparation and transport through nasal cell monolayer. AAPS PharmSciTech 7 (1) (2006) : E1-E10.

Hayashi, M., Hirasawa, T., Muraoka, T., Shiga, M., and Awaza, S. Comparison of water influx and sieving coefficient in rat jejunal, rectal and nasal absorption of antipyrine. Chemical and pharmaceutical bulletin 33 (1985) : 2149-2152.

Himmel, H.J., Downs, A.J., and Greene, T.M. Thermal and photochemical reaction of aluminum, gallium and indium atom (M) in the presence of ammonia: generation and characterization of the species M-NH$_3$, HMNH$_3$, MNH$_2$ and H$_2$MNH$_2$. Journal of the American Chemical Society 122 (40) (2000) : 9793-9807.

Hocart, M.J., Mackenzie, J.S., and Stewart, The IgG subclass responses to influenza virus haemagglutinin in the mouse: effect of route of inoculation. Journal of General Virology 70 (1989) : 809-818.

Hocart, M.J., Mackenzie, J.S., and Stewart, G.A. The immunoglobulin G subclass response of mice to influenza A virus: the effect of mouse strain, and the neutralizing abilities of individual protein A-purified subclass antibodies. Journal of General Virology 70 (1989) : 2439-2448.

HogenEsch, H. Mechanisms of stimulation of the immune response by aluminum adjuvants. Vaccine 20 (3) (2002) : 34-39.

Hsu, J., et al. Antivirals for Treatment of Influenza, A Systematic Review and Meta-analysis of Observational Studies. Annals of Internal Medicine 156 (7) (2012) : 512-524.

Huber, V.C., et al. Distinct Contributions of Vaccine-Induced Immunoglobulin G1 (IgG1) and IgG2a Antibodies to Protective Immunity against Influenza. Clinical and Vaccine Immunology 13 (9) (2006) : 981-990.

Illum, L. Chitosan and its use as a pharmaceutical excipient. Pharmaceutical Research 15 (1998) :1326-1331.

Illum L. Is nose-to-brain transport of drugs in man a reality? Journal of Pharmacy and Pharmacology 56 (2004) : 3-17.

Illum, L. Nanoparticulate Systems for Nasal Delivery of Drugs: A Real Improvement over Simple Systems? <u>Journal of Pharmaceutical Sciences</u> 96 (3) (2007) : 473-483.

Illum, L., Jabbal-Gill, I., Hinchcliffe, M., Fisher, A.N., and Davis, S.S. Chitosan as a novel nasal delivery system for vaccines. <u>Advanced Drug Delivery Reviews</u> 51(2001) : 81-96.

Ito, R., et al. Roles of anti-hemagglutinin IgA and IgG antibodies in different sites of the respiratory tract of vaccinated mice in preventing lethal influenza pneumonia. <u>Vaccine</u> 21 (2003) : 2362-2371.

Iwasaki, A. Mucosal dendritic cells. <u>Annual Review of Immunology</u> 25 (2007) : 381-418.

Iyer, S., Robinett, R.S.R., HogenEsch, H., and Hem, S.L. Mechanism of adsorption of hepatitis B surface antigen by aluminum hydroxide adjuvant. <u>Vaccine</u> 22 (2004) : 1475-1479.

Jabbal-Gill, I., Fisher, A.N., Rappuoli, R., Davis, S.S., and Illum, L. Stimulation of mucosal and systemic antibody responses against *Bordetella pertussis* filamentous haemagglutinin and recombinant pertussis toxin after nasal administrationwith chitosan in mice. <u>Vaccine</u> 16 (1998) : 2039-2046.

Jain, S., et al. Hospitalized Patients with 2009 H1N1 Influenza in the United States, April–June 2009. <u>New England Journal of Medicine</u> 361 (2009) : 1935-1944.

Jiang, H.-L., et al. The potential of mannosylated chitosan microspheres to target macrophage mannose receptors in an adjuvant-delivery system for intranasal immunization. <u>Biomaterials</u> 29 (12) (2008) : 1931-1939.

Kafshgari, M.H., Khorram, M., Khodadoost, M., and Khavari,S. Reinforcement of Chitosan Nanoparticles Obtained by an Ionic Cross-linking Process. Iranian Polymer Journal 20 (5) (2011) : 445-456.

Kaliner, M., Marom, Z., Patow, C., and Shelhamer, J. Human respiratory mucus. Journal of Allergy and Clinical Immunology 73 (1984) : 318-323.

Kamath, K. R., and Park, K. Mucosal adhesive preparations. In Swarbricks, J., and Boylan, J.C. Encyclopedia of Pharmaceutical Technology. 133-163. New York : Marcel Dekker, 1994.

Kang, M.L., et al. In vivo induction of mucosal immune responses by intranasal administration of chitosan microspheres containing Bordetella bronchiseptica DNT. European Journal of Pharmaceutics and Biopharmaceutics 63 (2006) : 215-220.

Kang, M.L., et al. Pluronic® F127 enhances the effect as an adjuvant of chitosan microspheres in the intranasal delivery of Bordetella bronchiseptica antigens containing dermonecrotoxin. Vaccine 25 (23) (2007) : 4602-4610.

Karlsson Hedestam, G.B., Fouchier, R.A.M., Phogat, S., Burton, D.R., Sodroski, J., and Wyatt, R.T. The challenges of eliciting neutralizing antibodies to HIV-1and to influenza virus. Microbiology 6 (2008) : 143-155.

Kato, Y., Onishi, H., and Machida, Y. Application of chitin and chitosan derivatives in the pharmaceutical field. Current Pharmaceutical Biotechnology 4 (2003) : 303-309.

Kelso, J.M. Safety of influenza vaccines. Current Opinion in Allergy & Clinical Immunology 12 (4) (2012) : 383-388.

Krauland, A.H., Guggi, D., and Bernkop-Schnuerch, A. Thiolated chitosan microparticles: a vehicle for nasal peptide drug delivery. <u>International Journal of Pharmaceutics</u> 307 (2006) : 270-277.

Kusonwiriyawong, C., Pichayakorn, W., Lipipun, V., and Ritthidej, G.C. Retained integrity of protein encapsulated in spray-dried chitosan microparticles. <u>Journal of Microencapsulation</u> 26 (2) (2009) : 111-121.

Kyd, J.M., Foxwell, A.R. and Cripps, A.W. Mucosal immunity in the lung and upper airway. <u>Vaccine</u> 19 (17-19) (2001) : 2527-2533.

Lear, J.D. Proton conduction through the M2 protein of the influenza A virus; a quantitative, mechanistic analysis of experimental data. <u>Federation of European Biochemical Societies letters</u> 552 (1) (2003) : 17-22.

Lim, S.T., Forbes, B., Martin, G.P., and Brown, M.B. In vivo and in vitro characterization of novel microparticulates based on hyaluronan and chitosan hydroglutamate. <u>AAPS PharmSciTech</u> 2 (4) (2001) : 1-12.

Lindblad, E.B. Aluminium adjuvants-in retrospect and prospect. <u>Vaccine</u> 22 (2004) : 3658-3668.

Lopez-Leon, T., Carvalho, E.L.S., Seijo, B., Ortega-Vinuesa, J.L., and Bastos-Gonzalez, D. Physicochemical characterization of chitosan nanoparticles: Electrokinetic and stability behavior. <u>Journal of Colloid and Interface Science</u> 283 (2005) : 344-351.

Madara, J.L. Modulation of tight junctional permeability. <u>Advanced Drug Delivery Reviews</u> 41(2000) : 251-253.

Makhlof, A., et al. Nanoparticles of glycol chitosan and its thiolated derivative significantly improved the pulmonary delivery of calcitonin. <u>International Journal of Pharmaceutics</u> 397 (1-2) (2010) : 92-95.

Mao, Z., Ma, L., Jiang, Y., Yan, M., Gao, C., and Shen, J. N,N,N-Trimethyl chitosan chloride as a gene vector: synthesis and application. <u>Macromolecular Bioscience</u> 7 (2007) : 855-863.

Martyn, C.N., Osmond, C., Edwardson, J.A., Barker, D.J.P., Harris, E.C., and Lacey, R.F. Geographical relation between Alzheimer's disease and aluminium in drinking water. <u>Lancet</u> 1 (1989) : 59-62.

McNeela, E.A., et al. A mucosal vaccine against diphtheria: formulation of cross reacting material (CRM(197)) of diphtheria toxin with chitosan enhances local and systemic antibody and Th2 responses following nasal delivery. <u>Vaccine</u> 19 (2000) : 1188-1198.

Mendelman, P.M., Cordova, J., and Cho, I. Safety, efficacy and effectiveness of the influenza virus vaccine, trivalent, types A and B, live, cold-adapted (CAIV-T) in healthy children and healthy adults. <u>Vaccine</u> 19 (2001) : 2221-2226.

Mokarram, R. and Alonso, M.J. Preparation and evaluation of chitosan nanoparticles containing Diphtheria toxoid as new carriers for nasal vaccine delivery in mice. <u>Archives of Razi Institute</u> 61(1) (2006) : 13-25.

Morefield, G.L., Sokolovska, A., Jiang, D., Hogen Esch, H., Robinson, J.P., and Hem, S.L. Role of aluminum-containing adjuvants in antigen internalization by dendritic cells in vitro. <u>Vaccine</u> 23 (2005) :1588-1595.

Mosmann, T.R., and Sad, S. The expanding universe of T-cell subsets: Th1, Th2 and more. <u>Immunology Today</u> 17(1996) :138-146.

Nair, H., et al. Global burden of respiratory infections due to seasonal influenza in young children: a systematic review and meta-analysis. Lancet 378 (2011) :1917-1930.

Nasti, A., et al. Chitosan/TPP and Chitosan/TPP-hyaluronic Acid Nanoparticles : Systematic Optimisation of the Preparative Process and Preliminary Biological Evaluation. Pharmaceutical Research 26 (8) (2009) : 1918-1930.

Neck Pain Blog. Nasopharynx [online]. 2011. Available from :http://www.painneck. com/images/nasopharynx.jpg [2013, 31 March]

Neutra, M.R. M cells in antigen sampling in mucosal tissues. Current Topics in Microbiology and Immunology 236 (1999) : 17-32.

Neutra, M.R., and Kozlowski, P.A. Mucosal vaccines: the promise and the challenge. Nature Reviews Immunology 6 (2006) : 148-158.

Ng, M., et al. Preparation and characterisation of new-polyaluminum chloride-chitosan composite coagulant. Water Research 46 (2012) : 4614-4620.

O'Hagan, D.T., and De Gregorio, E. The path to a successful vaccine adjuvant—'the long and winding road'. Drug Discovery Today 14 (2009) : 541-551.

Onishi, H. and Machida, Y. Biodegradation and distribution of water-soluble chitosan in mice. Biomaterials 20 (2) (1999) : 175-182.

Park, B.K., Lee, Y.S., and Koo, K.K. Preparation of highly porous aluminum hydroxide gels by hydrolysis of an aluminum sulfate and mineralizer. Journal of Ceramic Processing Research 11 (1) (2010) : 64-68.

Pichayakorn, W., Harikarnpakdee, S., Suksiengsri, S., Ritthidej, G.C., and Lipipun, V. Comparison of monoculture caco-2 cells, RPMI 2650 cells, and their coculture with raji cells: study in morphology, uptake and permeation of particulated drug delivery carriers. In Proceeding of the 6th World Meeting on Pharmaceutics, Biopharmaceutics and Pharmaceutical Technology. Barcelona, Spain, 2008.

Racaniello, V. Structure of influenza virus [online]. 2009. Available from : http://www.virology.ws/2009/04/30/structure-of-influenza-virus/ [2013, 31 March]

Ranjbar, B. and Gill, P. Circular Dichroism Techniques : Biomolecular and Nanostructural Analyses - A Review. Chemical Biology & Drug Design 74 (2009) : 101-120.

Rimaniol, A.C., et al. Aluminum hydroxide adjuvant induces macrophage differentiation towards a specialized antigen-presenting cell type. Vaccine 22 (2004) : 3127-3135.

Sarkar, M.A., Drug metabolism in the nasal mucosa. Pharmaceutical Research 9 (1992) : 1-9.

Scheiffele, P., Rietveld, A.,Wilk, T., and Simons, K. Influenza viruses select ordered lipid domains during budding from the plasmamembrane. Journal of Biological Chemistry 274 (4) (1999) : 2038-2044.

Schoell, I., Kopp, T., Bohle, B., and Jensen-Jarolim, E. Biodegradable PLGA particles for improved systemic and mucosal treatment of type I allergy. Immunology and Allergy Clinics of North America 26 (2006) : 349-364.

Schoell, I., et al. Anti-ulcer treatment during pregnancy induces food allergy in mouse mothers and a Th2-bias in their offspring. <u>Federation of American Societies for Experimental Biology journal</u> 21(4) (2007) : 1264-1270.

Schroeder, C., Heider, H., Moncke-Buchner, E., and Lin, T.I. The influenza virus ion channel and maturation cofactor M2 is a cholesterol-binding protein. <u>European Biophysics Journal</u> 34 (1) (2005) : 52-66.

Slütter, B., et al. Mechanistic study of the adjuvant effect of biodegradable nanoparticles in mucosal vaccination. <u>Journal of Controlled Release</u> 138 (2009) : 113-121.

Smith, J., Wood, E., and Dornish, M. Effect of chitosan on epithelial cell tight junctions. <u>Pharmaceutical Research</u> 21 (2004) : 43-49.

Soane, R.J., Hinchcliffe, M., Davis, S.S., and Illum, L. Clearance characteristics of chitosan based formulations in the sheep nasal cavity. <u>International Journal of Pharmaceutics</u> 217 (2001) : 183-191.

Spazierer, D., et al. T helper 2 biased de novo immune response to keyhole limpet hemocyanin in humans. <u>Clinical and Experimental Allergy</u> 39 (2009) : 999-1008.

Stephenson, I., et al. Phase I Evaluation of Intranasal Trivalent Inactivated Influenza Vaccine with Nontoxigenic *Escherichia coli* Enterotoxin and Novel Biovector as Mucosal Adjuvants, Using Adult Volunteers. <u>Journal of Virology</u> 80 (10) (2006) : 4962–4970.

Storni, T., Kundig, T.M., Senti, G., and Johansen, P. Immunity in response to particulate antigen-delivery systems. <u>Advanced Drug Delivery Reviews</u> 57 (2005) : 333-355.

Tang, Z.X., Qian, J.Q., and Shi, L.E. Preparation of chitosan nanoparticles as carrier for immobilized enzyme. Applied Biochemistry and Biotechnology 136 (1) (2007) : 77-96.

Tian, J., Yu, J., and Sun, X. Chitosan microspheres as candidate plasmid vaccine carrier for oral immunisation of Japanese flounder (Paralichthys olivaceus). Veterinary Immunology and Immunopathology 126 (2008) : 220-229.

Tsai, M.L., Chen, R.H., Bai, S.W., and Chen, W.Y. The storage stability of chitosan/tripolyphosphate nanoparticles in a phosphate buffer. Carbohydrate Polymers 84 (2011) : 756-761.

Tzoupanos, N.D., and Zouboulis, A.I. Novel inorganic-organic composite coagulants based on aluminium. Desalination & Water Treatment 13(1-3) (2010) : 340-347.

Ugwoke, M.I., Verbeke, N., and Kinget, R. The biopharmaceutical aspects of nasal mucoadhesive drug delivery. Journal of Pharmacy and Pharmacology 53 (2001) : 3- 21.

van der Lubben, I.M., Kersten, G., Fretz, M.M., Beuvery, C., Verhoef, J.C., and Junginger, H.E. Chitosan microparticles for mucosal vaccination against diphtheria : oral and nasal efficacy studies in mice. Vaccine 21 (2003) : 1400-1408.

van der Merwe, S.M., Verhoef, J.C., Verheijden, J.H.M., Kotze´, A.F., and Junginger, H.E. Trimethylated chitosan as polymeric absorption enhancer for improved peroral delivery of peptide drugs. European Journal of Pharmaceutics and Biopharmaceutics 58 (2004) : 225-235.

Varshosaz, J., Sadrai, H., and Alinagari, R. Nasal delivery of insulin using chitosan microspheres. Journal of Microencapsulation 21 (2004) : 761-774.

Vila, A., et al. Low molecular weight chitosan nanoparticles as new carriers for nasal vaccine delivery in mice. European Journal of Pharmaceutics and Biopharmaceutics 57 (1) (2004) : 123-131.

Vllasaliu, D., et al. Tight junction modulation by chitosan nanoparticles: Comparison with chitosan solution. International Journal of Pharmaceutics 400 (1-2) (2010) : 183-193.

Watson, S. What is the Flu? [online]. 2004. Available from : http://static.ddmcdn.com/ gif/flu-respiratory.gif [2013, 31 March]

World Health Organization. Influenza [online]. 2003. Available from : http://www.who.int/mediacentre/factsheets/2003/fs211/en/ [2013, 30 March]

World Health Organization. Influenza (Seasonal) [online]. 2009. Available from : http://www.who.int/mediacentre/factsheets/fs211/en/index.html [2013, 30 March]

World Health Organization. Influenza update [online]. 2013. Available from : http://www.who.int/influenza/surveillance_monitoring/updates/latest_update_G IP_surveillance/en/index.html [2013, 30 March]

World Health Organization. State of the Art of Vaccine Research and Development [online]. 2005. Available from : www.who.int/vaccine_research/documents/ Dip%20814.pdf [2013, 30 March]

Wu, H.Y. and Russell, M.W. Nasal lymphoid tissue, intranasal immunization, and compartmentalization of the common mucosal immune system. Immunologic Research 16 (1997) : 187- 201.

Wu, Y., Yang, W., Wang, C., Hu, J., and Fu, S. Chitosan nanoparticles as a novel delivery system for ammonium glycyrrhizinate. International Journal of Pharmaceutics 295 (1-2) (2005) : 235-245.

Xing, Y.L., et al. Preparation of alginate coated chitosan microparticles for vaccine delivery. BMC Biotechnology 8 (2008) : 89.

Yamamoto, H., Kuno,Y., Sugimoto, S., Takeuchi, H., and Kawashima, Y. Surface-modified PLGA nanosphere with chitosan improved pulmonary delivery of calcitonin by mucoadhesion and opening of the intercellular tight junctions. Journal of Controlled Release 102 (2) (2005) : 373-381.

Yin, L., Ding, J., He, C., Cui, L., Tang, C., and Yin, C. Drug permeability and mucoadhesion properties of thiolated trimethyl chitosan nanoparticles in oral insulin delivery. Biomaterials 30 (2009) : 5691-5700.

Yuan, Q., Shah, J., Hein, S., and Misra, R.D.K. Controlled and extended drug release behavior of chitosan-based nanoparticle carrier. Acta Biomaterialia 6 (3) (2010) : 1140-1148.

Zhang, J., Pekosz, A., and Lamb, R.A. Influenza virus assembly and lipid raft microdomains: a role for the cytoplasmic tails of the spike glycoproteins. Journal of Virology 74 (10) (2000) : 4634-4644.

Zhang, L., and Kosaraju, S.L. Biopolymeric delivery system for controlled release of polyphenolic antioxidants. European Polymer Journal, 43 (7) (2007) : 2956-2966.

Zijlstra, G.S., et al. Formulation and process development of (recombinant human) deoxyribonuclease I as a powder for inhalation. Pharmaceutical Development and Technology 14 (4) (2009) : 358-368.

APPENDIX

Table 6-1 Effects of concentration of chitosan solution and weight ratio of chitosan : TPP on nanoparticle formation and zeta potential. (Figure 4-1 and 4-2)

CS:TPP weight ratio	particle size (nm) (SD)		zeta potential (mV) (SD)	
	0.1 % CS	0.2 % CS	0.1 % CS	0.2 % CS
1.0	17,675.7 (3,177.78)	88,006.7 (87,473.50)	7.28 (0.39)	5.63 (0.15)
1.5	187,146.7 (99,217.01)	15,520.0 (4,880.28)	10.44 (4.52)	10.23 (0.41)
2.0	104.5 (4.71)	679.1 (122.32)	20.93 (0.84)	17.53 (0.31)
2.5	103.6 (4.60)	115.3 (2.16)	31.07 (2.25)	27.17 (0.42)
3.0	109.3 (3.05)	121.6 (1.70)	35.13 (3.97)	33.23 (1.47)

Table 6-2 Effects of pH of chitosan solution and weight ratio of chitosan : TPP on nanoparticle formation. (Figure 4-3)

CS:TPP weight ratio	particle size (nm) (SD)			
	pH 3.11	pH 4.5	pH 5.5	pH 6.5
2	114.2 (2.85)	169.2 (2.65)	195.9 (6.73)	172.7 (2.70)
3	96.4 (0.69)	95.7 (1.04)	195.7 (9.18)	227.0 (2.20)
4	111.4 (2.21)	268.5 (0.95)	268.5 (8.00)	241.5 (6.91)
5	135.1 (13.04)	299.3 (3.05)	299.3 (6.97)	293.1 (12.23)
6	143.0 (4.43)	359.3 (1.73)	359.3 (4.60)	343.2 (8.02)

Table 6-3 Effects of pH of chitosan solution and weight ratio of chitosan : TPP on zeta potential. (Figure 4-4)

CS:TPP weight ratio	zeta potential (mV) (SD)			
	pH 3.11	pH 4.5	pH 5.5	pH 6.5
2	19.40 (1.37)	10.80 (1.93)	8.35 (0.40)	6.85 (1.00)
3	28.40 (2.33)	15.70 (2.14)	11.41 (2.03)	5.95 (2.07)
4	32.80 (4.45)	14.50(2.63)	11.03 (1.54)	7.15 (2.90)
5	32.70 (4.84)	19.10 (2.70)	13.27 (2.20)	7.93 (2.60)
6	32.20 (6.20)	18.03 (3.09)	13.97 (2.06)	4.55 (3.25)

Table 6-4 The influence of order of mixing on particle size and zeta potential. (Figure 4-5 and 4-6)

order of mixing	particle size (nm) (SD)		zeta potential (mV) (SD)	
	pH 3.11	pH 4.5	pH 3.11	pH 4.5
A	223.1 (18.1)	127.9 (3.7)	37.97 (1.91)	16.77 (2.11)
B	195.9 (18.3)	118.5 (3.0)	36.47 (1.45)	16.63 (2.21)
C	169.4 (4.5)	114.1 (4.1)	37.57 (1.21)	16.93 (0.47)
D	160.9 (6.9)	193.6 (29.2)	35.87 (2.26)	17.43 (2.30)
E	168.7 (4.6)	139.2 (5.1)	38.00 (1.05)	19.40 (2.44)

A: mixed chitosan solution with Tween 80, then added alum, and TPP lastly.

B: mixed chitosan solution with alum, then add Tween 80, and TPP lastly.

C: mixed chitosan solution with TPP, then added Tween 80, and alum lastly.

D: mixed chitosan solution with Tween 80, then added TPP, and alum lastly.

E: mixed chitosan solution with TPP, then added Tween 80, and alum with tween 80 lastly.

Table 6-5 Effects of mixing time and amount of Tween 80 on nanoparticle formation and zeta potential. (Figure 4-7 and 4-8)

volume of 2% (w/v) tween 80	mixing time			
	particle size (nm) (SD)		zeta potential (mV) (SD)	
	30 min	60 min	30 min	60 min
0.5 ml	139.9 (10.2)	164.9 (19.6)	13.8 (0.3)	13.6 (2.3)
1.0 ml	128.3 (7.6)	197.6 (12.1)	16.6 (0.6)	15.9 (0.7)
1.5 ml	142.6 (7.3)	170.6 (65.3)	16.0 (2.6)	15.7 (0.4)

Table 6-6 Effects of aluminium hydroxide gel concentration on particle size and zeta potential. (Figure 4-9 and 4-10)

aluminium hydroxide gel concentration (mg/ml)	particle size (nm) (SD)	zeta potential (mV) (SD)
0.15	147.6 (11.7)	16.0 (1.1)
0.4	357.8 (31.0)	16.3 (2.3)
0.8	2,103.7 (337.2)	24.4 (1.2)
1.2	2,928.0 (1,131.9)	21.5 (3.2)
1.6	2,766.0 (451.5)	25.5 (1.6)

Table 6-7 Effects of method to incorporate BSA into chitosan nanoparticles on particle size. The number 1, 2 and 3 represented 0.1, 0.2 and 0.4 mg/ml of aluminium hydroxide gel in formulations with method A or B. (Figure 4-11)

formulation	particle size (nm) (SD)			
	day 1	day 3	day 5	day 10
A1	142.9 (6.3)	139.6 (5.2)	145.2 (4.2)	139.3 (4.3)
A2	197.3 (17.3)	206.5 (25.2)	234.6 (15.5)	233.4 (16.1)
A3	542.2 (110.4)	533.5 (124.2)	884.2 (206.3)	812.8 (150.1)
B1	140.4 (4.9)	138.2 (5.5)	153.1 (11.2)	139.7 (5.9)
B2	197.8 (26..7)	187.7 (22.0)	196.0 (21.5)	211.8 (28.2)
B3	249.4 (3.6)	354.8 (164.3)	402.0 (52.0)	639.7 (132.1)

Table 6-8 Effects of method to incorporate BSA into chitosan nanoparticles on zeta potential. The number 1, 2 and 3 represented 0.1, 0.2 and 0.4 mg/ml of aluminium hydroxide gel in formulations with method A or B. (Figure 4-12)

formulation	zeta potential (mV) (SD)			
	day 1	day 3	day 5	day 10
A1	14.44 (1.53)	15.28 (1.69)	14.10 (0.68)	15.79 (0.82)
A2	15.53 (1.58)	15.58 (0.70)	11.80 (1.38)	15.10 (1.54)
A3	16.91 (2.84)	18.79 (1.94)	19.63 (2.93)	20.09 (1.63)
B1	15.2 (1.89)	15.07 (2.58)	14.53 (0.45)	14.36 (1.24)
B2	13.97 (4.15)	15.22 (1.33)	18.50 (2.05)	15.77 (4.00)
B3	16.6 (0.78)	20.73 (1.69)	15.73 (4.16)	20.82 (3.04)

Table 6-9 Molar ellipticity of native BSA, BSA extracted from chitosan nanoparticles (CSNPs), chitosan nanoparticles with 0.1, 0.2 and 0.4 mg/ml (CSNPs+Al1, CSNPs+Al2 and CSNPs+Al3, respectively). (Figure 4-20)

Wavelength[nm]	native BSA	CSNPs	CSNPs+Al1	CSNPs+Al2	CSNPs+Al3
250	-0.038345	-0.300194	0.002871	-0.09715	-0.27309
249	-0.087537	-0.248851	-0.104047	-0.16607	-0.34063
248	-0.151418	-0.338924	-0.260608	-0.23578	-0.36191
247	-0.238608	-0.437113	-0.309708	-0.35828	-0.46084
246	-0.36001	-0.488705	-0.318659	-0.44344	-0.58999
245	-0.530892	-0.466774	-0.379985	-0.49431	-0.65269
244	-0.723705	-0.409788	-0.427414	-0.6179	-0.73638
243	-0.890242	-0.59543	-0.528386	-0.74434	-0.84161
242	-1.043764	-0.878389	-0.844285	-0.9522	-0.93371
241	-1.22131	-1.110961	-1.211099	-1.18662	-1.12727
240	-1.473922	-1.372469	-1.537312	-1.3551	-1.47347
239	-1.880452	-1.677722	-1.806201	-1.61899	-1.80906
238	-2.44975	-2.01125	-2.098045	-2.00044	-2.24357
237	-3.101386	-2.472461	-2.505957	-2.43486	-2.76244
236	-3.767104	-3.070061	-3.14285	-3.0299	-3.32872
235	-4.444405	-3.719656	-3.777294	-3.64983	-3.99426
234	-5.143543	-4.437755	-4.402263	-4.22417	-4.67732
233	-5.896277	-5.220391	-5.11541	-4.97732	-5.22649
232	-6.700946	-5.999834	-5.903715	-5.74272	-5.79427
231	-7.503536	-6.678409	-6.689866	-6.37487	-6.35031
230	-8.232324	-7.408305	-7.607124	-7.04615	-7.08145
229	-8.900323	-8.001018	-8.406182	-7.74088	-7.85315
228	-9.519212	-8.499624	-9.078615	-8.4398	-8.50993
227	-10.059084	-9.036451	-9.680097	-9.30957	-9.08431
226	-10.489445	-9.53546	-10.036951	-10.1625	-9.70137
225	-10.816579	-10.129536	-10.181176	-10.7359	-10.1258
224	-11.030344	-10.719247	-10.443413	-11.0317	-10.498
223	-11.137649	-11.178325	-10.830791	-11.2154	-10.7599
222	-11.246741	-11.650389	-11.161425	-11.4303	-11.0389
221	-11.379698	-12.079515	-11.369215	-11.7493	-11.29
220	-11.582403	-12.411087	-11.702068	-12.0333	-11.7069
219	-11.919522	-12.839828	-12.21967	-12.2073	-12.0167
218	-12.357574	-13.359719	-12.775181	-12.3859	-12.5239
217	-12.667168	-13.85578	-13.381598	-12.89	-13.1704

Wavelength[nm]	native BSA	CSNPs	CSNPs+Al1	CSNPs+Al2	CSNPs+Al3
216	-12.781482	-14.48495	-13.838574	-13.6011	-13.6605
215	-12.655023	-15.281864	-14.300583	-14.2771	-14.0532
214	-12.532413	-15.816977	-14.706656	-14.8457	-14.131
213	-12.696677	-15.970014	-15.177469	-15.0768	-14.2517
212	-13.343083	-16.043449	-15.633413	-14.9189	-14.7362
211	-14.174836	-16.216904	-16.043354	-15.6361	-15.3435
210	-14.805758	-16.847528	-16.285234	-16.1838	-16.046
209	-14.892142	-17.639185	-16.329933	-15.9214	-16.6258
208	-14.268769	-17.967499	-15.52691	-15.2128	-15.9837
207	-12.864939	-17.252176	-14.074377	-13.9647	-15.2231
206	-10.503514	-14.395941	-11.739545	-10.6597	-12.7137
205	-7.625034	-10.532108	-9.293507	-8.54725	-8.87663
204	-4.976144	-5.421934	-5.305246	-6.36713	-7.48493
203	-2.370648	2.233391	-0.667776	-4.60106	-3.94569
202	0.560952	9.438393	2.996583	-2.66534	5.214106
201	4.226201	13.489113	4.280527	0.725449	20.75435
200	9.176565	16.727831	3.255304	6.022559	45.44698

Table 6-10 The percentage of washed FITC-BSA representing the mucoadhesive property on mucous tissue of FITC-BSA in PBS buffer (control), chitosan nanoparticles (CSNPs) and chitosan nanoparticles conjugated with 0.1, 0.2 and 0.4 mg/ml of aluminium hydroxide gel (CSNPs+Al1, CSNPs+Al2 and CSNPs+Al3, respectively). (Figure 4-21)

time (min)	percentage of washed FITC-BSA (SD)				
	PBS	CSNPs	CSNPs+Al1	CSNPs+Al2	CSNPs+Al3
0	0	0	0	0	0
5	74.52 (5.84)	46.41 (4.02)	42.12 (3.63)	42.74 (6.19)	37.01 (2.48)
10	90.37 (4.61)	56.18 (6.78)	54.87 (4.16)	50.72 (6.38)	51.64 (6.93)
15	99.34 (5.89)	58.97 (8.13)	62.53 (6.17)	56.37 (8.28)	57.06 (5.88)
30	99.83 (3.94)	65.33 (5.58)	65.21 (9.51)	61.31 (6.57)	61.73 (6.43)
45	98.78 (2.43)	65.21 (3.30)	67.63 (5.67)	65.43 (6.05)	66.78 (6.24)
60	100.78 (4.26)	73.86 (5.38)	69.14 (5.12)	70.34 (2.77)	68.48 (5.63)

Table 6-11 The percentage of nasal cell viability after incubated with BSA loaded chitosan nanoparticles (CSNPs) and BSA loaded chitosan nanoparticles conjugated with 0.1, 0.2 and 0.4 mg/ml of aluminium hydroxide gel (CSNPs+Al1, CSNPs+Al2 and CSNPs+Al3, respectively). (Figure 4-22)

formulation	percentage of cell viability (SD)
CSNPs	102.66 (4.79)
CSNPs+Al1	100.25 (2.36)
CSNPs+Al2	99.83 (3.74)
CSNPs+Al3	81.97 (3.11)

Table 6-12 The average mean uptake cell count of RPMI 2650 cells, before uptake study and after 2 hours uptake studied of FITC-BSA in PBS buffer (PBS), FITC-BSA loaded chitosan nanoparticles (CSNPs), FITC-BSA loaded chitosan nanoparticles conjugated with 0.1, 0.2 and 0.4 mg/ml of aluminium hydroxide gel (CSNPs+Al1, CSNPs+Al2 and CSNPs+Al3, respectively). (Figure 4-24)

formulation	mean uptake cell count (SD)
cell	3.00 (0.15)
PBS	39.96 (2.86)
CSNPs	138.96 (47.78)
CSNPs+Al1	132.53 (7.47)
CSNPs+Al2	127.56 (34.29)
CSNPs+Al3	74.10 (5.30)

Table 6-13 The permeation data of FD-4 in PBS though cell culture and blank filter. (Figure 4-6)

time (min)	percentage of permeated FD-4 (SD)	
	blank filter	cell culture
0	0	0
30	13.50 (0.47)	0.84 (0.02)
60	20.93 (0.92)	1.75 (0.08)
120	35.70 (1.51)	3.29 (0.10)
180	47.02 (1.37)	5.10 (0.26)

Table 6-14 Effect of formulations on the TEER value during permeation study. FITC-BSA in PBS (PBS), FITC-BSA loaded chitosan nanoparticles (CSNPs), FITC-BSA loaded chitosan nanoparticles conjugated with 0.1, 0.2 and 0.4 mg/ml of aluminium hydroxide gel (CSNPs+Al1, CSNPs+Al2 and CSNPs+Al3, respectively). (Figure 4-27)

time (min)	TEER (% from initial value) (SD)				
	PBS	CSNPs	CSNPs+Al1	CSNPs+Al2	CSNPs+Al3
0	100.00 (0.79)	100.00 (6.54)	100.00 (3.67)	100.00 (4.28)	100.00 (7.04)
30	75.23 (4.20)	90.09 (10.24)	98.15 (4.24)	82.71 (2.80)	96.71(19.02)
60	73.39 (1.59)	89.15 (9.28)	95.83 (5.01)	85.51 (5.05)	83.10 (14.91)
120	72.94 (0.00)	84.91 (8.61)	95.37 (9.04)	82.24 (15.38)	95.77 (13.44)
180	72.48 (1.59)	83.96 (8.05)	95.37 (7.65)	81.31 (7.01)	95.3 (6.66)

Table 6-15 The permeation data of FITC-BSA in PBS (PBS), FITC-BSA loaded chitosan nanoparticles (CSNPs), FITC-BSA loaded chitosan nanoparticles conjugated with 0.1, 0.2 and 0.4 mg/ml of aluminium hydroxide gel (CSNPs+Al1, CSNPs+Al2 and CSNPs+Al3, respectively). (Figure 4-28)

time (min)	percentage of permeated FITC-BSA (SD)				
	PBS	CSNPs	CSNPs+Al1	CSNPs+Al2	CSNPs+Al3
0	0	0	0	0	0
30	0.68 (0.06)	0.25 (0.01)	0.28 (0.03)	0.24 (0.07)	0.30 (0.02)
60	1.20 (0.04)	0.50 (0.11)	0.56 (0.09)	0.47 (0.12)	0.49 (0.02)
120	2.48 (0.01)	1.25 (0.14)	1.35 (0.06)	1.13 (0.13)	2.18 (0.06)
180	3.68 (0.12)	2.24 (0.16)	2.52 (0.38)	1.15 (0.22)	2.01 (0.12)

Table 6-16 The amount of lysated BSA-FITC from each formulation after permeation study. FITC-BSA in PBS buffer (PBS), FITC-BSA loaded chitosan nanoparticles (CSNPs), FITC-BSA loaded chitosan nanoparticles conjugated with 0.1, 0.2 and 0.4 mg/ml of aluminium hydroxide gel (CSNPs+Al1, CSNPs+Al2 and CSNPs+Al3, respectively). (Figure 4-29)

formulation	lysated BSA-FITC concentration (μg/ml) (SD)
PBS	6.00 (0.51)
CSNPs	30.65 (2.60)
CSNPs+Al1	36.66 (5.63)
CSNPs+Al2	26.82 (3.75)
CSNPs+Al3	14.47 (5.44)

Table 6-17 IgG Anti-influenza (H1N1) antigen-specific total serum IgG responses in mice after intranasal vaccination with the antigen solution, antigen loaded chitosan nanoparticles, antigen loaded chitosan nanoparticles conjugated with aluminium hydroxide gel, and intramuscular vaccination with antigen solution. (Figure 4-31)

Formulation	route	IgG titers (SD, No. of responded mice)		
		day 21	day 42	day 56
PBS	i.n.	0	-	-
Ag-Solution	i.n.	100.0 (0,2)	100.0 (0,3)	100.0 (0,4)
Ag-CSNPs	i.n.	100.0 (0,3)	280.0 (402.0,5)	485.7 (481.0,7)
Ag-CSNPs-Al	i.n.	400.0 (519.6,3)	614.3 (481.1,7)	887.5 (318.0,8)
Ag-Solution	i.m.	1000.0 (0,8)	-	-

Table 6-18 IgG1 Anti-influenza (H1N1) antigen-specific total serum IgG responses in mice after intranasal vaccination with the antigen solution, antigen loaded chitosan nanoparticles, antigen loaded chitosan nanoparticles conjugated with aluminium hydroxide gel, and intramuscular vaccination with antigen solution. (Figure 4-32)

Formulation	route	IgG1 titers (SD, No. of responded mice)		
		day 21	day 42	day 56
PBS	i.n.	0	-	-
Ag-Solution	i.n.	100.0 (0,2)	400.0 (519.6,3)	460.0 (493.0,5)
Ag-CSNPs	i.n.	700.0 (520.0,3)	640.0 (493.0.0,5)	1,900.0 (2,600.0,7)
Ag-CSNPs-Al	i.n.	1,000.0 (0,4)	2,028.6 (3,540.6,7)	3,137.5 (4,247.0.0,8)
Ag-Solution	i.m.	3,250.0 (4,166.2,8)	-	-

Table 6-19 IgG2a Anti-influenza (H1N1) antigen-specific total serum IgG responses in mice after intranasal vaccination with the antigen solution, antigen loaded chitosan nanoparticles, antigen loaded chitosan nanoparticles conjugated with aluminium hydroxide gel, and intramuscular vaccination with antigen solution. (Figure 4-33)

Formulation	route	IgG2a titers (SD, No. of responded mice)		
		day 21	day 42	day 56
PBS	i.n.	0	-	-
Ag-Solution	i.n.	100.0 (0,2)	400.0 (519.6,3)	460.0 (493.0,5)
Ag-CSNPs	i.n.	640.0 (493.0,5)	2,050.0 (3,920.0,6)	3,442.9 (4,491.0,7)
Ag-CSNPs-Al	i.n.	1,450.0 (3,469.1,8)	3,025.0 (4,322.9,8)	6,625.0 (4,657.9,8)
Ag-Solution	i.m.	6,512.5 (4,821.2,8)	-	-

Table 6-20 Anti-influenza (H1N1) antigen-specific S-IgA titers in nasal lavages of mice after intranasal vaccination with the antigen solution, antigen loaded chitosan nanoparticles, antigen loaded chitosan nanoparticles conjugated with aluminium hydroxide gel, and intramuscular vaccination with antigen solution. (Figure 4-34)

Formulation	route	IgA titers (SD, No. of responded mice)
PBS	i.n.	0
Ag-Solution	i.n.	10 (0,2)
Ag-CSNPs	i.n.	33 (46,7)
Ag-CSNPs-Al	i.n.	42 (49,8)
Ag-Solution	i.m.	1 (0,1)
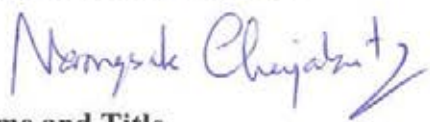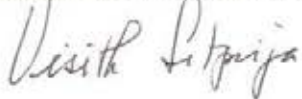
Chulalongkorn University Animal Care and Use Committee

Certificate of Project Approval	☐ Original ☐ Renew
Animal Use Protocol No. 12-33-015	**Approval No. 12-33-015**

Protocol Title
Chitosan nanoparticles with aluminium hydroxide gel as nasal delivery system for influenza vaccine

Principal Investigator
GARNPIMOL C. RITTHIDEJ, Ph.D.

Certification of Institutional Animal Care and Use Committee (IACUC)
    This project has been reviewed and approved by the IACUC in accordance with university regulations and policies governing the care and use of laboratory animals. The review has followed guidelines documented in Ethical Principles and Guidelines for the Use of Animals for Scientific Purposes edited by the National Research Council of Thailand.

Date of Approval	Date of Expiration
August 21, 2012	August 21, 2015

Applicant Faculty/Institution
Faculty of Pharmaceutical Sciences, Chulalongkorn University, Phyathai Road., Pathumwan
BKK-THAILAND. 10330

Signature of Chairperson	Signature of Authorized Official
Name and Title	**Name and Title**
THONGCHAI SOOKSAWATE, Ph.D.	PARKPOOM TENGAMNUAY, Ph.D.
Chairman	Associate Dean (Research and Academic Service)

    The official signing above certifies that the information provided on this form is correct. The institution assumes that investigators will take responsibility, and follow university regulations and policies for the care and use of animals.
    This approval is subjected to assurance given in the animal use protocol and may be required for future investigations and reviews.

Queen Saovabha Memorial Institute Animal Care and Use Committee

Certificate of Project Approval	✓☐ Original ☐ Renew
Protocol No. 4/2012	
Protocol Title Chitosan nanoparticles with aluminium hydroxide gel as nasal delivery system for influenza vaccine	
Principle Investigator Anawatch Mitpratan	

Certification of Institutional Animal Care and Use Committee (QSMI-ACUC)

This project has been reviewed and approved by the committee in accordance with Queen Saovabha Memorial Institute regulations and policies governing the care and use of laboratory animals. The review has followed guidelines documented in Ethical Principles and Guidelines for the Use of Animals for Scientific Purposes edited by National Research Council of Thailand.

Date of Approval September 25, 2012	**Date of Expiration** September 25, 2014

Applicant Institution

Queen Saovabha Memorial Institute, Thai Red Cross Society

Signature of Chairperson	**Signature of Authorized Official**
Narongsak Chaiyabutr (signature)	*Visith Sitprija* (signature)
Name and Title Prof. Dr. Narongsak Chaiyabutr Chairman	**Name and Title** Prof. Dr. Visith Sitprija Director of Queen Saovabha Memorial Institute

The official signing above certifies that the information provided on this form is correct. The institution assumes that investigators will take responsibility, and follow institute regulations and policies for the care and use of animals.

This approval is subjected to assurance given in the animal use protocol and may be required for future investigations and reviews

BIOGRAPHY

Mr.Anawatch Mitpratan was born on March 30, 1975, in Bangkok, Thailand. He received his Bachelor of Science in Pharmacy in 1998 from the Faculty of Pharmaceutical Sciences, Chulalongkorn University, Bangkok, Thailand. He entered studying in the Master's Degree in Industrial Pharmacy Program in the Faculty of Pharmaceutical Sciences, Chulalongkorn University, Thailand in 2010.